

**VIRUS-HOST INTERACTIONS AT THE MATERNAL-FETAL INTERFACE**

by

**Elizabeth Brianne Delorme-Axford**

B.S. Biological Sciences, State University of New York College at Brockport, 2006

M.S. Biological Sciences, State University of New York College at Brockport, 2008

Submitted to the Graduate Faculty of  
the School of Medicine in partial fulfillment  
of the requirements for the degree of  
Doctor of Philosophy

University of Pittsburgh

2013

UNIVERSITY OF PITTSBURGH

SCHOOL OF MEDICINE

This dissertation was presented

by

Elizabeth Brianne Delorme-Axford

It was defended on

March 14, 2013

and approved by

Dr. Ora Weisz, Committee Chair, Professor, Department of Medicine

Dr. Yoel Sadovsky, Professor, Department of OB/GYN

Dr. Jennifer Condon-Jeyasuria, Assistant Professor, Department of OB/GYN

Dissertation Advisor: Dr. Carolyn Coyne, Assistant Professor, Department of Microbiology  
and Molecular Genetics

## VIRUS-HOST INTERACTIONS AT THE MATERNAL-FETAL INTERFACE

Elizabeth Delorme-Axford, PhD

University of Pittsburgh, 2013

Strategies to protect against viral infections are essential during pregnancy. Maternal-fetal transmission can have serious pathological outcomes, including fetal infection, growth restriction, birth defects, and/or death. Throughout pregnancy, the placenta (composed of polarized trophoblasts amid stromal and vascular arrangements) is an indispensable tissue that forms a barrier at the maternal-fetal interface. Viruses have likely evolved specific mechanisms to exploit the protective functions of placental trophoblasts to initiate fetal infection. Despite the severity of pathologic disease associated with fetal viral infection, little is known regarding virus-host interactions at the maternal-fetal interface. In this work, we have examined the mechanisms by which – 1) placental trophoblasts protect against invading viruses and 2) coxsackievirus B (CVB), a virus associated with fetal pathology, gains entry into polarized trophoblasts. As a model, we have used cultured primary human trophoblasts (PHTs) and immortalized human (BeWo) trophoblasts.

We have found that PHTs are highly resistant to infection by six disparate viruses. PHTs transfer this resistance to non-placental recipient cells through exosome-mediated delivery of select placental microRNAs (miRNAs). We show that members of the chromosome 19 miRNA cluster (C19MC), which are almost exclusively expressed in the primate placenta, are packaged within trophoblast-derived exosomes, and attenuate viral replication in recipient cells by inducing autophagy.

To study CVB entry into placental trophoblasts, we have merged virological and cell biological techniques, combined with pharmacological inhibitors and siRNAs directed against diverse cellular endocytic and signaling components, to characterize the pathways hijacked by CVB to promote its entry into human trophoblasts. We found the kinetics of CVB entry and uncoating in placental trophoblasts similar to those described in polarized intestinal epithelial cells. CVB entry into placental trophoblasts requires decay accelerating factor (DAF) binding, and is associated with the relocalization of virus from the apical surface to intercellular tight junctions. We have identified a divergent mechanism for CVB entry that is independent of clathrin, caveolae, and dynamin II but is dependent on lipid-rafts and Src family tyrosine kinase signaling. Our studies model viral transmission and infection at the maternal-fetal interface, and have the therapeutic potential for preventing prenatal infections, pre-term labor, and birth defects.

## TABLE OF CONTENTS

<b>ABSTRACT.....</b>	<b>III</b>
<b>LIST OF TABLES.....</b>	<b>X</b>
<b>LIST OF FIGURES.....</b>	<b>XI</b>
<b>PREFACE.....</b>	<b>XIII</b>
<b>1.0 INTRODUCTION.....</b>	<b>1</b>
<b>1.1 PLACENTAL TROPHOBLASTS.....</b>	<b>1</b>
<b>1.1.1 Syncytiotrophoblasts.....</b>	<b>3</b>
<b>1.1.2 Villous cytotrophoblasts.....</b>	<b>4</b>
<b>1.2 INFECTIONS DURING PREGNANCY.....</b>	<b>5</b>
<b>1.2.1 TORCH Infections.....</b>	<b>7</b>
<b>1.2.1.1 Toxoplasmosis.....</b>	<b>8</b>
<b>1.2.1.2 Rubella virus.....</b>	<b>9</b>
<b>1.2.1.3 Cytomegalovirus (CMV).....</b>	<b>9</b>
<b>1.2.1.4 Herpes simplex viruses 1 and 2 (HSV-1 and -2).....</b>	<b>10</b>
<b>1.2.2 Coxsackievirus B (CVB).....</b>	<b>11</b>
<b>1.3 VIRUS ENTRY.....</b>	<b>12</b>
<b>1.3.1 Virus entry mechanisms.....</b>	<b>12</b>
<b>1.3.2 VSV entry.....</b>	<b>14</b>

1.3.3	CVB entry into polarized epithelia.....	14
1.4	EXOSOMES.....	16
1.5	MICRORNAS (MIRNAS) .....	20
1.5.1	Overview and biogenesis .....	20
1.5.2	Antiviral miRNAs .....	23
1.5.3	Chromosome 19 miRNA cluster (C19MC).....	24
1.6	AUTOPHAGY .....	26
1.6.1	Introduction to autophagy .....	26
1.6.2	Autophagy as an antiviral host defense mechanism .....	29
1.6.3	Autophagy as a post-birth survival mechanism.....	30
1.7	CLASSICAL ANTIVIRAL TYPE I INTERFERON (IFN) SIGNALING ..	30
1.8	GOALS OF THIS DISSERTATION.....	33
2.0	PLACENTAL EXOSOMES CONFER VIRAL RESISTANCE.....	36
2.1	INTRODUCTION .....	36
2.2	RESULTS.....	37
2.2.1	Primary human trophoblasts (PHTs) resist virus infection.....	37
2.2.2	Conditioned PHT medium confers viral resistance.....	38
2.2.3	PHT exosomes confer viral resistance.....	42
2.2.4	C19MC-derived miRNAs confer viral resistance .....	43
2.2.5	Conditioned PHT medium and exosomes induce autophagy .....	45
2.2.6	Antiviral effects of C19MC miRNAs are not the result of type I IFN signaling .....	48
2.2.7	C19MC-derived miRNAs induce autophagy.....	49

2.2.8	Autophagy is a mechanism of viral resistance .....	52
2.2.9	Model.....	54
2.3	DISCUSSION.....	56
3.0	CVB ENTRY INTO HUMAN PLACENTAL TROPHOBLASTS .....	61
3.1	INTRODUCTION .....	61
3.2	RESULTS .....	62
3.2.1	BeWo cells are an appropriate model to study virus-host interactions at the maternal-fetal interface.....	62
3.2.2	DAF is required for efficient CVB entry .....	63
3.2.3	Kinetics of CVB entry into BeWo trophoblasts .....	64
3.2.4	CAR does not internalize with CVB during entry .....	65
3.2.5	Clathrin endocytosis is not required for CVB entry.....	67
3.2.6	Dynamin II is not required for CVB entry into placental trophoblasts	71
3.2.7	Lipid rafts but not caveolae are required for CVB entry .....	72
3.2.8	Macropinocytosis is not required for CVB entry.....	75
3.2.9	CVB entry is dependent on Src family tyrosine kinases .....	78
3.2.10	CVB entry into primary human trophoblasts (PHTs) .....	80
3.3	DISCUSSION.....	82
4.0	CONCLUSIONS .....	87
4.1	PLACENTAL EXOSOMES CONFER VIRAL RESISTANCE.....	87
4.2	CVB ENTRY INTO HUMAN PLACENTAL TROPHOBLASTS.....	94
4.3	CONCLUDING REMARKS .....	96
5.0	MATERIALS AND METHODS .....	98

<b>5.1</b>	<b>CELLS .....</b>	<b>98</b>
<b>5.2</b>	<b>VIRUSES .....</b>	<b>99</b>
<b>5.3</b>	<b>VIRUS EXPANSION AND PREPARATION .....</b>	<b>100</b>
<b>5.3.1</b>	<b>VSV.....</b>	<b>100</b>
<b>5.3.2</b>	<b>CVB .....</b>	<b>100</b>
<b>5.3.3</b>	<b>Neutral red labeled CVB .....</b>	<b>101</b>
<b>5.4</b>	<b>PLAQUE ASSAYS .....</b>	<b>101</b>
<b>5.4.1</b>	<b>VSV.....</b>	<b>101</b>
<b>5.4.2</b>	<b>CVB .....</b>	<b>102</b>
<b>5.4.3</b>	<b>Neutralizing virus plaque assays .....</b>	<b>103</b>
<b>5.5</b>	<b>MODIFIED TCID50 VIRUS TITERING ASSAYS.....</b>	<b>103</b>
<b>5.6</b>	<b>ANTIBODIES .....</b>	<b>103</b>
<b>5.7</b>	<b>PHARMACOLOGICAL AGENTS.....</b>	<b>104</b>
<b>5.7.1</b>	<b>Autophagy assays.....</b>	<b>104</b>
<b>5.7.2</b>	<b>CVB entry assays .....</b>	<b>104</b>
<b>5.8</b>	<b>CONDITIONED MEDIUM TREATMENT.....</b>	<b>105</b>
<b>5.9</b>	<b>EXOSOME ISOLATION .....</b>	<b>106</b>
<b>5.10</b>	<b>TRANSFECTIONS .....</b>	<b>107</b>
<b>5.10.1</b>	<b>Plasmid transfection .....</b>	<b>107</b>
<b>5.10.2</b>	<b>miRNA transfection .....</b>	<b>107</b>
<b>5.10.3</b>	<b>siRNA (small interfering RNA) transfection.....</b>	<b>107</b>
<b>5.11</b>	<b>VIRUS INFECTION ASSAYS.....</b>	<b>108</b>
<b>5.12</b>	<b>NEUTRAL RED INFECTIOUS CENTER ASSAY.....</b>	<b>109</b>

<b>5.13</b>	<b>VIRUS ENTRY ASSAYS.....</b>	<b>111</b>
5.13.1	U2OS .....	111
5.13.2	BeWo cells.....	111
5.13.3	PHTs.....	111
<b>5.14</b>	<b>CHOLERA TOXIN B AND TRANSFERRIN UPTAKE ASSAY .....</b>	<b>112</b>
<b>5.15</b>	<b>IMMUNOSTAINING.....</b>	<b>112</b>
5.15.1	General protocol.....	112
5.15.2	Serial staining for virus entry assay .....	113
5.15.3	Immunofluorescence and confocal microscopy.....	113
5.15.4	Quantification and analysis.....	114
<b>5.16</b>	<b>TRANSMISSION ELECTRON MICROSCOPY (TEM) .....</b>	<b>114</b>
<b>5.17</b>	<b>RNA EXPRESSION STUDIES .....</b>	<b>115</b>
5.17.1	RNA isolation .....	115
5.17.2	cDNA synthesis.....	116
5.17.3	RT-qPCR (Real time quantitative polymerase chain reaction).....	116
<b>5.18</b>	<b>IMMUNOBLOTS .....</b>	<b>117</b>
<b>5.19</b>	<b>REPORTER GENE ASSAY.....</b>	<b>118</b>
<b>5.20</b>	<b>STATISTICAL ANALYSIS .....</b>	<b>118</b>
<b>APPENDIX A .....</b>		<b>119</b>
<b>APPENDIX B .....</b>		<b>129</b>
<b>BIBLIOGRAPHY .....</b>		<b>131</b>

## LIST OF TABLES

Table 1.1. Differences between placental cytotrophoblasts and syncytiotrophoblasts.....	5
Table 1.2. Pattern recognition receptors that detect viral components. ....	32
Table 2.1. Groups of C19MC miRNA mimics. ....	45
Table 5.1. Real-time PCR primers.....	117

## LIST OF FIGURES

Figure 1.1. Human placental structure .....	3
Figure 1.2. Viruses enter cells through a variety of pathways.....	13
Figure 1.3. Exosome release and uptake.....	19
Figure 1.4. Processing mature miRNAs through the miRISC .....	22
Figure 1.5. Multiple pathways to autophagy .....	29
Figure 2.1. Conditioned PHT medium and exosomes confer viral resistance to recipient cells ..	38
Figure 2.2. PHT cells resist virus infection.....	40
Figure 2.3. The antiviral effects of PHT conditioned medium .....	41
Figure 2.4. PHT and exosomal C19MC miRNAs confer viral resistance to recipient cells.....	44
Figure 2.5. PHT-derived exosomes induce autophagy in recipient cells.....	47
Figure 2.6. Medium from PHT cells induces autophagy in recipient cells.....	48
Figure 2.7 The antiviral effects of conditioned PHT medium are not due to type I IFN .....	51
Figure 2.8. C19MC miRNAs induce autophagy.....	52
Figure 2.9. Suppression of autophagy abrogates C19MC-mediated antiviral effects .....	54
Figure 2.10. Model depicting the exosome-mediated transfer of C19MC miRNAs .....	55
Figure 3.1. DAF is required for efficient CVB infection of placental trophoblasts .....	63
Figure 3.2. Kinetics of CVB entry into placental trophoblasts.....	66

Figure 3.3. Clathrin-mediated endocytosis is not required for CVB entry into BeWo trophoblast cells ..... 70

Figure 3.4. Dynamin II and clathrin heavy chain siRNAs inhibit transferrin uptake ..... 71

Figure 3.5. Lipid rafts, but not caveolin, are required for CVB entry ..... 75

Figure 3.6. Macropinocytosis is not involved in CVB entry into placental trophoblasts ..... 78

Figure 3.7. CVB entry is dependent on Src family tyrosine kinases ..... 80

Figure 3.8. CVB entry into primary human trophoblasts requires lipid rafts ..... 82

Figure 5.1. Culturing recipient cells with conditioned PHT medium ..... 105

Figure 5.2. Modified NRIC (Neutral Red Infectious Center) Assay ..... 110

## PREFACE

This dissertation would not have been possible without the abundant support of several individuals. I owe sincere thankfulness to my mentor, Dr. Carolyn Coyne. Thank you for allowing me to join your lab and allowing me to explore my scientific interests. Your thoughtful guidance, support, and encouragement over the years have made me a better person and a better scientist. Without your continuous determination to help me to succeed, I would not be where I am today. I am forever grateful for all that you have taught and helped me.

I would like to thank Dr. Yoel Sadovsky for agreeing to meet with Carolyn and I several years ago to teach us about placental trophoblasts. This was the start of an incredible collaboration between our labs that took us scientifically to places we could not have imagined. Thank you for all of your guidance and generosity. I would like to acknowledge my dissertation committee members – Drs. Ora Weisz and Jennifer Condon-Jeyasuria for your guidance and support over the years.

I would like to thank members of the Coyne lab (past and present) – Stefanie Morosky, Dr. Becky Bozym, Katie Harris, and Jana Jacobs – for your support and camaraderie. I would also like to acknowledge members of the Sadovsky lab (past and present) for their significant contributions to this work – Dr. Rogier Donker, Dr. Jean-Francois Mouillet, Dr. Tianjiao Chu, Dr. Yingshi Ouyang, Lori Rideout, Magda Jennings, Judy Ziegler, Elena Sadovsky, and Avi Bayer. I would also like to thank those who have generously provided scientific advice and

reagents essential to these studies: Drs. Adrian Morelli, Donna Stolz, Saumen Sarkar, Fred Homa, Jon Boyle, and Bill Goins (University of Pittsburgh), Jeffrey Bergelson, and Chonsaeng Kim (University of Pennsylvania). I have also been fortunate enough to be a recipient of a Teaching Fellowship awarded through the University of Pittsburgh School of Medicine and the Cell Biology graduate program, which has greatly helped to financially support my studies over the years and provided me with invaluable teaching experience.

I also cannot thank my family enough for all of the support that I have received over the years. To my parents Jeff and Kim Delorme, thank you for always encouraging me, loving me, and providing numerous opportunities throughout my life. I would also like to thank my aunt Michele Kearney for always being a source of support and guidance. Emily Wickline, thank you for being such a great friend over the past few years. Lastly, I am grateful to my husband Brian Delorme-Axford for never giving up on me. I could not have made it through graduate school without your endless support. Thank you for always being a constant source of love and encouragement, even when you had no idea what I was talking about.

## 1.0 INTRODUCTION

### 1.1 PLACENTAL TROPHOBLASTS

The placenta is a highly unique tissue, formed only during pregnancy, which is absolutely essential for maintaining and sustaining the development of a fetus. The primordial placenta begins to form approximately 6-7 days post-conception [1] and *reviewed* [2]. The placenta is primarily composed of specialized epithelial cells known as trophoblasts [3], and is derived from the outer trophoblast layer of the blastocyst during development of the conceptus [2]. The inner layer of the blastocyst will eventually form the developing embryo [3]. About one week post-conception, the trophoblastic cells begin to superficially invade the maternal uterine epithelium, *reviewed* [4]. The placenta proper begins to form as the trophoblast layer develops into a fused outer layer of multinucleated syncytiotrophoblasts and an inner layer of mononuclear cytotrophoblasts [4]. Around five weeks of pregnancy, the first cytotrophoblasts cells migrate from the placenta to differentiate and further invade into the spiral arteries of the endometrial wall [2, 5].

The placenta serves as the foremost maternofetal barrier during pregnancy by facilitating exchanges between maternal and fetal circulation [3]. Within the sterile environment of the uterus, the placenta also maintains a microbial-free milieu through both its highly complex architecture and innate immune functions, further described below [6]. As pregnancy progresses, the placental structure becomes more architecturally complex and defined; full

placental modification is complete by 16 weeks of pregnancy (**Figure 1.1**) [4, 7]. Beyond 16 weeks, further arrangements only occur at the primary villi [4]. The placenta is composed of villous tree structures (or villi) formed by intricate arrangements of stroma (a mesenchymal core of supportive connective tissue), fetal blood vessels that interdigitate throughout the villi, and trophoblasts (**Figure 1.1B**) [4, 8]. The hemochorial placental villi are composed of syncytiotrophoblasts, which are in direct contact with maternal blood. Therefore, the syncytiotrophoblasts serve as an initial line of defense against any probable invading pathogens. Progenitor cytotrophoblast cells underlie the syncytiotrophoblast layer and sit on a basement membrane anchored to the stroma. Beyond the main villous arrangement extend the extravillous cytotrophoblasts, which invade into the maternal uterine wall, or decidua.

Moreover, in addition to the inherent structural complexity of the placenta, there are numerous APPs (antimicrobial proteins and peptides) secreted by the placenta into the amniotic fluid within the fetal compartment, *reviewed* [6]. These APPs include lactoferrin (bactericide and fungicide [9]), bactericidal permeability-increasing protein (BPI), histones H2A and H2B (inhibit the bacterial endotoxin activity of LPS, lipopolysaccharide) [10], and  $\alpha$ -defensins (bactericide, fungicide, protozoacide, and enveloped virucide [11]) [6]. Interestingly, this points to a key, active role for the placenta in mediating antimicrobial defense, and contrasts with previous theories wherein pregnancy is viewed as an immunosuppressed state to support and prevent rejection of the semi-allogeneic fetus [12, 13]. However, there remains much to be discovered regarding the plethora of mechanisms the placenta must maintain to prevent the spread of infectious diseases to the fetus during pregnancy.

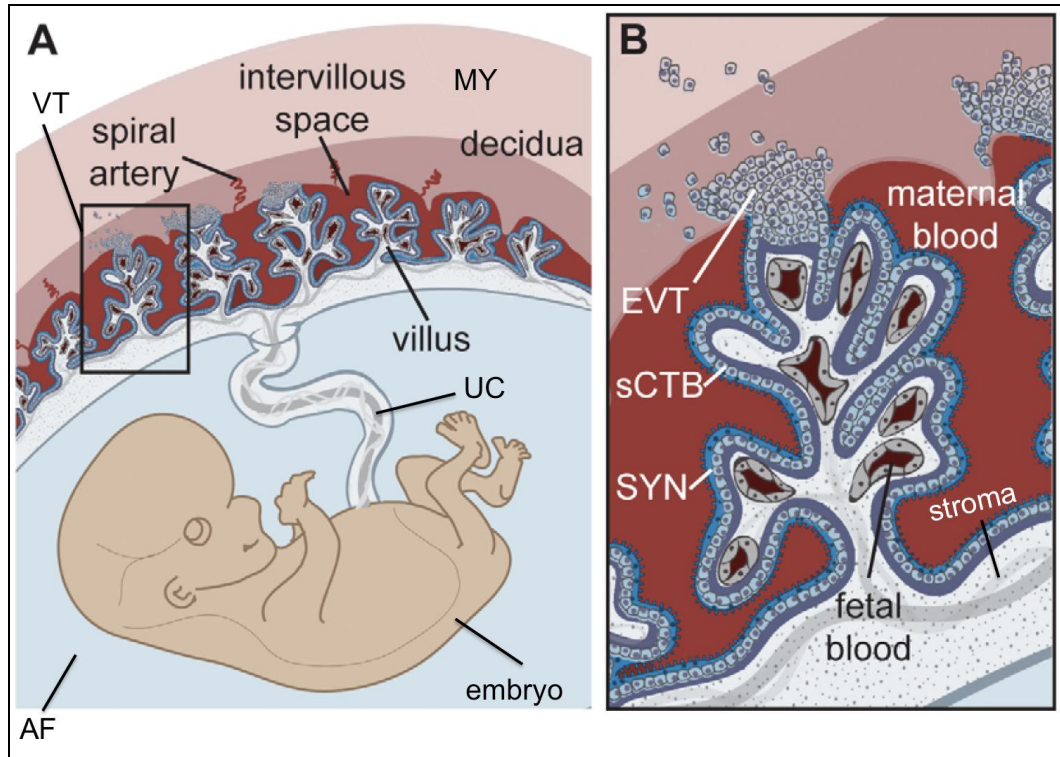


**Figure 1.1. Human placental structure.** (A) Shown is a schematic of the human placenta at approximately 6 weeks of pregnancy. Maternal features: MY (myometrium), spiral arteries, decidua (or the uterine lining during pregnancy), and intervillous space. Embryonic features: VT (villous tree), UC (umbilical cord), AF (amniotic fluid), and embryo. (B) Shown is an enlarged view of the box in A (villous tree). EVT (extravillous trophoblasts) invade and anchor the placenta into the decidual wall. STB (syncytiotrophoblasts) overlay the villous tree and are in direct contact with maternal blood. sCTB (subsycytial cytotrophoblasts) lie between the STB and basement membrane of the villous tree. Villous trees are formed with a core of stroma amid fetal blood vessels. Figure modified from Robbins JR *et al.* 2010, full reference in text.

### 1.1.1 Syncytiotrophoblasts

The syncytiotrophoblasts are highly polarized and maintain a dense layer of microvilli at the apical surface (**Table 1.1**) [14]. These microvilli are critical to facilitate the exchange of nutrients, gases, and wastes between the mother and the fetus. Furthermore, the syncytiotrophoblasts are multinucleated, terminally differentiated cells which no longer undergo mitotic division [14]. The syncytiotrophoblasts appear to be active participants in antimicrobial defense during pregnancy. Several lines of evidence support a role for the syncytiotrophoblasts as an antimicrobial bottleneck in preventing pathogen transmission across the remainder of the

placental unit (see section **1.2, “Infections During Pregnancy”**) [7, 8, 15-19]. Exchange of gas, nutrients, and wastes occurs via the syncytiotrophoblast layer, either actively or passively [14]. The syncytiotrophoblasts are also the major synthesizers for critical hormones necessary for sustaining the pregnancy including: hCG (human chorionic gonadotropin), hCS (human chorionic somatotropin; also known as hPL or human placental lactogen), other hGHs (human growth hormones), oxytocin, leptin, erythropoietin, CRH (corticotropin-releasing hormone), hPRL (human prolactin), and PTHrP (parathyroid hormone-related protein) [3, 14].

### **1.1.2 Villous cytotrophoblasts**

Cytotrophoblasts form the cellular barrier underlying the syncytiotrophoblast layer (**Table 1.1**). These cells lie on a basement membrane covering the placental villi [14]. In contrast to the syncytiotrophoblast, the cytotrophoblasts are mononuclear cells that continue to undergo proliferation. Cytotrophoblasts function as undifferentiated progenitors for both the overlying syncytiotrophoblasts and the extravillous invasive trophoblasts that serve to anchor the placenta into the maternal uterine wall [5]. Throughout pregnancy the cytotrophoblasts are mitotically active until they fuse to form a syncytium to replenish the syncytiotrophoblast layer. The cytotrophoblast stratum is a continuous monolayer but becomes increasingly discontinuous throughout the duration of pregnancy [3, 14]. The precise mechanisms guiding cytotrophoblast to syncytiotrophoblast fusion are currently under debate. However, the proportion of cytotrophoblastic to syncytialized nuclei persists at a ratio of approximately 1:9 throughout pregnancy [14]. Together, both the syncytiotrophoblast and the cytotrophoblast cells form an innate fetoplacental defense unit against pathogen invasion.

**Table 1.1. Differences between placental cytotrophoblasts and syncytiotrophoblasts.**

<b>Placental Trophoblasts</b>		
	<b>Syncytiotrophoblasts (STB)</b>	<b>Cytotrophoblasts (CTB)</b>
<b>Localization</b>	Faces maternal blood, between CTB and maternal blood	Fetal interface, between the basement membrane and STB layer
<b>Nucleation</b>	Multinuclear	Mononuclear
<b>Monolayer</b>	Yes	Yes during early gestation but becomes discontinuous during the second trimester
<b>Polarity</b>	Fully polarized	Dependent on monolayer confluence and trimester
<b>Differentiation state</b>	Differentiated, post-mitotic	Undifferentiated progenitors, may progress to STB

## **1.2 INFECTIONS DURING PREGNANCY**

A significant and complex, yet inadequately characterized epithelial barrier that is absolutely essential for protection from invading pathogens, are the polarized trophoblasts of the human placenta. The placenta constitutes the major physical and cellular barrier at the maternal-fetal interface, and serves as the main site for gas and nutrient exchange between mother and fetus. As mentioned above (see section 1.1, “**Placental Trophoblasts**”), the syncytiotrophoblast cells lie in direct contact with maternal blood, and therefore comprise the initial line of defense against entering viruses. Additionally, gas and nutrient exchange primarily occurs across the syncytiotrophoblast layer and between the fetal capillaries located within the stroma of the

villous trees [7]. Therefore, it is easy to see how any pathogens potentially present within the maternal blood could easily be transmitted to the fetus.

*In utero* viral transmission from mother to fetus can potentially occur by four transit routes: (a) maternal endothelial microvasculature to endovascular extravillous cytotrophoblasts, (b) infected macrophages from maternal blood to placental trophoblast populations, (c) ascending infection (via the urogenital tract) culminating in vertical and/or (d) paracellular routes mainly through maternal blood via the syncytiotrophoblast and fetal capillaries. Currently, the molecular mechanisms by which pathogens cross from the maternal to fetal to cause infection remain poorly defined.

Historically, the literature investigating host-pathogen interactions at the maternal-fetal interface has been limited. Recently, however, a series of papers have been published investigating key prenatal pathogens (such as *Listeria monocytogenes* and *Toxoplasma gondii*) and transmission of infection into the trophoblasts of placental explants [7, 8, 19]. Robbins *et al.* initially identified that *Listeria monocytogenes* infected various trophoblast populations with varying efficiencies [7]. These studies were performed using first trimester human placental explant cultures grown in on Matrigel extracellular matrix (ECM) substrates [7]. Remarkably, this model retains the *in vivo* architecture of the placenta including the syncytiotrophoblast covering of the villous trees, the underlying cytotrophoblasts, and the invasive extravillous trophoblasts (EVTs). Robbins and colleagues found that *L. monocytogenes* primarily initiated infection at the villous cytotrophoblasts, which were not covered by a syncytiotrophoblast layer, while the syncytiotrophoblasts resisted infection [7]. Subsequent studies by Zeldovich *et al.* demonstrated that *L. monocytogenes* was trapped within vacuoles, late endosomes, and/or acidified lysosomes within isolated, purified EVT's or within EVT's of placental explants [8],

which could severely limit the spread of bacteria throughout the rest of the placental organ. Similarly, Robbins *et al.* examined *Toxoplasma gondii* parasitic infection in placental explants [19]. Interestingly, only EVT's or subsyncytial cytotrophoblasts (in which overlying syncytiotrophoblast breaks were present) were susceptible to infection [19]. Also in this study, the syncytiotrophoblasts were most resistant to infection and colonization by *T. gondii* [19]. Clearly, investigation into the routes by which diverse pathogens initiate vertical transmission to gain access to the fetal compartment is a key area for research; not only to advance our understanding of host-pathogen interactions and the diverse mechanisms that cells employ to defend themselves against microbial invasion, but also for its significance in maternal-fetal health. Knowledge gained by further investigation into pathogen invasion at the maternal-fetal interface has the therapeutic potential to reduce the incidences of fetal infection and death, pre-term labor, and birth defects *in utero*.

### **1.2.1 TORCH Infections**

During pregnancy, any maternal infection can potentially lead to vertical transmission and subsequent fetal disease. However, primary TORCH perinatal infections have been identified as being particularly detrimental with highly pathological outcomes. The term TORCH was initially coined by Nahmias *et al.* to designate microorganisms associated with known congenital and fetal disease [20]. Common neonatal clinical presentations of TORCH agents include: growth retardation, hepatosplenomegaly, jaundice, hemolytic anemia, microcephaly/hydrocephaly, intracranial calcification, pneumonitis, myocarditis, cardiac abnormalities, chorioretinitis, keratoconjunctivitis, cataracts, glaucoma, and hydrops [21]. TORCH infections include toxoplasmosis, other [such as Parvovirus B19, varicella zoster virus

(VZV), human immunodeficiency virus (HIV), enteroviruses, and/or the bacteria *Listeria monocytogenes* and *Treponema pallidum* (the causative agent of syphilis)], rubella, cytomegalovirus, and herpes simplex viruses type 1 and 2 [20-24]. The acronym was later proposed to be expanded to TORCHES (to now include syphilis) [25]. There is currently controversy regarding routinely screening for the TORCHES panel in the clinic due to the cost-effectiveness versus the benefits outcome; officially, it is currently not recommended to do so [24]. Nevertheless, some clinics routinely screen for the main TORCHES pathogens and select others, such as HIV. The main TORCH microorganisms are further described in detail below.

#### **1.2.1.1 Toxoplasmosis**

Toxoplasmosis is caused by the protozoan parasite *Toxoplasma gondii* [26]. It can be spread through undercooked, contaminated food or through accidental ingestion of *Toxoplasma* oocytes following contact with infected cat feces. If vertical transmission of *Toxoplasma gondii* occurs during pregnancy, it can result in devastating effects to the fetus. The severity of clinical manifestations are somewhat dependent on which stage of pregnancy fetal infection occurs [24]. If infection occurs in the first trimester, fetal death is often the result [24]. Second trimester infections commonly cause eye problems (chorioretinitis), hydrocephalus, and/or intracranial calcifications in the developing brain [24]. Third trimester infections are often asymptomatic, but the fetus may present with pathologies later on including fever, intrauterine growth restriction (IUGR), microcephaly, seizure, hearing loss, maculopapular rash, jaundice, hepatosplenomegaly, anemia, and lymphadenopathy [24]. If infection does occur during pregnancy, mothers may remain asymptomatic, and diagnoses are typically made through serologic testing [26]. Current therapies aimed towards treating *in utero Toxoplasma gondii* infections include drugs, such as pyrimethamine and sulfadiazine, supplemented with folinic

acid; however, this does not eliminate all of the parasites completely [26]. Thus, continued investigation into therapeutic strategies for prevention and full eradication of maternal-fetal infection with *Toxoplasma gondii* is critical for reducing the incidences of fetal death and/or birth defects.

#### **1.2.1.2 Rubella virus**

Rubella is a member of the *Rubivirus* genus within the *Togaviridae* family, and an enveloped virus with a positive-sense ssRNA genome of 9.7 kb. Rubella virus infections *in utero* can lead to deafness, cataracts, heart defects, mental retardation, and liver and spleen damage [27]. Fortunately, there is a vaccine available (MMR – measles, mumps, and rubella). Modern vaccine programs have been successful in nearly eradicating congenital rubella disease; however, prenatal rubella infections are still possible [21]. However, there is no specific treatment for pregnant mothers infected with rubella virus [28]. The only available therapeutic option is non-specific immune globulin; however, this does not ensure complete inhibition of fetal transmission [28].

#### **1.2.1.3 Cytomegalovirus (CMV)**

Human cytomegalovirus (hCMV) is a member of the  $\beta$ -herpesvirus family. CMV is an enveloped virus with a large, dsDNA genome of approximately 240 kb. Furthermore, CMV remains a significant cause of disease in neonate and immunocompromised populations. *In utero* CMV infections are one of the most detrimental prenatal and neonatal pathogens, causing symptoms such liver, lung, and spleen pathologies, jaundice, seizures, and/or IUGR [29]. Permanent and long-term effects of congenital CMV infection include hearing and/or vision loss, small head, mental disabilities, lack of coordination, seizures, and/or death [29]. Unfortunately,

there are currently limited therapeutic strategies aimed at treating CMV infections *in utero* and in affected neonates. In cases of severe CMV infection, antiviral therapy will likely only have a modest effect on improving neonatal outcome [30]. Existing treatment options include using CMV immune globulin in pregnant mothers and the antiviral nucleoside analog ganciclovir in infected neonates [30]. Therefore, investigation into the causes and potential therapeutic approaches is key to preventing CMV-related birth defects and neonatal diseases.

#### **1.2.1.4 Herpes simplex viruses 1 and 2 (HSV-1 and -2)**

Herpes simplex viruses-1 and -2 (HSV-1 and -2) are members of the  $\alpha$ -herpesvirus family, enveloped viruses with linear dsDNA genomes of 152 and 155 kb, respectively. HSV-1 is the causative agent of cold sores, and HSV-2 is associated with genital ulcers. Vertical transmission is relatively low (~5%), and the greatest risk of HSV transmission occurs during vaginal birth [31, 32]. If a mother has an active genital HSV infection the risk of transmission to the fetus during labor is around 80% [31]. HSV infections acquired *in utero* can cause miscarriage but can also be characterized by symptoms such as skin lesions or scarring, eye wounds (chorioretinitis, microphthalmia, cataract), neurologic issues (intracranial calcifications, microcephaly, seizures, encephalomalacia, IUGR, and psychomotor developmental delays, or even stillbirth, *reviewed* [32]. Neonatal HSV infection acquired during vaginal delivery is characterized by: 1) skin, eye, or oral lesions which can progress to encephalitis, 2) HSV encephalitis (that can progress to neurologic morbidity), 3) multi-organ system pathology (including central nervous system, liver, lung, brain, adrenals, skin, eye and/or mouth) with a mortality risk >80% without treatment [32]. The best preventative measure is to establish whether the pregnant mother has, or is at risk for acquiring, HSV. The mother can be treated with antiviral drugs such as acyclovir or valacyclovir during the third trimester can prevent

active HSV infections; however, these therapies are not approved for use during pregnancy [32]. If the mother does have an active HSV infection at the time of birth, neonatal transmission can be reduced by cesarean delivery [32]. However, if fetal transmission has already occurred and the neonate presents with symptoms of HSV infection shortly after birth, treatment with the antiviral agent acyclovir can be used to prevent progression of the disease [32]. Unfortunately, if severe pathologies exist, antiviral therapy may not be enough to guarantee increased survival. Thus, development of improved approaches to both prevention and treatment of neonatal infectious diseases is crucial to reducing incidences of pre-term delivery, birth defects, and death.

### **1.2.2 Coxsackievirus B (CVB)**

Group B coxsackieviruses (CVBs) are non-enveloped, positive-sense single-stranded RNA viruses and enteric members of the family *Picornaviridae*. CVB infections are generally asymptomatic or cause mild flu-like symptoms in most healthy individuals. However, for reasons that are unclear, CVB infections can also result in severe pathologies, such as aseptic meningitis, myocarditis, and pancreatitis [33, 34].

Maternal CVB infection and consequential fetal transmission have been associated with severe pathological outcomes, including miscarriage [35], stillbirth [36], fetal sepsis [37] and death [38, 39], fetal myocarditis [40-42], meningoencephalitis [43], hydrops fetalis [44], congenital skin lesions [45], aseptic meningitis [46], neurodevelopmental delays [47], and the development of type I diabetes [48, 49] and thyroiditis later in life [50]. Currently, testing for enterovirus infections during pregnancy is not routine, and thus there is a lack of data regarding its prevalence. Nonetheless, the consequential detrimental fetal pathologies of undetected and

untreated *in utero* enterovirus infections further demonstrates how critical it is to further our understanding of host-pathogen interactions at the maternal-fetal interface.

## 1.3 VIRUS ENTRY

### 1.3.1 Virus entry mechanisms

Viruses gain entry into host cells through a variety of ways, including classical endocytic routes such as through clathrin- [51] or caveolar-dependent [52], or via macropinocytosis *reviewed* [53]. Additionally, other viruses may internalize via mechanisms that combine aspects of multiple endocytic mechanisms (such as CVB [54, 55]) or that utilize unconventional pathways to gain access to hosts, such as caveolar-independent lipid-raft pathways [56] or clathrin- and lipid-raft-independent routes such as human papillomavirus 16 (HPV-16) [57] (**Figure 1.2**). Moreover, the same virus may exploit diverse mechanisms and activate multiple signaling cascades, depending on cell type (organ of origin, non-polarized v. polarized, undifferentiated v. differentiated, cell line v. primary cell) and the particular subset of proteins and co-factors present within that cell; for further review see [58].

Briefly, clathrin-dependent endocytosis involves the uptake of vesicles coated with clathrin and requires dynamin II and the recruitment of various adaptor complexes such as AP2 (adaptor protein 2) and accessory proteins such as AP180 and epsin [59]. Internalization of clathrin-coated vesicles by this endocytic route may be ligand-dependent or constitutive [60]. Incoming vesicles fuse with early endosomes, wherein cargo is sorted and either recycled to the cell surface or trafficked further along the endosomal pathway to multivesicular bodies or lysosomes [61]. Caveolae are a subdomain of lipid rafts, forming morphologically distinct

invaginations ( $\Omega$  shaped, 50-100 nm) at the plasma membrane, *reviewed* [62, 63]. However, endocytosis of caveolae structures is not constitutive, is triggered by specific ligands, and requires dynamin II [62, 64, 65]. Importantly, caveolae may also serve as scaffolds for the organized assembly of signaling molecules [66]. Lipid rafts are defined as detergent resistant, highly liquid-ordered, hydrophobic plasma membrane microdomains composed primarily of cholesterol and sphingolipids [62]. Non-caveolar lipid rafts are devoid of caveolin-1 and caveolae, and may or may not require dynamin II for internalization. Macropinocytosis is a non-clathrin, non-caveolar, dynamin-independent mechanism that requires actin for the non-specific uptake of fluid and other cargo, *reviewed* [53, 67]. The incoming vesicles termed macropinosomes (0.5-10  $\mu\text{m}$ ) are formed by the closure of actin-dependent membrane ruffles [68, 69].

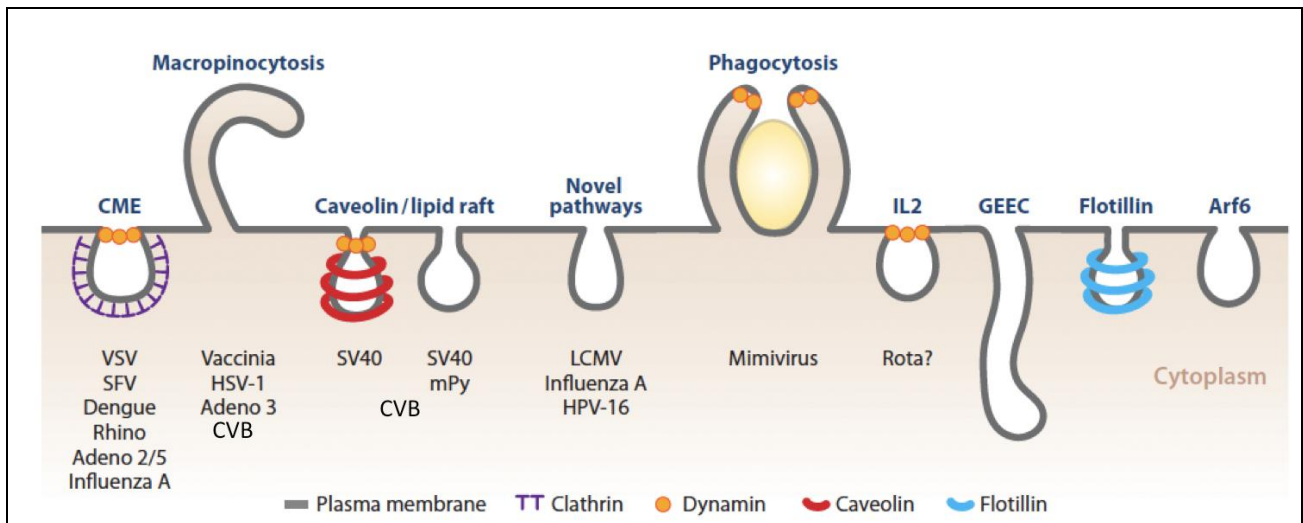


**Figure 1.2. Viruses enter cells through a variety of pathways.** Shown is a schematic of diverse viruses and the endocytic mechanisms utilized to enter host cells, including CME (clathrin-mediated endocytosis), macropinocytosis, caveolin and/or lipid-rafts, and other novel pathways. The beads at the neck of the endocytic vesicle indicate mechanisms that require the GTPase dynamin II. Additional pathways that viruses use may include phagocytosis or the IL-2-dependent route. Mechanisms that may be used but have not yet been identified to be required by any viruses, such as GEEC (GPI-enriched endocytic compartments), flotillin, and Arf6 (ADP-ribosylation factor 6). Figure modified from Mercer J *et al.* 2010, full reference in text.

### **1.3.2 VSV entry**

Vesicular stomatitis virus (VSV) is an enveloped member of the *Rhabdoviridae* family, and a negative-sense ssRNA virus with a genome of 11 kb, *reviewed* [70, 71]. VSV can infect both insects and mammals (typically cattle), but rarely humans [70]. VSV was selected in these studies because it is an excellent model virus with a well characterized endocytic mechanism and is particularly sensitive to host antiviral strategies such as a type I interferon (IFN) [72] and autophagy [73-75]. To enter cells, VSV usurps the host clathrin machinery, as demonstrated by prior studies utilizing siRNAs towards clathrin heavy chain, dominant-negative mutants of Eps15 (or epidermal growth factor substrate 15, a clathrin adaptor protein), and chlorpromazine, a pharmacological inhibitor of clathrin [51]. Later reports confirmed that VSV internalization occurred very quickly (within three minutes) and was dependent on the GTPase dynamin II (dyn II), but not clathrin adaptor complex AP2 [76]. VSV virions were present within early endosomes within one to two minutes following entry [76]. The low pH environment of the early endosome was required for the induction of conformational changes within VSVG (VSV glycoprotein), resulting in virion acidification for subsequent uncoating [71]. These studies overturned previous models in which decreased pH (6.2) was thought to contribute to alterations in VSVG, leading to fusion between the VSV viral envelope and the early endosome membrane [77, 78].

### **1.3.3 CVB entry into polarized epithelia**

Enteroviruses (including CVB) are spread primarily via the fecal-oral route whereby, an individual is exposed upon consuming fecally contaminated food. The virus must first enter the

polarized epithelial cells of the gastrointestinal (GI) tract to initiate host entry and infection [79]. Despite the obvious barrier that a polarized epithelial monolayer poses, pathogens, such as CVB, have evolved to exploit protective cellular mechanisms, such as components of junctional complexes, endocytic pathways, and signaling networks, to enter hosts.

There are six serotypes of CVB (CVB1-6); all of which require the coxsackievirus and adenovirus receptor (CAR), a tight junction (TJ)-localized type I transmembrane protein, to enter and infect cells [80-82]. A subset of CVB serotypes (CVB1, CVB3-RD, CVB5) also utilize decay-accelerating factor (DAF or CD55) as a secondary receptor for virus attachment and entry [54, 83-86]. DAF, a GPI-anchored apical surface membrane protein, localizes to the apical surface of polarized intestinal epithelial cells [54, 85]. We previously demonstrated that CVB3-RD exploits a unique mechanism of entry in polarized intestinal epithelial cells [54, 55] and further *reviewed* [58]. CVB initially utilizes DAF as an attachment factor at the apical surface, and following binding, CVB induces DAF clustering [54]. CVB and DAF complexes traffic to the TJ via DAF-mediated Abl signaling and Rac-dependent actin reorganization; whereby CVB subsequently interacts with CAR for events required for entry [54, 87]. Earlier work has demonstrated that CVB enters by a lipid-raft dependent, dynamin-independent mechanism that combines features of caveolar endocytosis and macropinocytosis in polarized intestinal epithelial cells and requires Src kinases Abl and Fyn [54, 55]. Activation of Fyn kinase is required for caveolin phosphorylation prior to CVB internalization at the TJ [54]. Endocytosis of TJ protein occludin, along with small GTPases Rab34 and Rab5 were found to be required for CVB entry. In contrast, CVB entry into polarized HBMEC (human brain microvascular endothelial cells) requires caveolar endocytosis, dynamin II, and unidentified Src family tyrosine kinases (SFKs) [88]. However, in non-polarized HeLa cells, dynamin II and lipid rafts were necessary for CVB

entry, while clathrin and caveolin-1 were not [89]. Additionally, unknown tyrosine kinases were necessary for early events in CVB infection but were not required for entry [89]. Thus, it has become apparent that CVB entry varies across non-polarized (HeLa) and various polarized epithelial and endothelial cell types (Caco-2, HBMEC) [54, 55, 88, 89].

## 1.4 EXOSOMES

Exosomes are extracellular vesicles approximately 30-100 nm in size released by most cell types, and have a characteristic density ranging from 1.13-1.19 g/mL, *reviewed* [90-92]. Exosomal vesicles have been isolated *in vivo* from various sources, including urine, blood plasma, amniotic fluid, breast milk, synovial fluid, epididymal fluid, ascites pleural effusions, and bronchoalveolar lavage fluid [92]. Exosomes have recently gained much interest in the literature mainly due to their roles as cargo nanovesicles [93, 94] and as modulators of intercellular communication [92, 94-96]. Various components have been identified to be exosomal cargo, including protein, mRNAs, and small RNAs such as miRNAs [94, 97]. The exosomal membrane is composed of cholesterol, sphingomyelin- and ceramide-rich lipid rafts [98]. These small vesicles are sensitive to disruption by various methods including repeated freeze/thaw and sonication [99, 100].

Not only do mammalian cells utilize exosomes for mediating intercellular communication, but viruses have usurped these mechanisms as well [101-103]. For example, components of human tumor virus EBV (Epstein Barr virus) was recently found within exosomes released from nasopharyngeal carcinomas (NPC) [102]. These exosomes contained latent EBV, EBV LMP1 (latent membrane protein 1), viral miRNAs, and signal transduction molecules [102]. More recently, Dreux *et al.* published that exosomes containing hepatitis C

virus (HCV) particles from infected, permissive Huh-7.5 cells were sufficient to activate type I IFN signaling in non-permissive pDCs (plasmacytoid dendritic cells) [103]. Moreover, the exosomes containing the viral RNA were transferred between cells in a process requiring Annexin A2 (ANXA2), an RNA-binding protein necessary for multivesicular body (MVB) biogenesis, and various ESCRT proteins (CHMP4B, Atg4B, and TSG101) – factors necessary for exosome biogenesis [103]. Taken together, these studies indicate that both cells and pathogens utilize exosomes to facilitate critical roles in shaping the gene expression and signaling responses of their target recipient cells.

The mechanisms of exosome biogenesis have been controversial and not well defined in the literature to date. One model of exosome biogenesis proposes that exosomes are generated within late endosomes, or MVBs, and are subsequently released into the extracellular space via fusion with the plasma membrane of the exosome-producing cell (**Figure 1.3**). Within the MVBs, ILVs (or intraluminal vesicles) are formed from the inward budding of the MVB membrane, giving rise to the subsequently released vesicles known as exosomes [92, 97]. However, Booth *et al.* argued that Jurkat T cells produce exosomes from outward budding at discrete regions of the plasma membrane; these vesicles were also positive for exosomal markers such as the lipid N-Rh-PE and tetraspannins CD63 and CD81 [104]. Similarly, the role of the ESCRT (endosomal sorting complex required for transport) machinery has been contentious with various groups debating its involvement [105-107]; while others cite no evidence for its connection [95, 104, 108]. Furthermore, exosomes are characterized by a particular subset of markers, including those that are commonly present in MVBs such as TSG101, Alix, and Gag, among others [109], supporting that exosomes biogenesis conceivably is regulated through the

MVB pathway. Additionally, exosome protein composition may be (and likely is) dependent on the cell type from which the exosome is derived.

Likewise, the mechanisms by which exosomes are internalized into their target cells, and the factors responsible for mediating the intended recipient cell selection are somewhat controversial. Feng *et al.* recently published that the internalization of exosomes occurs via phosphoinositide 3-kinase (PI3K)-dependent and dynamin II-dependent phagocytosis [110]. However, another group – Parolini *et al.* described that exosome uptake was dependent on a low-pH membrane fusion event between the exosome and the recipient cell [111]. It is possible that these exosome internalization events are cell-type dependent and contingent on whether the exosomes in question are targeted for a particular recipient cell type. For example, *does that cell have the correct docking factors or is the uptake process somewhat non-specific if the particular recipient cell is **not** the intended target?* There is a void in the literature regarding exosomal target cell selection, and identification of both the cell and exosomal factors involved in exosome uptake. New evidence has suggested that the specific tetraspannin protein components anchored into the exosomal membrane may be key determinants in selecting which cells are targeted for internalizing a particular subset of exosomes [112]. Recently, exosomes have become the focus of pharmaceutical interest; these small vesicles have therapeutic promise as potential vaccine candidates, tumor immunotherapy modulators, and biomarkers (for diagnostic and prognostic purposes) [109].

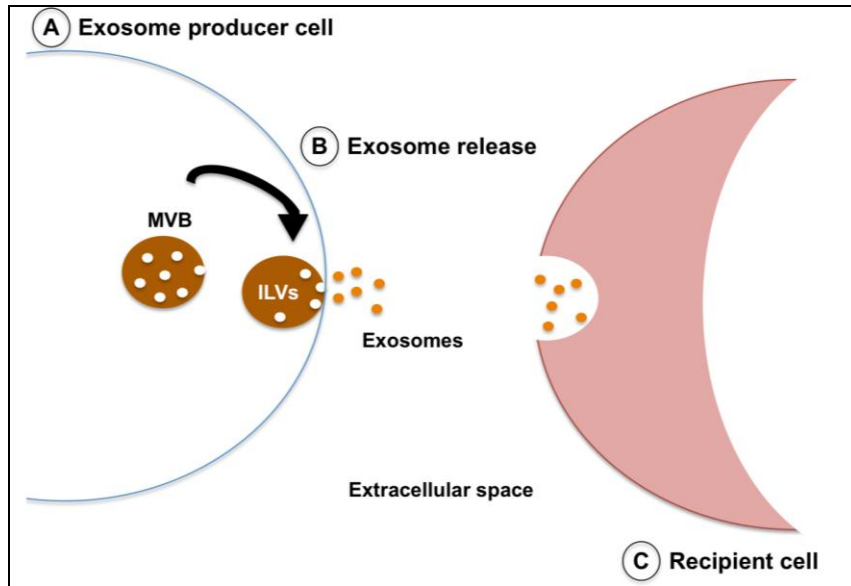


**Figure 1.3. Exosome release and uptake.** (A) Shown is a schematic of exosome biogenesis through fusion of MVBs (containing ILVs) with the plasma membrane of the producer cell. (B) Exosomes are released into the extracellular space, and (C) are taken up by recipient cells by endocytic mechanisms that are currently under debate.

Intriguingly, circulating exosomes are a normal feature of human pregnancy [98]. Placental exosomes have been isolated from the blood of pregnant women [113, 114], supernatants of cultured trophoblast cells [115], and trophoblast cell lines [116]. The syncytiotrophoblast cells are believed to release the exosomes, which may mediate “fetal-maternal cross-talk for adaptation of the maternal organism to the ongoing pregnancy,” *reviewed* [98]. Thus far, these and/or additional roles for placental exosomes have not been further defined or experimentally established in the literature.

## 1.5 MICRORNAS (MIRNAS)

### 1.5.1 Overview and biogenesis

Mature microRNAs (miRNAs) are small (19-25 nt), non-coding ssRNAs that typically downregulate select messenger RNAs (mRNAs) post-transcriptionally *reviewed* [117] and described further below. However, recent literature has shown that miRNAs can also function to post-transcriptionally stabilize or upregulate mRNA expression [118, 119]. One mechanism by which stabilization of the target mRNA occurs is by miRNA binding to the 3'UTR (untranslated region) of the target mRNA to prevent RBPs (RNA binding proteins) from mediating RNA degradation [119].

RNA polymerase II (Pol II) directs the transcription of most primary miRNA (pri-miRNA) genes [120, 121]; whereas RNA Pol III mediates the transcription of other pri-miRNAs [117, 122]. The resulting pri-miRNA transcripts have structures similar to that of mRNA with 5' methylguanosine caps (5' m<sup>7</sup>GpppN) and 3' polyA tails [121] and *reviewed* [123]. As shown in **Figure 1.4**, pri-miRNAs are generated into precursor miRNAs (pre-miRNAs) by a 'microprocessor' complex, consisting of RNase III enzyme Drosha and DGCR8 (DiGeorge syndrome critical region gene 8) in the canonical pathway of miRNA biogenesis [117]. Pre-miRNAs (60-80 nt), characterized by their distinct hairpin secondary structure, are then exported from the nucleus to the cytoplasm. This process is dependent on both RAS-related nuclear protein-guanosine triphosphate (RAN-GTP) and Exportin-5. Mature miRNAs are produced by RNase III Dicer and TRBP [HIV trans-activating response (TAR) RNA binding protein]-dependent cleavage of the hairpin stem to generate a duplex miRNA/miRNA\* [124]. The duplex undergoes strand separation, and one strand of the miRNA is selectively loaded into the

miRNA-induced silencing complex (miRISC), which consists of a core of Argonaute2 (Ago2) and GW182 (glycine-tryptophan repeat containing protein of 182 kDa), Dicer, and TRBP [123, 125]. To note, there are at least four Argonaute proteins in the mammalian system (Ago1-2), but only Ago2 is associated with miRISC mRNA degradation [123, 126]. However, the precise mechanism governing miRISC strand selection is currently under debate [127]. Although recent evidence has suggested that there is a structural bias for strand selection based on the stem loop position within each strand of the duplex miRNA, which could allow for more efficient miRISC assembly [128]. Khvorova *et al.* have described that strand selection and subsequent miRISC loading is dependent on the thermodynamic stability of the base pairs of each duplex strand at its 5' end; the strand with the less stable base pair is subsequently selected and loaded onto the miRISC for mRNA targeting [129] and *reviewed* [130].

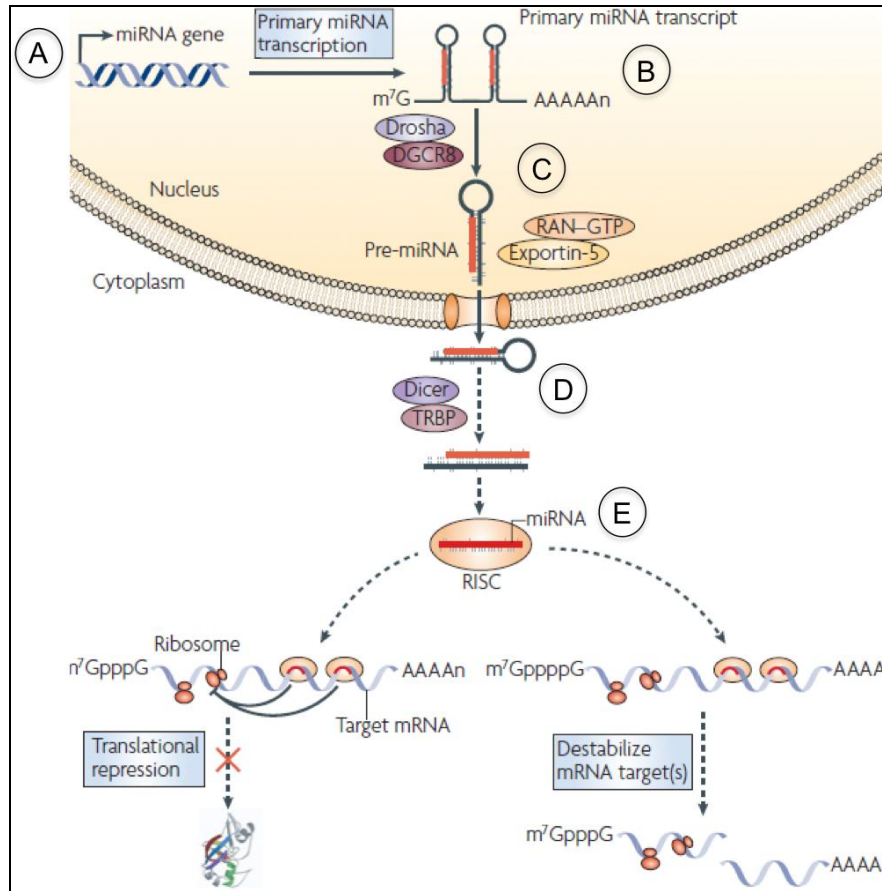


**Figure 1.4. Processing mature miRNAs through the miRISC.** Shown is an overview of miRNA biogenesis. (A) Either RNA Pol II or III directs pri-miRNA transcription. (B) Pri-miRNA transcripts are structurally similar to mRNAs with 5' methylguanosine caps (5' m<sup>7</sup>GpppN) and 3' polyA tails. (C) Pri-miRNAs are generated into pre-miRNAs by a 'microprocessor' complex, consisting of RNase III enzyme Drosha and DGCR8 (DiGeorge syndrome critical region gene 8). Pre-miRNAs have distinct hairpin secondary structures, and are exported from the nucleus to the cytoplasm (a RAN-GTP- and Exportin-5-dependent process). (D) Mature miRNAs are produced by RNase III Dicer and TRBP-dependent cleavage of the hairpin stem to produce a duplex miRNA/miRNA\*. (E) The duplex undergoes strand separation, and one miRNA strand is selectively loaded onto the miRISC. Figure modified from Lodish HF *et al.* 2008, full reference in text.

The mature miRNA guides the RISC to its target mRNA, and depending on the degree of complementarity between the miRNA and 3'UTR mRNA target, the miRNA either: represses translation or induces mRNA degradation [117]. The seed sequence (nt 2-7 or 2-8) located in the 5' conserved region of the miRNA, largely directs which genes will be targeted. A single miRNA can potentially interact with (and target) hundreds of mRNAs to regulate global gene expression [131-133]. Prediction software tools such as TargetScan (<http://www.targetscan.org>)

use miRNA seed sequence predictions to calculate expected mRNA targets. In addition to the transfer of miRNAs via exosomes, it has also been reported that miRNAs associate in non-vesicle form *in vivo*, bound to components of the RISC complex such as Ago2 [134].

### 1.5.2 Antiviral miRNAs

Viruses have evolved extraordinary mechanisms to subvert and manipulate the host innate immune response. More recently, miRNAs have emerged as strategic participants in virus-host interactions. Host miRNAs can influence either antiviral or proviral responses [135]. Similarly, certain viruses, including members of the herpesvirus and polyomavirus families, encode for miRNAs to regulate the expression of host and/or viral genes during infection [136]. Thus, an increased awareness of miRNA functioning during infection will provide insight into the multifaceted interplay between viral and host defense mechanisms.

Recently, miR-199a-3p, a cellular miRNA, was identified by Santhakumar *et al.* to confer antiviral effects against a panel of  $\alpha$ ,  $\beta$ , and  $\gamma$  Herpesviruses [including HSV-1, murine cytomegalovirus (MCMV), and murine herpesvirus-68 (MHV-68)] in a combined miRNA mimic-inhibitor genome-wide screen [135]. Following the screen, four miRNAs (including miR199a-3p) were found to have antiviral effects as indicated by low levels of viral replication with the miRNA mimic, and by enhanced replication with an antagonist (anti-miRNA) [135]. To further assess the effects of the identified antiviral miRNAs, each miRNA was overexpressed in NIH 3T3 cells [135]. Cells were then infected with the herpesvirus panel as described or Semliki Forest virus (SFV), a positive-sense ssRNA virus. SFV was used for comparison because it increased the diversity of the viruses tested, and the antiviral effects of miR-199a-3p were further validated through these studies. The authors concluded that the observed phenotype of miR-

199a-3p was most likely due to the targeting of host genes, rather than direct targeting of virus-specific sequences. Direct targeting of viral mRNA was less probable due to the high sequence diversity of each viral genome tested. Analysis of predicted miR-199a-3p targets revealed pathways that may be important for suppressing viral infection, including PI3K/Akt, ERK/MAPK, and oxidative stress signaling [135]. However, the validation of these targets, and the mechanism(s) by which miR-199a-3p mediates antiviral signaling is currently unknown. These findings were significant because although antiviral miRNAs have been previously described, a genome-wide screen for broadly antiviral cellular miRNAs had never before been reported.

Interestingly, work by Pedersen *et al.* has demonstrated that IFN- $\beta$  also impacts host miRNA expression during virus infection [137]. However, the eight host miRNAs that were identified to be upregulated by IFN- $\beta$  had sequence-predicted targets within the HCV genome to directly target the virus for RNA degradation, reducing viral replication [137]. More recently, Witwer *et al.* showed that, following HIV infection, select miRNAs (miR-26a, -34a, -145, and let-7b) inhibited IFN- $\beta$  secretion [138]. This further demonstrated that viruses subvert host miRNA networks to promote their infectious life cycles. Taken together, these data point towards a role for viruses in manipulating host miRNAs, to activate or suppress cellular pathways, and/or to potentially target viral genomes directly to attenuate virus infection. Clearly, elucidation of virus-host miRNA interactions are necessary to help us to better understand the complex interplay between invading pathogens and host immune defense systems.

### **1.5.3 Chromosome 19 miRNA cluster (C19MC)**

The human chromosome 19 miRNA cluster (C19MC) is the largest known human miRNA

cluster, comprising 46 miRNAs that are highly expressed in the human placenta and trophoblastic exosomes [113, 115, 116, 139-142]. C19MC-associated miRNAs are almost exclusively expressed in the placenta with both inheritance and expression solely derived from the paternally expressed allele [140]. Although less common, C19MC miRNAs have been identified to be expressed in very rare, aggressive brain tumors and liver cancers [143-145] and further *reviewed* [146]. The C19MC is expressed on region 19q13.41 of chromosome 19, spans over 100 kb, and is primate-specific [147] and *reviewed* [141]. C19MC miRNAs are transcribed by RNA Pol II, and are thought to be transcribed as a long non-coding transcript from which mature miRNAs are generated [141] and *reviewed* [148]. Furthermore, using miRNA profiling, recent work has detected the relatively high expression of the majority of C19MC-associated mature miRNAs in PHT-derived exosomes, and found a strong correlation between C19MC miRNA levels in PHT cells and PHT-derived exosomes [115, 139]. Interestingly, C19MC miRNAs have been detected in the plasma of pregnant women [115, 116, 139], and blood plasma levels of C19MC miRNAs “decrease dramatically after delivery” [116]. Furthermore, Luo *et al.* reported that circulating C19MC miRNAs were lower during the first-trimester of pregnancy compared to full-term [116]. In correlation to this, clinical reports describe pathogen infection occurring during the first trimester as being associated with more severe and dangerous pathological outcomes than infection during later stages of pregnancy [149, 150]. Luo *et al.* also described the presence of C19MC miRNAs in exosomes from cultured trophoblast cells [116]. Thus far, the functions of the C19MC associated miRNAs during pregnancy have not yet been described in the literature.

## 1.6 AUTOPHAGY

### 1.6.1 Introduction to autophagy

Autophagy is an evolutionarily conserved process of cellular “self-eating” that degrades aged organelles, protein aggregates, and ubiquitylated cargo by the formation of autophagosomes, double-membrane vesicles, for fusion with lysosomes *reviewed* [151]. Under resting conditions, basal levels of autophagy are very low [151]. However, multiple forms of stimuli and cell stress can induce autophagy (**Figure 1.5**), including cellular development and differentiation, nutrient deprivation, oxidative and endoplasmic reticulum (ER) stress, accumulation of aged organelles, hypoxia, and pathogen infection [151-154]. Under normal cellular conditions, various molecules function as inhibitors of autophagy, such as the class I PI3K/Akt signaling pathway, nutrient abundance, and cytoplasmic p53 [155, 156]. Downstream of PI3K/Akt, mTOR (mammalian target of rapamycin) is a potent negative regulator of autophagy [157]. mTOR forms a complex with ULK1, Atg13, and FIP200 – known as mTORC1 (mammalian target of rapamycin complex-1) – to inhibit autophagy [155]. ULK1 and Atg13 are hyperphosphorylated by mTOR, thus maintaining repression of the autophagy pathway [155].

During autophagy, structures known as autophagosomes are formed, which are characterized by double- or multi- membranes (approximately 300-900 nm) [158]. There are four distinct phases of ATG (autophagy-related gene) activity throughout the progression of autophagic flux, *reviewed* [159]. The first stage is known as the initiation phase (or the nucleation step) of autophagosome formation and involves the mTORC1, the ULK1/2, and the Class III PI3K complexes, *reviewed* [156, 159]. However, the source(s) of the autophagosome membrane has been under constant debate with various groups citing mitochondrial origin [160],

endoplasmic reticulum, plasma membrane, and/or Golgi, *reviewed* [161]. In the canonical pathway of autophagy (under conditions such as nutrient deprivation), mTOR association with ULK1-Atg13-Fip200 is limited and ULK1 and Atg13 remain hypophosphorylated, allowing for membrane expansion and the generation of the isolation membrane, or phagophore [159, 161]. Along different arms of the pathway, eukaryotic initiation factor-2 $\alpha$  (eIF2 $\alpha$ ), c-jun-N-terminal kinase-1 (JNK1), various GTPases, and intracellular calcium act upstream to induce autophagy [159]. This activates the Class III PI3K complex, composed of vacuolar protein-sorting-34 (VPS34), VPS15, Beclin-1, ATG14, AMBRA1, UVRAG (ultraviolet radiation resistance-associated gene protein), and Rubicon [156, 159]. The complex generates phosphatidylinositol-3-phosphate (PI3P), possibly on the ER membrane [156, 159]. Rubicon negatively regulates the fusion of autophagosomes and lysosomes by interacting with UVRAG [156]. Its direct binding with BCL2 and BCL-X<sub>L</sub> negatively regulates beclin-1. At the ER, the factor DFCP1 prepares for the expansion of the phagophore into a structure known as the omegasome [156, 161]. Additional proteins such as ATG9, WIPI1-4, and VMP1 are present on the preliminary autophagic membrane [156].

In the second stage of autophagy (also known as the elongation step) vesicle extension and completion occurs through two separate, conserved ubiquitin-like conjugation systems [156, 159]. The first system requires the ATG12-conjugation system involving a heterotrimeric complex ATG16L1-ATG12-ATG5, which is localized to the isolation membrane and crucial for LC3-PE (phosphatidylethanolamine) conjugation [156, 159]. The ATG12-complex is required for proper elongation [156]. ATG7, an E1-like enzyme, and ATG10, an E2-like enzyme, promote the association of the heterotrimeric ATG12-complex on the autophagosome membrane [156, 159].

The second system – the LC3-conjugation system – is indispensable for membrane expansion and closure [156]. The LC3-conjugation system is comprised of LC3 (microtubule-associated protein light chain-3) and additional autophagy related factors – ATG7, ATG4A-D, and ATG3 [156, 159]. LC3 is present at both the inner and outer autophagosome membrane with adapter functions for other substrates (including p62, NBR1, and NDP52) at the inner membrane [156]. LC3-I (18-kDa molecular weight protein) is converted to its secondary form LC3-II (16-kDa molecular weight protein) by ATG7- and ATG4-mediated cleavage, followed by ATG3-mediated PE (phosphatidylethanolamine)-lipidation at a conserved glycine residue at the LC3 C-terminus [159]. The completion of the autophagosome is followed by an ATG9 and ATG19 concerted removal of the ATG12 complex and outer membrane-associated LC3. The third phase consists of autophagosome docking and fusion with lysosomes, to form autolysosomes. The final step is the degradation of the autolysosome vesicle and its cargo, which is completed by lysosomal cathepsins B, D, and L. As autophagy is an evolutionarily conserved cell survival and recycling pathway, the residual by-products of lysosomal degradation – such as amino acids and lipids – are exported to the cytoplasm for the anabolic generation of new macromolecules [162, 163]. More recently, alternatives of the canonical pathway have been identified (e.g. independent of ‘required’ factors [164, 165]) and variations (such as mitophagy, lipophagy, virophagy, pexophagy, etc.) further complicate an already convoluted and inherently complex primordial biological mechanism.

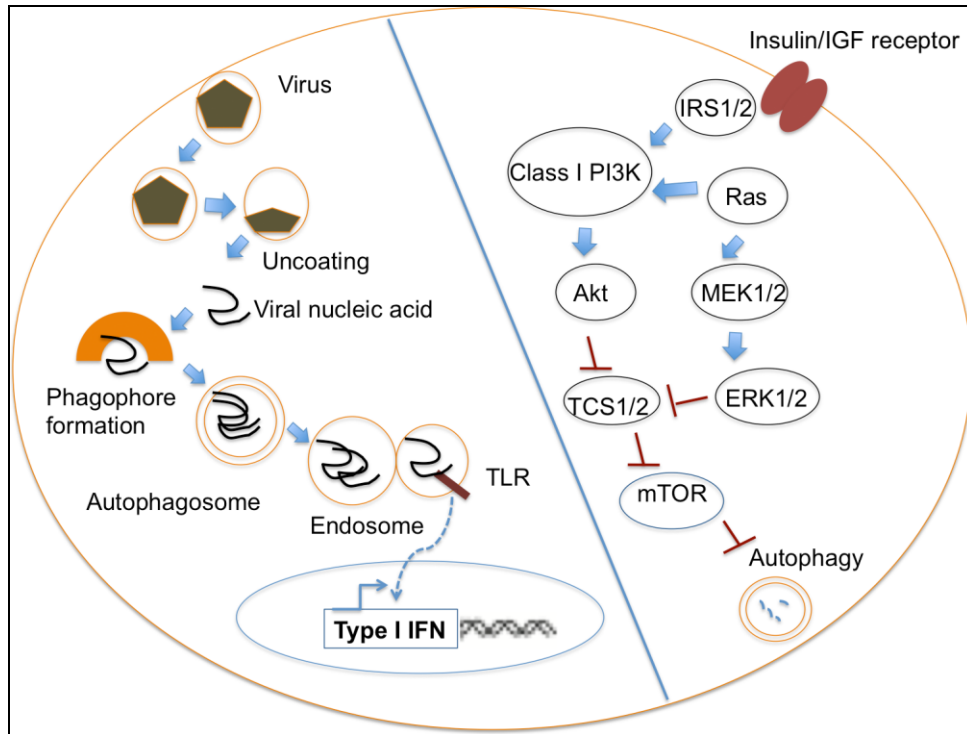


**Figure 1.5. Multiple pathways to autophagy.** Shown is a schematic demonstrating two of the myriad of pathways leading to the autophagic response. (Left) Autophagy as an antiviral innate immune response downstream of TLR signaling following the recognition of viral nucleic acids. (Right) Autophagy is induced in response to cellular nutrient deprivation.

## 1.6.2 Autophagy as an antiviral host defense mechanism

The autophagy pathway also participates in antiviral host defense by: targeting cytoplasmic viruses for lysosomal degradation (known as xenophagy or virophagy) [166], limiting viral replication [74, 167], and/or interacting with innate immune components such as toll-like receptors (TLRs) and associated adaptors [168, 169]. Previous work has indicated that autophagy may be required for the activation of antiviral IFN-mediated signaling by certain viruses [73, 170, 171]. Autophagosome-mediated sequestration of viral antigens was required for recognition and innate immune signaling by endosomal toll-like receptor-7 (TLR7) [73, 171].

Several viruses have been identified to be susceptible to host-induced antiviral autophagy including Sindbis virus [167], tobacco mosaic virus [172], and VSV [73-75]. Other viruses have

evolved mechanisms to overcome autophagy such as HSV-1 [173-175], human cytomegalovirus (hCMV) [176, 177], Kaposi's sarcoma herpesvirus (KSHV), and human immunodeficiency virus (HIV), *reviewed* [159]. However, certain viruses usurp the host autophagy machinery to promote and enhance their replication such as HCV [178], the picornaviruses poliovirus (PV) [179] and CVB [180, 181], VZV, EBV, (Epstein-Barr virus), hepatitis B virus (HBV), HPV-16, parvovirus B19, simian virus-40 (SV40), influenza A virus, and dengue virus *reviewed* [159].

### **1.6.3 Autophagy as a post-birth survival mechanism**

Autophagy has been recognized as a critical post-birth survival mechanism during the early neonatal starvation period [154, 182-184]. This is especially important in the time immediately following birth when the supply of nutrients, which had been driven by the placenta, is no longer available [154, 182]. Mouse pups deficient in an essential autophagy factor *Atg5* (and thus could not undergo autophagy) died within one day post-delivery compared to wild-type littermates [182]. Numerous studies have indicated that loss of vital pro-autophagy genes including *Atg3*, *Atg7*, *Atg9*, *Atg16L1*, *Beclin-1*, and *FIP-200* lead to early embryonic lethality, *reviewed* [154]. Autophagy is essential for maintaining survival immediately following birth, prior to the availability of mother's milk for neonatal nourishment.

## **1.7 CLASSICAL ANTIVIRAL TYPE I INTERFERON (IFN) SIGNALING**

Interferons (IFNs) are key regulators of host antiviral innate and adaptive immune responses [185]. Type I IFNs include IFN- $\alpha$  (of which there are 13 subtypes in humans) and IFN- $\beta$  (one

gene in humans), *reviewed* [186]. Following microbial challenge, pathogen-associated molecular patterns (PAMPs) are recognized by pattern-recognition receptors (PRRs) of the innate immune system, such as TLRs, retinoic-acid-inducible gene I (RIG-I)-like helicase (RLH) family members including RIG-I and MDA5 (melanoma differentiation associated gene 5), or DNA-dependent activator of IFN-regulatory factors (DAI), *reviewed* [186]. For specific viral PAMPs recognized by various PRRs, see **Table 1.2**. PRR recognition of PAMPs leads to downstream activation of transcription factors, such as NF- $\kappa$ B (nuclear factor- $\kappa$ B) and IRFs (IFN regulatory factors) for the downstream activation of type I IFNs and select pro-inflammatory cytokines [186]. TLRs initiate downstream host defense signaling cascades through the recruitment of adaptors (such as MyD88, Toll/IL-1R (TIR) homology domain-associated protein (TIRAP)/MyD88-adaptor-like (MAL), TIR-domain-containing adaptor protein-inducing IFN- $\beta$  (TRIF)/TIR-domain-containing-molecule 1 (TICAM1), and TRIF-related adaptor molecule (TRAM), *reviewed* [187]. Certain viral TLRs, including TLR3, 7, 8, and 9 localize to endosomes; others, such as TLR2 and 4 localize to the cell membrane (**Table 1.2**). Viral PAMP stimulation of TLRs (and other PRRs) triggers transcription and extracellular secretion of type I IFN.

**Table 1.2. Pattern recognition receptors that detect viral components.**

PPR	PAMPs	Localization
TLR2	Viral envelope and structural proteins	Transmembrane
TLR3	dsRNA	Endosomal
TLR4	Viral envelope glycoproteins	Transmembrane
TLR7	ssRNA	Endosomal
TLR8	ssRNA	Endosomal and ER
TLR9	DNA CpG motifs	Endosomal
RLH (RIG-I, MDA5)	dsRNA, 5'-triphosphate of ssRNA	Cytosolic
DAI	dsDNA	Cytosolic

Both IFN- $\alpha$  and IFN- $\beta$  exert their downstream effects by binding to type I IFN- $\alpha/\beta$  receptors (IFNAR1/2) located at the cell membrane [188]. Activation of IFNAR1/2 results in downstream signaling via the JAK-STAT signaling pathway. JAKs, or Janus kinases, are a receptor tyrosine kinase family including JAK1-3 and TYK2, whose self-phosphorylation serves as a docking site for the recruitment of STATs (signal transduction and activators of transcription) [186]. Following recruitment, STATs are phosphorylated, and then dissociate from their receptors to form hetero- or homo-dimers. STAT dimers migrate to the nucleus to bind promoter cis-elements containing ISREs (IFN-stimulated response elements) to potentially induce the transcription of hundreds of antiviral IFN-stimulated genes (ISGs) [185, 186]. ISGs, such as RNA-dependent protein kinase (PKR), oligo-adenylate synthetase (OAS), myxovirus-resistance protein (Mx) GTPase, and ribonuclease L (RNase L) exert a variety of antiviral

effects, including degradation of viral nucleic acids, inhibition of viral replication and gene translation to suppress infection [189].

## 1.8 GOALS OF THIS DISSERTATION

At the present time, our current knowledge regarding virus-host interactions at the maternal-fetal interface during pregnancy is limited. The damaging fetal pathologies resulting from prenatal infections are clear, including but are not limited to: miscarriage, *in utero* fetal disease (sepsis, myocarditis, meningoencephalitis, aseptic meningitis, hydrops fetalis), stillbirth, pre-term labor, and neonatal pathologies (deafness, blindness, mental retardation, seizures, neurodevelopmental delays, and congenital lesions), and the development of childhood disease (type I diabetes and thyroiditis). Existing strategies to protect against, or to treat, *in utero* pathogen infections during pregnancy are limited.

Elucidation of the endocytic pathways and host signaling events associated with virus entry and trophoblast-mediated host defense are key factors for investigating and modeling pathogen transmission and infection during pregnancy. Presently, the endocytic and signaling mechanisms utilized by viruses to enter and infect placental trophoblasts are unknown. Similarly, the defense mechanisms (used by trophoblasts to protect the developing embryo from pathogen invasion and infection) are poorly understood. These studies also have the therapeutic potential for preventing prenatal infections, pre-term labor, and birth defects. Specific targeting of molecular mediators of virus infection in the placenta is critical for reducing the incidences of prenatal infections and their resulting pathologies *in utero*.

In the first chapter of these studies, our initial goal was to investigate the susceptibility of *in vitro* cultures of primary human trophoblast (PHT) cells (isolated from normal term placentas) to virus infection. Surprisingly, we observed that PHTs were highly resistant to infection by a panel of disparate viruses (CVB, PV, VSV, VV, CMV, HSV-1). Furthermore, we uncovered the remarkable finding that conditioned medium harvested from PHTs is sufficient to confer viral resistance to recipient cells. Our second aim was to determine the component found within PHT conditioned medium that was responsible for conferring the viral resistant phenotype to recipient cells. Unexpectedly, we found that PHT-derived exosomes present within the conditioned media were capable of inducing antiviral effects. Our third objective was to determine the component within PHT-derived exosomes that was sufficient for producing the antiviral phenotype in recipient cells. Interestingly, we identified three antiviral members (miR-512-3p, miR-516b-5p, miR-517-3p) of the chromosome 19 microRNA (miRNA) cluster (C19MC), which are expressed almost exclusively in the placenta and trophoblastic exosomes [113, 115, 139, 140]. Our fourth goal was to elucidate a possible mechanism by which the placental exosomes exerted their antiviral effects. We found that autophagy was induced by PHT conditioned medium, PHT-derived exosomes, and by the identified antiviral C19MC miRNAs, and was sufficient to function in an antiviral capacity.

The first aim of the second chapter of this dissertation was to investigate the endocytic mechanism by which Coxsackievirus B (CVB), a virus known to cause prenatal and neonatal pathologies, enters trophoblast cells. We discovered that CVB hijacks a non-clathrin, non-caveolar, lipid-raft dependent but dynamin II-independent pathway to enter and infect trophoblasts. Our second objective was to determine host signaling pathways required for CVB entry into trophoblasts. We found that CVB requires Src family tyrosine kinases to enter and

infect trophoblast cells. Our final goal was to compare CVB entry in immortalized BeWo and primary trophoblasts. We found that the entry kinetics and the requirement for lipid rafts were strikingly similar for CVB entry into either immortalized or primary trophoblasts. Taken together, this work provides valuable insight into critical interactions between viruses and trophoblasts at the maternal-fetal interface.

## **2.0 PLACENTAL EXOSOMES CONFER VIRAL RESISTANCE**

### **2.1 INTRODUCTION**

Strategies to reduce fetal infection are essential during pregnancy, where maternal to fetal transmission of microbes can adversely impact the developing embryo, both prenatally and post-birth [47, 190, 191]. Within the human hemochorial placental villi, the multinucleated syncytiotrophoblasts are in direct contact with maternal blood, and constitute a primary epithelial barrier for mediating fetal defense against invading microbes. Currently, there are limited therapeutic options to prevent maternal-fetal transmission of pathogens during pregnancy. Additionally, little is known regarding the mechanisms regulating pathogen entry and invasion, transmission, and host defense at the maternal-fetal interface.

In this chapter, we have examined the susceptibility of primary placental human trophoblast (PHT) cells to infection by diverse viruses, and the mechanisms by which these cells transfer and induce viral resistance to recipient cells. Our studies model viral transmission and infection in the placenta, and have the therapeutic potential for preventing prenatal infections, pre-term labor, and birth defects. These results illuminate pathways employed by human trophoblasts to suppress viral infections systemically by conferring viral resistance to non-placental cells, suggesting a novel mechanism for shielding placental and maternal cells against viral infections during pregnancy.

## 2.2 RESULTS

### 2.2.1 Primary human trophoblasts (PHTs) resist virus infection

To model virus-host interactions at the maternal-fetal interface and to investigate the susceptibility of primary human trophoblasts (PHTs) to virus infection, we infected PHT cells<sup>1</sup> with a panel of viruses including coxsackievirus B3 (CVB), poliovirus (PV), vesicular stomatitis virus (VSV), vaccinia virus (VV), herpes simplex virus-1 (HSV-1), and human cytomegalovirus (CMV) (**Figure 2.1a**). We found that PHT cells were highly resistant to infection by all of the viruses we tested (CVB, PV, VSV, VV, HSV-1, CMV), when compared to non-PHT (e.g. HeLa, human foreskin fibroblast (HFF), U2OS, and/or Vero) cells as assessed by immunofluorescence microscopy, RT-qPCR, or TC-ID50 assays (**Figure 2.1a** and **Figure 2.2a-d**). This lack of viral replication was not due to inefficient viral binding and/or entry as virus was observed to internalize in PHTs but this did not lead to a productive infection (**Figure 2.2e**). In fact, early gene expression of DNA viruses HSV-1 (Tk or thymidine kinase) and VV (rpo35) was barely initiated compared to non-PHT cells, indicating that inhibition of replication occurred very early in the virus life cycle (**Figure 2.2d**). Additionally, we did not detect any defects in common endocytic pathways utilized by viruses for their entry such as clathrin- or caveolar-mediated, by transferrin (Tfn) and cholera toxin B (CTB) uptake assays (**Figure 2.2f**). Transferrin (tfn) uptake is dependent on clathrin- [192], and CTB is dependent upon caveolar or non-caveolar lipid raft-mediated endocytosis [28, 110, 111]. We also obtained no evidence of pre-existing antiviral and inflammatory signaling in PHTs as assessed by IRF3 (IFN regulatory factor 3) or NF- $\kappa$ B subunit p65 translocation (**Figure 2.7a**).

---

<sup>1</sup> PHT cells provided by Dr. Yoel Sadovsky (Magee Womens Research Institute, Pittsburgh, PA).

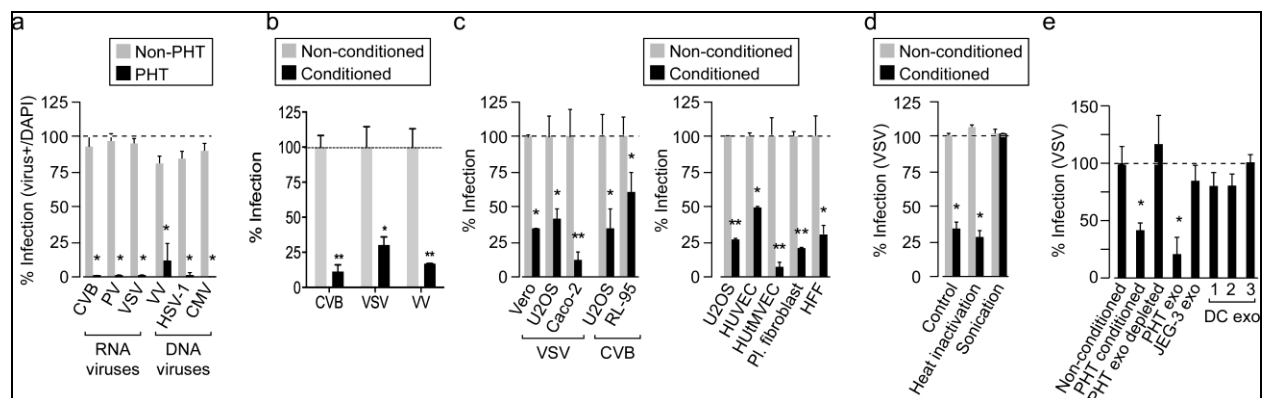


**Figure 2.1. Conditioned PHT medium and exosomes confer viral resistance to recipient cells.** (a) PHT or non-PHT cells were infected with a panel of viruses, including coxsackievirus B (CVB), poliovirus (PV), vesicular stomatitis virus (VSV), vaccinia virus (VV), herpes simplex virus-1 (HSV-1), and cytomegalovirus (CMV). Non-PHT cells were as follows: HeLa (CVB, PV), U2OS (VSV, HSV-1, and VV), and human foreskin fibroblasts (HFF, CMV). Shown are the percent of infected cells (assessed by IF; \* $p < 0.0001$ ). (b) Non-PHT recipient cells were exposed for 24 hr to non-conditioned or conditioned PHT medium, and then infected with CVB, VSV, or VV. Non-PHT cells were as follows: HFF (CVB) and U2OS (VSV, VV). Shown are the percent of infected cells [assessed by IF (CVB, VSV) or RT-qPCR (VV); \* $p < 0.05$ , \*\* $p < 0.005$ ]. (c) Left, cells were exposed to non-conditioned or conditioned PHT medium for 24 h, and then infected with VSV or CVB. Right, primary cells were infected with VSV following exposure to non-conditioned or conditioned PHT medium (\* $p < 0.05$ , \*\* $p < 0.005$ ). (d) Conditioned PHT medium was subjected to heat inactivation or sonication prior to 24 hr exposure to Vero cells, then infected with VSV. Percent infection assessed as in (a); \* $p < 0.0001$ ). (e) U2OS cells were exposed for 24 hr to non-conditioned, conditioned, exosome-depleted conditioned medium, exosomes purified from PHT, JEG-3, or from three preparations of murine dendritic cell (DC), and then infected with VSV. Percent infection assessed as in (a); (\* $p < 0.0005$ ). Each PHT exosome preparation was derived from a different placental preparation.

## 2.2.2 Conditioned PHT medium confers viral resistance

To identify the factor responsible for conferring viral resistance in PHT cells, we tested whether PHT conditioned medium (isolated from naïve PHT cells 48-72 hr post-plating) could transfer viral resistance to non-PHT recipient cells (Figure 2.1b-c, Figure 2.3a,d-e and Figure 2.7e). We found that exposure of diverse non-PHT recipient cells (U2OS, RL-95, Caco-2, Vero, and/or HT1080) for 24 hr prior to infection significantly decreased the replication of CVB, VSV, or VV by immunofluorescence microscopy, RT-qPCR, luciferase, and/or TCID50 assay (Figure 2.1b-c, Figure 2.3a,d-e and Figure 2.7e). We observed antiviral effects with multiple viruses across numerous conditioned medium samples isolated from independent and unrelated PHT preparations (Figure 2.3d-e and Figure 2.7e). Shown are only a sampling as we have tested >20

independent conditioned medium preps from individual PHT cell culture isolations. PHT conditioned medium not only conferred antiviral effects in several immortalized cell types (**Figure 2.1b-c**, left panel, **Figure 2.3a,d-e** and **Figure 2.7e**), but also in physiologically relevant fetal and/or maternal cells human umbilical vein endothelial cells (HUVEC), human uterine microvascular endothelial cells (HUtMVEC), human placental fibroblasts, and HFFs (**Figure 2.1c**, right panel). In contrast, conditioned medium from other cell types such as immortalized trophoblast BeWo cells had no effect on virus infection (**Figure 2.3b**). This effect was not the result of direct neutralization of the virus as incubating virus alone in the presence of conditioned medium and subsequently performing plaque assays had no effect on viral titers (**Figure 2.3c**). Similar to what we had observed in the PHT cells, we found that VV early gene expression was poorly initiated, as measured by rpo35 mRNA expression (a subunit encoding the DNA-directed RNA polymerase expressed within 2 hr of virus entry [193, 194]), suggesting that infection had not initiated in recipient cells cultured in conditioned PHT medium (**Figure 2.3e**). Together, this data indicated that an antiviral factor secreted by PHT cells into the medium was capable of transferring viral resistance to non-placental recipient cells.

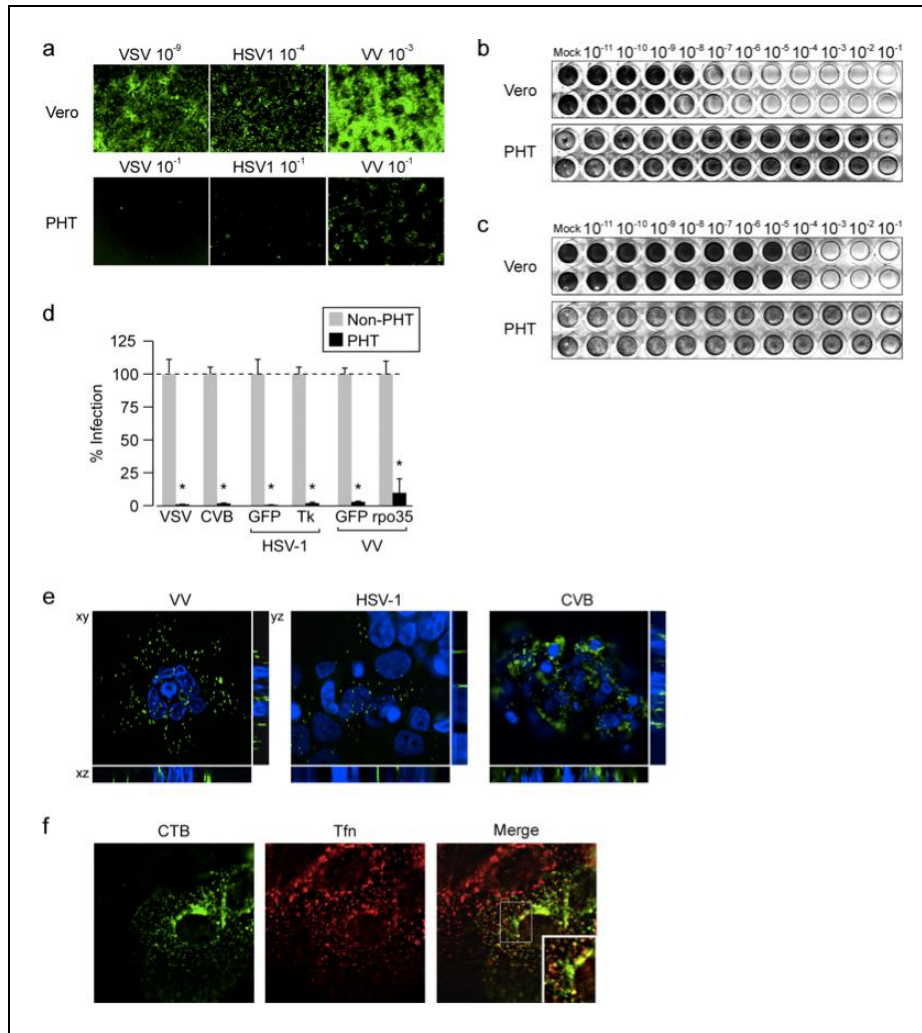


**Figure 2.2. PHT cells resist virus infection.** (a) Vero (top) or PHT (bottom) cells were infected with the indicated dilutions of GFP-VSV, GFP-HSV-1, or YFP-VV for ~40-45 hr. Shown are representative immunofluorescent images. (b) TCID50 assays for VSV in either Vero (top) or PHT (bottom) cells. Cells were infected with the indicated serial dilutions of virus for ~40-45 hr and then stained with crystal violet. (c) TCID50 assays for CVB in either Vero (top) or PHT (bottom) cells. Cells were infected with the indicated serial dilutions of virus for ~40-45 hr and then stained with crystal violet. (d) PHT and U2OS cells were infected in parallel with CVB, VSV, HSV-1, or VV for ~6-7 hr. Relative CVB, VSV, HSV-1 (VP26-GFP or early gene Tk) or VV (GFP or early gene rpo35) RNA was assessed by RT-qPCR (\* $p < 0.0001$ ). (e) Virus entry assays were performed in PHT cells with PV, HSV-1, VV, or CVB (60 min post-infection). DAPI-stained nuclei are shown in blue and viruses are shown in green. (f) Cholera toxin subunit B (CTB) (green) and transferrin (Tfn) (red) uptake in PHT cells. PHT cells were exposed to Alexa Fluor-488 conjugated CTB and Alexa Fluor-594 conjugated Tfn for 60 min at 37 °C, fixed, and assessed using confocal microscopy. Shown are representative images of internalized CTB and Tfn. Inset, 3x zoom.

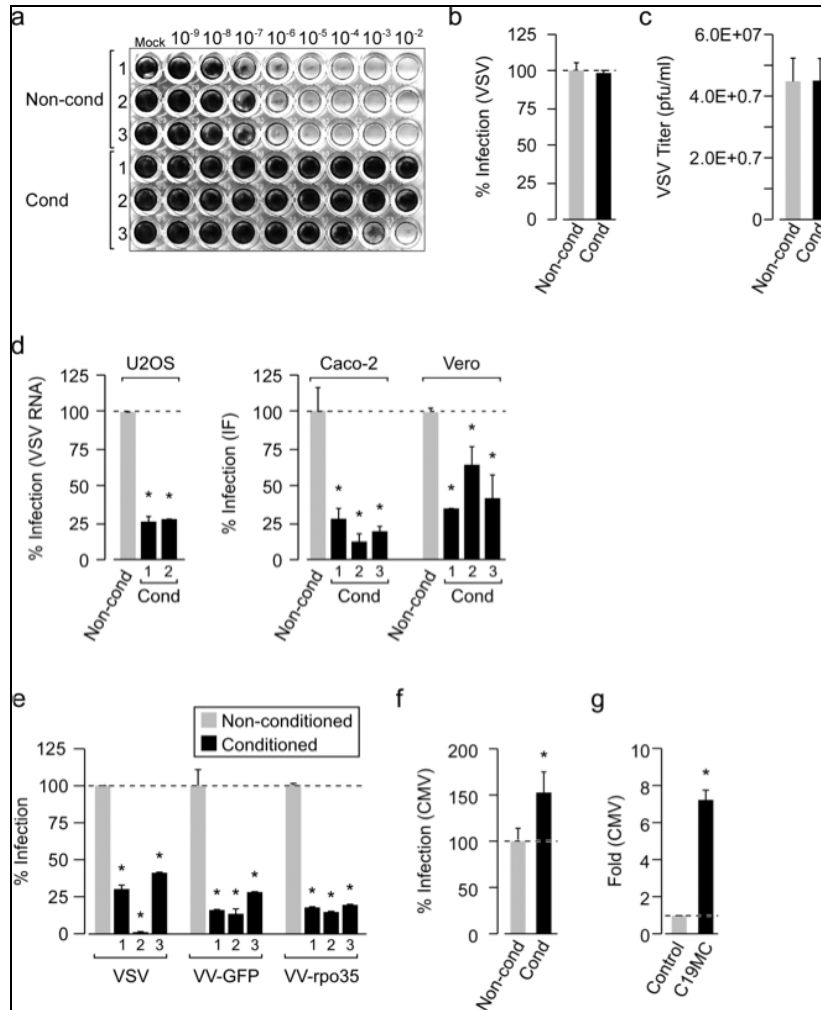


**Figure 2.3. The antiviral effects of PHT conditioned medium.** (a) TCID<sub>50</sub> assays for VSV in Vero cells pretreated for 24 hr non-conditioned medium (top, in triplicate) or three independent preparations of conditioned PHT medium. Cells were infected in the indicated dilution of virus in the presence of non-conditioned or conditioned medium for ~40-45 hr and then stained with crystal violet. (b) Vero cells were exposed to non-conditioned (Non-cond) or conditioned (Cond) medium isolated from BeWo cells for 24 hr and then infected with VSV. Shown is the percent of infected cells (as assessed by IF). (c) VSV was incubated in non-conditioned (Non-cond) or conditioned (Cond) PHT medium (in the absence of cells) for 1 hr at 37°C then plaque assays performed. Shown are VSV titers (in pfu/mL). (d) Left, U2OS cells were exposed to non-conditioned (Non-cond) or conditioned (Cond) media from two independent PHT preparations and infected with VSV. Relative VSV RNA was assessed by RT-qPCR (\*p<0.0001). Right, Caco-2 or Vero cells were exposed to conditioned (Cond) medium isolated from four independent preparations of PHT cells for 24 hr prior to infection with VSV. Shown are the percent of infected cells as assessed by IF (\*p<0.0005). (e) U2OS cells exposed to non-conditioned or conditioned PHT medium were infected with VSV or VV for ~6 hr. Relative VSV or VV (early gene rpo35 or early gene GFP) RNA was assessed by RT-qPCR (\*p<0.0001). (f) HFF cells were exposed to non-conditioned (Non-cond) or conditioned PHT media for 24 hr before and during infection with CMV. Shown is the percent of infected cells (assessed by IF; \*p<0.05). (g) U2OS cells stably expressing control- or C19MC-BAC were infected with CMV, and infection levels assessed by RT-qPCR. Data are shown as fold-change over control (\*p<0.0001). In all panels, data are displayed as mean ±SD.

### 2.2.3 PHT exosomes confer viral resistance

Based on our data obtained with the PHT conditioned medium, it was clear that a specific factor present in the medium was capable of conferring viral resistance to non-placental recipient cells. To examine and identify the factor present in the PHT conditioned medium, we subjected the medium to a variety of treatments, and found that the antiviral effect was not diminished by heat-inactivation or RNase treatment (**Figure 2.1d** and data not shown). However, the transfer of viral resistance was abolished by sonication and partially eliminated by repeated freeze-thawing (**Figure 2.1d** and data not shown). Interestingly, exosomes are sensitive to disruption by sonication and repeated freeze/thaw and [99, 100]. Exosomes also function as cargo nanovesicles [93, 94] and mediators of intercellular communication [92, 94-96]. Consequently, we investigated the role of PHT-derived exosomes in transferring viral resistance to recipient cells<sup>2</sup> (**Figure 2.1e**). We found that exosomes purified from PHT conditioned medium reduced VSV infection in recipient cells, and that the antiviral effect was lost using conditioned medium depleted of PHT exosomes (**Figure 2.1e**). In contrast, exosomes isolated from other cell types such as JEG-3, an immortalized human placental choriocarcinoma cell line, or primary murine dendritic cells had little to no effect on VSV infection (**Figure 2.1e**). Altogether, these data directly support that PHT-derived exosomes are a key component within conditioned PHT medium with the capability to transfer viral resistance non-placental recipient cells.

---

<sup>2</sup> Purified exosomes and exosome-depleted conditioned media were provided by Dr. Yoel Sadovsky (Magee Womens Research Institute, Pittsburgh, PA).

#### 2.2.4 C19MC-derived miRNAs confer viral resistance

The transfer of mRNA, miRNA, and proteins via exosomes facilitates intercellular communication [94-96]. Intriguingly, placental trophoblasts and trophoblast-derived exosomes almost exclusively express miRNAs from the primate-specific chromosome 19 miRNA cluster (C19MC) [113, 115, 116, 139-142]. Although C19MC miRNAs are among the most abundant miRNAs in human trophoblasts and exosomes [115], their function remains unknown. We therefore investigated whether expression of the entire C19MC could induce viral resistance in non-PHT cells (U2OS). U2OS cells were stably transfected with either a control-BAC (bacterial artificial chromosome) or a BAC-expressing the entire C19MC<sup>3</sup> (**Figure 2.4a**). VSV infection was significantly reduced in U2OS cells stably expressing a C19MC-encoding BAC compared to cells expressing the control-BAC (**Figure 2.4a**). To narrow down which C19MC miRNAs may be selectively involved in mediating antiviral effects, we transiently transfected U2OS cells with miRNA mimics of 16 C19MC-derived miRNAs (representing the most highly expressed miRNAs and/or the two subfamilies of the C19MC [115, 195]); this markedly diminished VSV infection (**Figure 2.4b** and **Table 2.1**).

---

<sup>3</sup> Stable control- and C19MC-BAC U2OS cells were provided by Dr. Yoel Sadovsky (Magee Womens Research Institute, Pittsburgh, PA).

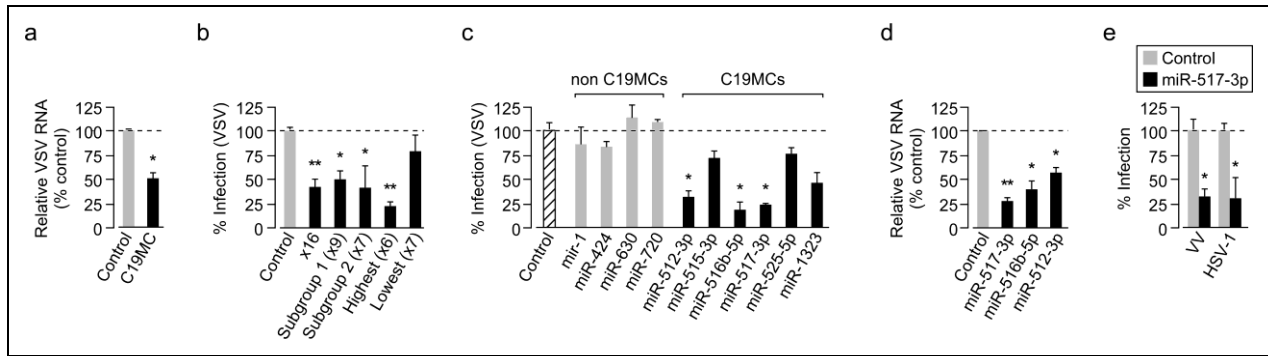


**Figure 2.4. PHT and exosomal C19MC miRNAs confer viral resistance to recipient cells.** (a) U2OS cells stably expressing control- or C19MC-BAC were infected with VSV (infection levels assessed by RT-qPCR; \* $p < 0.0001$ ). (b) U2OS cells were transfected with C19MC miRNA mimics that represent the miRNA sub-groups detailed in Table 2.1 or control mimics, and then infected with VSV (shown as percent infected cells assessed by IF; \* $p < 0.05$ , \*\* $p < 0.001$ ). (c) U2OS cells transfected with mimics of the six highest expressed C19MC miRNAs, scrambled control, or non-C19MC (miR-1, -424, -630, -720) miRNA mimics were infected with VSV (infection level assessed by IF or qPCR; \* $p < 0.0005$ ). (d) U2OS cells transfected with mimics of the top three antiviral C19MC miRNAs or with scrambled control mimics were infected with VSV (infection assessed by RT-qPCR; \* $p < 0.05$ , \*\* $p < 0.0001$ ). (e) U2OS cells, transfected with scrambled control or miR-517b mimics, were infected with VV or HSV-1 [infection assessed as in (D); \* $p < 0.0001$ ].

We also observed a potent inhibition of VSV infection using miRNA mimics of the highest expressed C19MC miRNAs [115], but not with the lowest expressed miRNAs (**Figure 2.4b** and **Table 2.1**). To identify individual antiviral C19MC miRNAs, we transiently transfected singular mimics from among the highest expressed C19MC (**Figure 2.4c** and **Table 2.1**). A significant reduction of VSV infection was detected with mimics of miR-517-3p, -516b-5p, and -512-3p (**Figure 2.4c-d**). We did not detect any appreciable effect on VSV infection with several non-C19MC-associated miRNAs, including miR-1, 424, -630, and -720<sup>4</sup>. (**Figure 2.4c**). Similarly, we found that miR-517-3p also decreased infection by the DNA viruses VV and HSV-1, suggesting a broadly antiviral function for this miRNA (**Figure 2.4e**).

<sup>4</sup> Data for experiments involving miR-1, -630, and -720 were provided by were provided by Dr. Yoel Sadovsky (Magee Womens Research Institute, Pittsburgh, PA).

**Table 2.1. Groups of C19MC miRNA mimics.**

16 C19MC miRNAs	Subgroup 1 9 C19MC miRNAs	Subgroup 2 7 C19MC miRNAs	6 highest expressed C19MC miRNAs	7 lowest expressed C19MC miRNAs
miR-517-3p	miR-517-3p		miR-517-3p	
miR-1323		miR-1323	miR-1323	
miR-516b-5p		miR-516b-5p	miR-516b-5p	
miR-525-5p		miR-525-5p	miR-525-5p	
miR-512-3p		miR-512-3p	miR-512-3p	
miR-515-3p	miR-515-3p		miR-515-3p	
miR-518e	miR-518e			
miR-515-5p		miR-515-5p		
miR-517c	miR-517c			
miR-519c-3p	miR-519c-3p			miR-519c-3p
miR-520h	miR-520h			miR-520h
miR-519d	miR-519d			miR-519d
miR-518b	miR-518b			miR-518b
miR-512-5p		miR-512-5p		miR-512-5p
miR-520c-3p	miR-520c-3p			miR-520c-3p
miR-518a-5p		miR-518a-5p		miR-518a-5p

### 2.2.5 Conditioned PHT medium and exosomes induce autophagy

Viruses have developed exceptional strategies to evade and hijack cellular immune mechanisms. A variety of exceptional host cell strategies have been identified as critical components in mammalian innate immune regulation during viral infection. One vital mechanism by which host cells protect against invading pathogens is through autophagy (see section **1.6**, “**Autophagy**”), an evolutionarily conserved lysosomal degradation pathway. The autophagy pathway participates in antiviral host defense by: targeting cytoplasmic viruses for lysosomal degradation (known as xenophagy or more recently, virophagy) [166], limiting viral replication [74, 167], and/or interacting with innate immune components such as TLRs and associated adaptors [73, 168, 169]. Remarkably, we found that exposure of recipient cells (U2OS, Vero) to PHT conditioned medium or to purified PHT-derived exosomes (as assessed by the formation of mRFP-LC3b-positive punctae and by electron microscopy), whereas conditioned-medium depleted of PHT-exosomes had no effect (**Figure 2.5a-b** and **Figure 2.6a-b**). Furthermore, PHT

conditioned medium induced the upregulation (>2-fold) of several key pro-autophagy transcripts (e.g., ATG4C, UVRAG, LC3A, and PIK3C3) while having no effect on other innate immune pathway components (e.g. toll-like receptors, interferon regulatory factors, cytokine-mediated signaling) in U2OS cells exposed to conditioned PHT medium (**Figure 2.6c** and **Appendix B**), supporting the induction of autophagy. Additionally, the pharmacological agent 3-methyladenine (3-MA), an inhibitor of the type III PI3K critical for autophagosome biogenesis [196], inhibited canonical autophagic induction in recipient cells exposed to conditioned PHT medium (**Figure 2.5c**). Lastly, we investigated VSV entry into recipient cells that had been previously cultured in conditioned PHT medium, and found that incoming VSV particles were trafficked to LC3b-positive punctae, suggesting that viruses are shuttled from the endosomal to the autophagic pathway for degradation, limiting viral replication (**Figure 2.5d**).

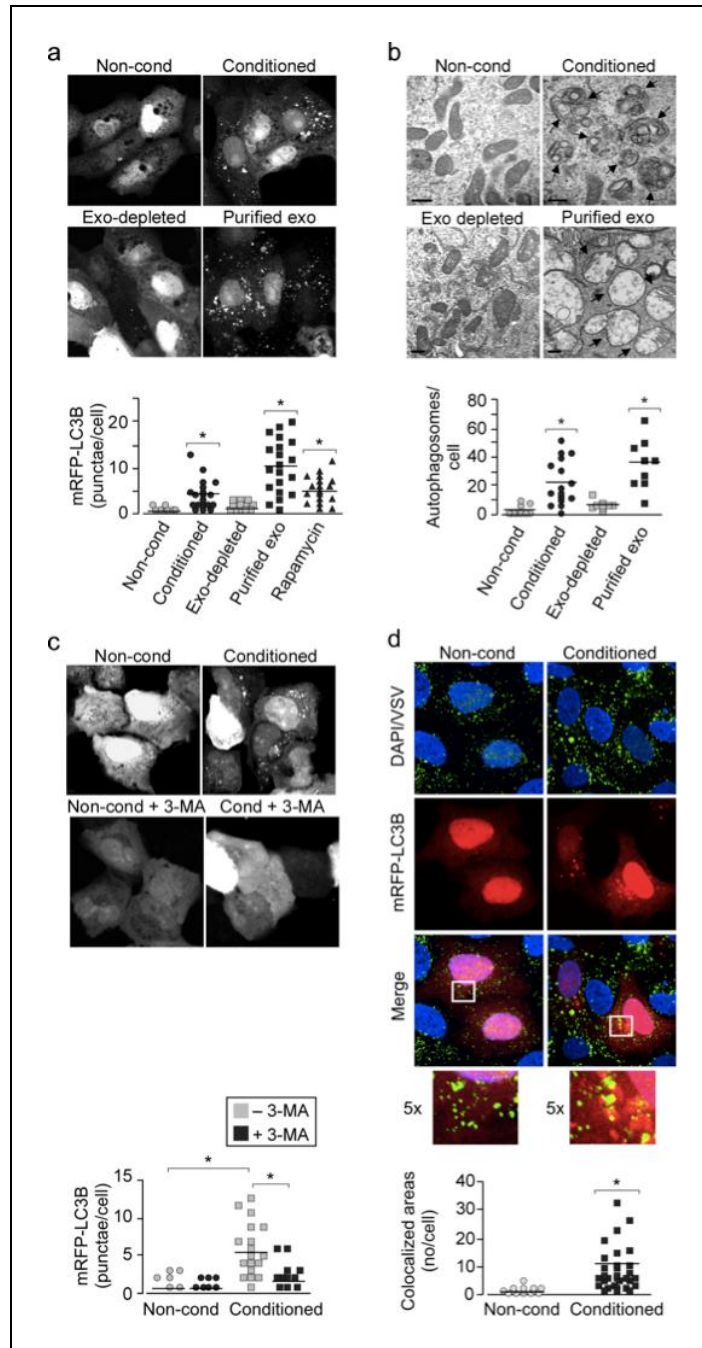


**Figure 2.5. PHT-derived exosomes induce autophagy in recipient cells.** (a) U2OS cells transfected with mRFP-LC3b were exposed to non-conditioned (Non-cond), PHT conditioned (Conditioned), exosome-depleted conditioned PHT medium (Exo-depleted), or purified PHT exosomes (Purified exo) for 24 hr. LC3b punctae formation was assessed by confocal microscopy. Top, confocal micrographs. Bottom, quantification of mRFP-LC3b punctae per cell (\* $p < 0.0001$ ). (b) Top, electron micrographs of cells exposed to non-conditioned or conditioned PHT medium (Vero), exosome-depleted conditioned PHT medium (Vero), or purified PHT exosomes (U2OS). Arrows denote autophagosomes. Bar=500 nm. Bottom, (Figure 2.5 continued) quantification of electron micrographs of cells exposed to non-conditioned (Vero and U2OS), conditioned PHT media samples (Vero and U2OS), exosome-depleted conditioned medium (Vero), or purified PHT exosomes (U2OS) (\* $p < 0.0001$ ). (c) U2OS cells transfected with mRFP-LC3b were exposed to non-conditioned or conditioned PHT medium in the absence or presence of 3-MA for 8 hr as indicated. LC3b punctae formation assessed by confocal microscopy. Top, confocal micrographs.

(**Figure 2.5 continued**) Bottom, quantification of mRFP-LC3b punctae (\* $p < 0.0005$ ). (**d**) Top, immunofluorescence images of VSV entry into U2OS cells transiently transfected with mRFP-LC3b exposed to non-conditioned (left) or conditioned (right) PHT medium. VSV particles are shown in green and DAPI-stained nuclei are shown in blue (inset, 5x magnification). Areas of colocalization appear as yellow. Bottom, quantification of the extent of colocalization between VSV particles and mRFP-LC3B positive punctae (\* $p < 0.0001$ ).

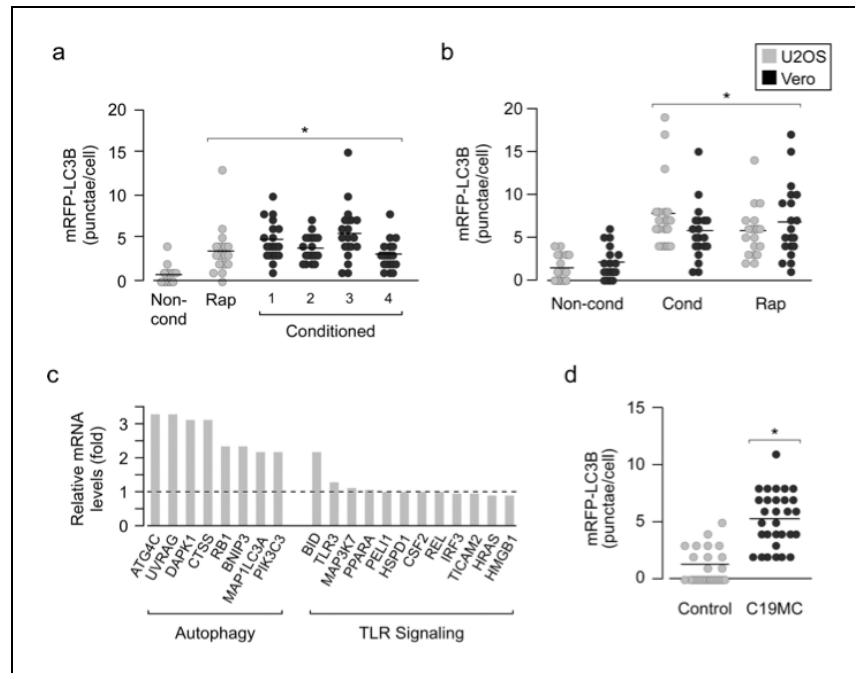


**Figure 2.6. Medium from PHT cells induces autophagy in recipient cells.** (a) Vero cells were transfected with mRFP-LC3b and at 24 hr post-transfection were exposed for 24 hr to either non-conditioned (Non-cond) or conditioned medium isolated from four independent PHT preparations. Cells were exposed to rapamycin (Rap) as a positive control. Shown are the levels of autophagic induction as determined by quantification of mRFP-LC3b positive punctae (\* $p < 0.0001$ ). (b) Vero and U2OS cells were co-transfected with mRFP-LC3b and then exposed to non-conditioned (Non-cond) or conditioned PHT medium (Cond) 24 hr post-transfection. Cells were exposed to rapamycin (Rap) as a positive control. Shown are the levels of autophagic induction as determined by quantification of mRFP-LC3b positive punctae by confocal microscopy (\* $p < 0.0001$ ). (c) Relative mRNA levels in U2OS cells exposed to non-conditioned or conditioned PHT medium for 24 hr, and analyzed using autophagy or toll-like receptor (TLR)-targeted RT-qPCR arrays. (d) U2OS cells stably expressing a control- or C19MC-BAC were transfected with mRFP-LC3b, fixed after 48 hr, and analyzed for mRFP-LC3b punctae by confocal microscopy (\* $p < 0.0001$ ).

## 2.2.6 Antiviral effects of C19MC miRNAs are not the result of type I IFN signaling

In contrast, we detected no effect of PHT conditioned medium or C19MC-associated miRNAs on the induction of the canonical antiviral type I IFN signaling (**Figure 2.7b-g**). We also observed antiviral effects of conditioned PHT medium in HT1080 Jak1-deficient cells that fail to

respond to type I IFNs (and cannot induce downstream antiviral signaling), further supporting that induction of type I IFNs is not the major pathway responsible for conferring viral resistance in recipient cells (**Figure 2.7e**). We found no evidence of: type I IFNs present in conditioned PHT medium by performing enzyme-linked immunosorbent assay (ELISA) for IFN- $\beta$  (data not shown), or induction of a type I IFN response as measured by reporter gene assay for IFN- $\beta$  or ISRE activity with conditioned medium cultured on cells for 24 hr (**Figure 2.7b-c**). We also did not observe any indication of a hyper-activated IFN-response in recipient cells cultured with conditioned PHT medium, and transfected with the synthetic dsRNA analog poly(I:C) (a ligand of the antiviral toll-like receptor-3, TLR3 [197]) (**Figure 2.7b**). Additionally, there was no evidence of IRF3 nuclear translocation in recipient U2OS cells exposed to conditioned PHT medium or in U2OS C19MC-BAC cells (**Figure 2.7d,f**), or the induction of ISGs such as ISG56 as assessed by RT-qPCR (**Figure 2.7g**).

### **2.2.7 C19MC-derived miRNAs induce autophagy**

We next investigated whether C19MC miRNAs were capable of inducing autophagy as we had previously observed their role in transferring type I IFN-independent viral resistance. Transfection of U2OS cells with mimics of the six highest expressed C19MC miRNAs (**Figure 2.8a-b**), or stably expressing the C19MC-BAC (**Figure 2.6d**), or mimics of individual C19MC miRNAs that significantly decreased viral infection (**Figure 2.8c**) induced autophagy (as assessed by mRFP-LC3b punctae formation and/or electron microscopy). Next, we investigated whether the observed increase in the number of autophagosomes was due to autophagic flux (rather than a block of downstream degradation) (**Figure 2.8d**). During autophagy, p62 links LC3-II with ubiquitylated substrates, associates with autophagosomes, and undergoes

degradation by autolysosomes [198]. p62 is a marker of autophagic flux, as expression levels decrease during prolonged autophagy. Our results indicated a characteristic decrease in p62 expression in U2OS C19MC-BAC cells compared to control-BAC, supporting that the upregulation of autophagy was due to increased flux through the autophagic pathway (**Figure 2.8d**).

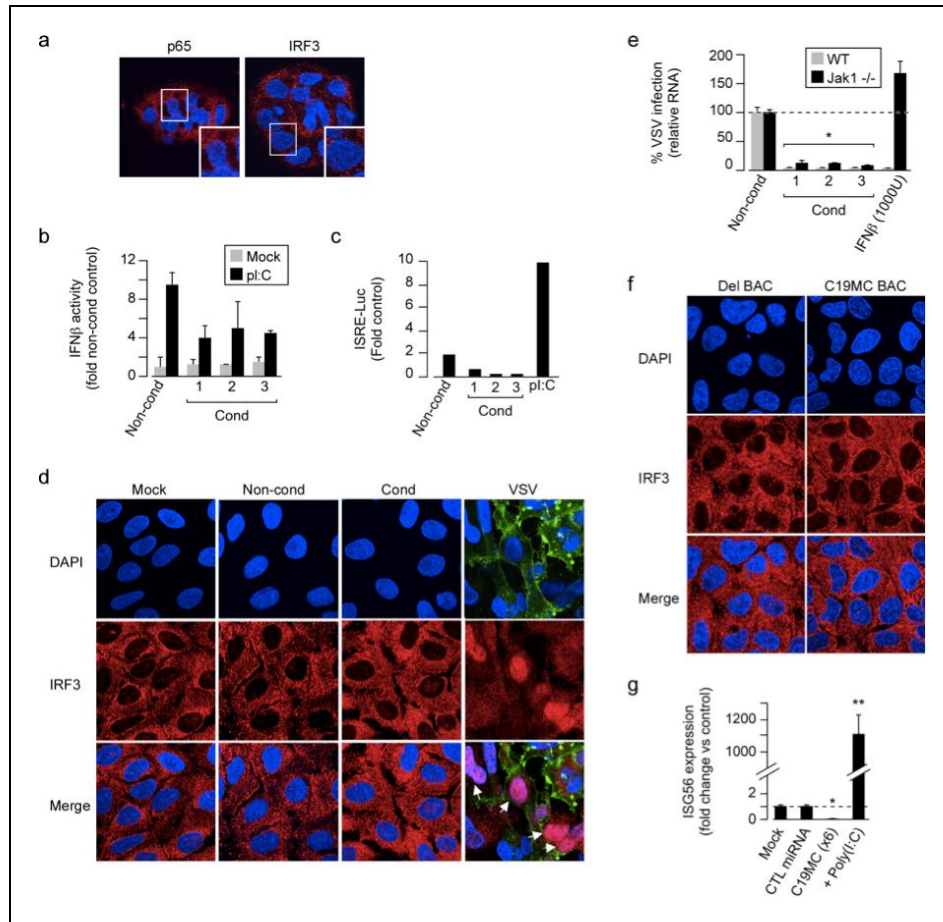


**Figure 2.7 The antiviral effects of conditioned PHT medium are not due to type I IFN.** (a) Confocal micrographs of PHT cells stained with anti-NF- $\kappa$ B p65 subunit or IRF3 antibodies (red). DAPI-stained nuclei are shown in blue. (b) IFN- $\beta$  luciferase assays in U2OS cells exposed to non-conditioned (Non-cond) medium of three independent preparations of conditioned PHT medium (Cond). In parallel, exposed cells were transfected with 1  $\mu$ g poly(I:C). (c) ISRE luciferase assays in U2OS cells exposed to non-conditioned medium (Non-cond) or three independent preparations of conditioned PHT medium (Cond). As a positive control, naïve cells were transfected with 1  $\mu$ g poly(I:C). (d) Immunofluorescence microscopy for IRF3 (red) in control (mock-exposed) U2OS cells or cells exposed to non-conditioned (Non-cond) or conditioned PHT medium (Cond). As a positive control, naïve cells were infected with VSV (right, green). DAPI-stained nuclei are shown in blue. (e) Control (wt) or JAK-deficient (U4A) HT1080 cells were exposed to non-conditioned (Non-cond) or three independent (preparations of conditioned PHT medium (Cond) and infected with VSV. In parallel, cells were exposed to 1000 U of purified human IFN- $\beta$ . Shown are the relative amounts of VSV RNA as assessed by RT-qPCR and normalized to non-conditioned control-treated cells (\* $p$ <0.0001). (f) Immunofluorescence microscopy for IRF3 (red) and DAPI-stained nuclei (blue) in control Del-BAC or C19MC-expressing BAC U2OS cells. (g) ISG56 mRNA levels as assessed by in mock (non-transfected) U2OS cells or cells transfected with control (CTL) miRNA mimics or mimics of the highest six expressed C19MC-associated miRNAs (\* $p$ <0.05, \*\* $p$ <0.0001). In parallel, cells were transfected with 1  $\mu$ g poly(I:C) as a positive control. In (B, C, F, and H) panels, data are displayed as mean  $\pm$ SD.

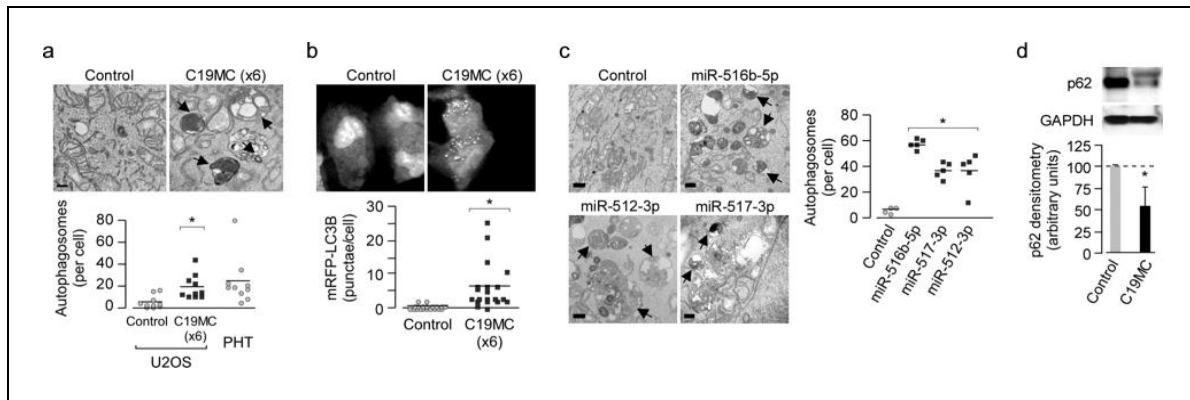


**Figure 2.8. C19MC miRNAs induce autophagy.** (a) Top, electron micrographs of U2OS cells transfected with scrambled control or the six highest expressed C19MC miRNA mimics (**Table 2.1**). Black arrows denote autophagosomes and/or autolysosomes. Bar=500 nm. Bottom, quantification of electron micrographs shown at top ( $*p<0.005$ ), or in PHT cells. (b) U2OS cells were transfected with mRFP-LC3b and either scrambled control or the six highest expressed C19MC miRNA mimics. Top, confocal micrographs. Bottom, quantification of mRFP-LC3b punctae per cell ( $*p=0.0005$ ). (c) Left, electron micrographs of U2OS cells transfected with scrambled control or the most robust antiviral miRNA mimics. Black arrows denote autophagosomes and/or autolysosomes. Bar=500 nm. Right, quantification of adjacent electron micrographs ( $*p<0.005$ ). (d) Top, a representative immunoblot for p62 or GAPDH in U2OS cells stably transfected with either control Del- or C19MC-BAC. Bottom, densitometry of p62 levels (normalized to GAPDH) from three independent immunoblots ( $*p<0.05$ ).

## 2.2.8 Autophagy is a mechanism of viral resistance

In these studies, we have observed and reported a clear inhibition of viral replication and a pronounced induction of autophagy in recipient cells cultured in conditioned PHT medium and in cells expressing C19MC-derived miRNAs (**Figure 2.5a-b**, **Figure 2.6a-b,d** and **Figure 2.8**). We next wanted to investigate whether the antiviral effects observed were the result of the increased autophagy. To do so, we treated cells with 3-MA which stably expressing either the entire C19MC- or control-BAC (a pharmacological inhibitor of autophagosome biogenesis [196]) (**Figure 2.9a**). We found that 3-MA treatment restored VSV infection (as assessed by relative RNA using RT-qPCR) in C19MC-BAC cells (**Figure 2.9a**). We further validated our results by silencing Beclin-1 (which is critical for the induction of autophagy [199] and *reviewed in* [200]) with RNAi, and found that loss of Beclin-1 partially restored VSV infection in C19MC-

BAC expressing cells<sup>5</sup> (**Figure 2.9b**). As we had previously observed very high basal levels of autophagy in PHTs (**Figure 2.8a**), we examined whether addition of 3-MA would enhance virus infection in PHTs (**Figure 2.9c**). Interestingly, treatment of PHT cells with 3-MA bolstered VSV infection as measured by viral RNA (**Figure 2.9c**). Although the overall level of infection remained fairly low (~10% overall infection), suggesting additional mechanisms are involved in the protection of PHT cells from pathogens. Taken together, these data demonstrate that the upregulation of autophagy is crucial for the antiviral effect of C19MC miRNAs.

---

<sup>5</sup> Data related to beclin-1 silencing experiments were provided by Dr. Yoel Sadovsky (Magee Womens Research Institute, Pittsburgh, PA).

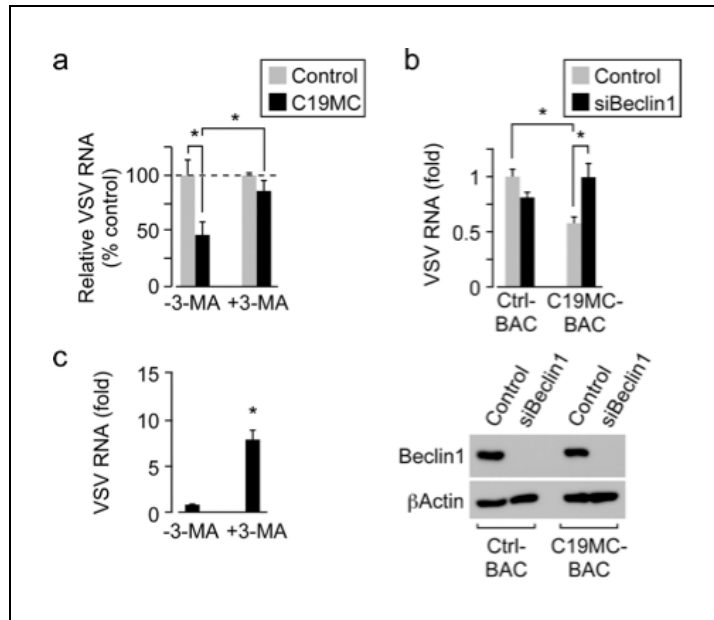


**Figure 2.9. Suppression of autophagy abrogates C19MC-mediated antiviral effects.** (a) U2OS cells transfected with scrambled control or miRNA mimics of the six most prevalent C19MC miRNA mimics. Cells were exposed to 3-MA before and during VSV infection. Relative VSV RNA was analyzed by RT-qPCR (\* $p < 0.0005$ ). (b) U2OS cells stably expressing control- or C19MC-BAC transfected with scrambled control siRNA or beclin-1 siRNA for 72 hr were infected with VSV, and relative infection was determined by RT-qPCR (\* $p < 0.05$ , determined using ANOVA with Bonferroni's correction). Bottom, immunoblots for beclin-1 or actin in cells transfected as described above. (c) PHT cells were treated with 3-MA for 30 min prior to infection with GFP-VSV (in the presence of 3-MA). Relative VSV RNA was analyzed by RT-qPCR (\* $p < 0.005$ ).

## 2.2.9 Model

Our current model for the transfer of viral resistance between placental trophoblasts and recipient cells at the maternal-fetal interface is delineated in the schematic shown in **Figure 2.10**. Placental trophoblasts, which are highly resistant to virus infection and exhibit high resting levels of autophagy prior to viral stimulation, secrete exosomes containing C19MC-miRNAs into the extracellular space (**Figure 2.10**). Exosomes harboring C19MC miRNAs are taken up by, as yet, unidentified recipient cells. Internalization of the exosomes enables the release of the miRNAs into the recipient cell for targeting of mRNAs, ultimately altering recipient cell gene expression. Through as yet unrevealed mRNA targets, autophagy is upregulated in the recipient cell (**Figure 2.10**). Entering viruses (such as VSV) utilize the host cell endosomal pathway to initiate their

trafficking for uncoating and replication. Through either endosome-autophagosome fusion (forming an amphisome), or an as yet unidentified mechanism, virus becomes sequestered within autophagosomes (**Figure 2.5d** and **Figure 2.10**). Autophagic flux promotes progression of the virion-bound autophagosomes through the pathway, wherein autophagosomes fuse with lysosomes (forming autolysosomes), and the autophagic cargo (including virus) are subsequently degraded. Thus, this model was conceived based on the data presented in this chapter and provides a mechanism by which maternal-fetal tissues are protected from invading microbes during pregnancy.

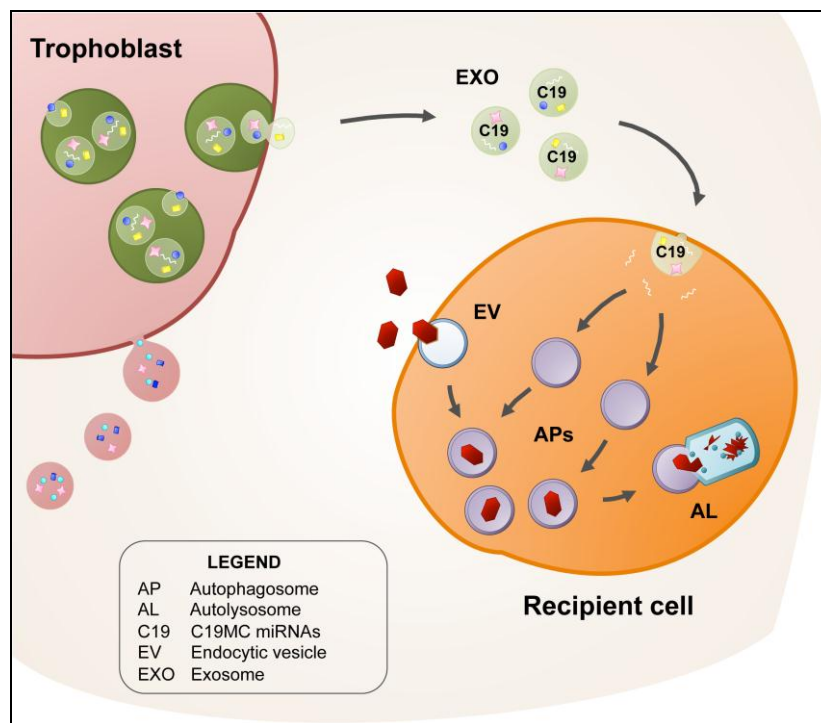


**Figure 2.10. Model depicting the exosome-mediated transfer of C19MC miRNAs.** Primary placental trophoblasts release exosomes (EXO) containing C19MC miRNAs (C19), which are taken up by recipient cells. The C19MC miRNAs induce autophagy by targeting as-yet unidentified mRNAs. Incoming viral particles (in red) are likely trafficked in endocytic vesicles (EV) from the endosomal pathway into pre-existing autophagosomes (APs), which then fuse with lysosomes to form autolysosomes (AL), as a mechanism to degrade these virus-containing vesicles.

## 2.3 DISCUSSION

The placenta is a critical physical and immunological barrier for fetal protection from invading pathogens throughout pregnancy. In this chapter, we have presented the remarkable finding that primary human trophoblast (PHT) cells are resistant to infection by a panel of disparate viruses (e.g. CVB, PV, VSV, VV, HSV-1, CMV) as measured by multiple assays (immunofluorescence, luciferase, RT-qPCR, and TCID50) (**Figure 2.1a** and **Figure 2.2a-d**). These antiviral effects were not due to pre-existing type I IFN or NF- $\kappa$ B inflammatory signaling, or to defects in virus entry or host endocytic routes (either expression or function) (**Figure 2.2e-f** and **Figure 2.7a**). The block of replication occurred very early in the viral life cycle as overall viral RNA (VSV, CVB) and early gene expression of HSV-1 gene Tk (thymidine kinase) and VV gene rpo35 (encoding a subunit of a DNA-directed RNA polymerase that is expressed within 2 h post-entry [193, 194] is inhibited in PHT cells (**Figure 2.2d**).

Furthermore, PHTs were able to transfer viral resistance to non-placental, recipient cells through trophoblast conditioned medium, trophoblast-derived exosomes, stable expression of the entire C19MC, or select miRNAs from the primate- and placenta-specific chromosome 19 miRNA cluster (C19MC), which are cargo of PHT exosomes (**Figure 2.1b-e**, **Figure 2.3a,d-e**, **Figure 2.4** and **Figure 2.7e**). Moreover, sonication and depletion of exosomes from conditioned PHT medium completely abrogated the antiviral effect (**Figure 2.1d-e**). We found no evidence a factor in conditioned trophoblast medium capable of directly neutralizing the virus, as incubating virus in conditioned medium alone had no detectable effect on virus titer (**Figure 2.3c**). We also found that inhibition of viral replication occurred early in the virus life cycle as expression of a VV early gene rpo35 was also inhibited in recipient cells exposed to conditioned PHT medium (**Figure 2.3e**).

Although the target cells of these exosomes have yet to be identified *in vivo*, the data presented in this chapter demonstrates that relevant maternal-fetal cell types such as placental fibroblasts, human uterine maternal vascular endothelial cells (HUtMVEC), human umbilical vein endothelial cells (HUVEC), and human uterine epithelial (RL-95) cells are receptive and become antiviral following exposure to conditioned trophoblast medium (**Figure 2.1c**). During pregnancy, the placenta may serve as an antimicrobial conduit by secreting trophoblastic exosomes and antiviral miRNAs into maternal circulation. Taken together, these data uncover a pathway that may serve to defend the developing fetus and surrounding maternal tissues against microbial invaders.

Additionally, our data demonstrate that conditioned PHT medium, purified PHT exosomes, stably expressing the entire C19MC, or select miRNAs of the C19MC family potently stimulate autophagy as assessed by multiple assays (LC3b-positive punctae, electron microscopy, and p62 autophagic flux; **Figure 2.5a-b**, **Figure 2.6** and **Figure 2.8**). Exosome depletion of conditioned trophoblast medium did not induce autophagy (**Figure 2.5a-b**). Autophagy is a critical antimicrobial host defense pathway [74, 156, 166-169]. Surprisingly, we found no role for type I IFN signaling in recipient cells following exposure to conditioned trophoblast medium or when expressing C19MC miRNAs using a variety of assays (JAK1<sup>-/-</sup> deficient cells, luciferase assays for the IFN- $\beta$  or ISRE promoters, IRF3 translocation, ISG induction by RT-qPCR, and ELISA for IFN- $\beta$ ) (**Figure 2.7b-g** and data not shown).

Inhibition of C19MC-induced autophagy by either the pharmacological agent 3-MA or by siRNA-mediated silencing of autophagy factor beclin-1 was sufficient to restore viral infection (**Figure 2.9a-b**). Considering that at least one of the viruses tested in this study (eg. CVB [180, 181]) may actually benefit from the formation of autophagic vesicles as a mechanism

to enhance replication; CVB was nevertheless susceptible to the antiviral effects of C19MC miRNAs. However, in contrast to autophagy pathways induced following host viral recognition, cells, which have either been exposed to PHT conditioned medium, PHT exosomes, or transfected with C19MC miRNAs, exhibit robust levels of autophagy *prior* virus exposure. Based on our evidence with VSV entry into cells undergoing C19MC miRNA-induced autophagy (**Figure 2.5d**), entering viruses may be shuttled to endosomes for subsequent trafficking to the autophagic pathway for degradation, significantly impacting viral uncoating and/or replication. Further supporting our model (**Figure 2.10**) and as mentioned earlier, both PHTs and recipient cells expressed very low levels of early gene expression when infected with HSV-1 and/or VV (**Figure 2.2d** and **Figure 2.3f**), suggesting that inhibition of replication occurs very early in the virus life cycle. Moreover, by electron microscopy, PHT cells demonstrated very high baseline levels of autophagy (*without* viral challenge) (**Figure 2.8a**) and the application of autophagy inhibitor 3-MA enhanced viral susceptibility (**Figure 2.9c**), implying that autophagy may be one mechanism by which PHT cells defend against viral invaders. However, these results do not exclude other mechanisms for viral resistance in placental trophoblasts or other functions by which autophagy may benefit the maternal-fetal unit.

In contrast to the other viruses investigated in this study, exposure to conditioned PHT medium and expression of the entire C19MC-BAC, significantly increased CMV infection (**Figure 2.3f-g**). This revealed that while C19MC miRNAs inhibited the replication of many of the viruses we have tested (VSV, CVB, HSV-1, VV), as-yet unknown mechanisms may account for the functioning of C19MCs in a proviral way to bolster CMV infection. Intriguingly, congenital CMV infection is one of the most dangerous prenatal and neonatal pathogens, leading to temporary symptoms such liver, lung, and spleen pathologies, jaundice, seizures, and/or IUGR

[29]. Permanent and long-term effects of congenital CMV infection include hearing and/or vision loss, small head, mental disabilities, lack of coordination, seizures, and/or death [29]. However, our data and the findings of others indicate that syncytiotrophoblasts are highly resistant to infection by CMV and other microbes, and that the cytotrophoblasts may be a key entry site for facilitating pathogen invasion into the fetal compartment [7, 8, 15-19]. Interestingly, CMV is also known to counteract antiviral autophagy in response to virus stimulation [176, 177]. A virus related to CMV – HSV-1 also has measures to thwart antiviral autophagy [173-175], but it remains sensitive to the antiviral effects of C19MC miRNAs (**Figure 2.4e**). However, the specific mechanism(s) underlying the upregulation of CMV infection by C19MC miRNAs are likely complex, involving diverse viral and/or cellular strategies.

This work demonstrates a role for transferrable, autophagy-dependent antiviral responses (**Figure 2.10**). Whereas our data demonstrates the effect of select C19MC miRNAs – miR-512-3p, -516b-5p, and -517-3p – on viral infection and autophagy, the targets involved in mediating these antiviral and pro-autophagy responses have not yet been identified. Although the search for the mRNA targets of miR-512-3p, -516b-5p, and -517-3p and other C19MC miRNAs are ongoing. It is possible that other, as-yet untested members of the C19MC could be involved in antiviral responses, perhaps synergistically with those select miRNAs that we have so far identified. A further complication of trying to identify miRNA targets is the sheer magnitude of the number of miRs (~46) that are C19MC family members. Additionally, mRNA targets may be targeted for degradation or for upregulation of gene expression (see section **1.5 “MiRNAs”**). Furthermore, the possibility exists that there may be other components present within PHT conditioned medium or exosomes that contribute to the observed antiviral effects that have yet to be recognized. These components may interact with a network of C19MC miRNAs and/or their

targets to mount antiviral responses, spanning diverse and possibly redundant pathways. Thus, C19MC miRNAs may direct a pathogen-specific response, facilitating the deployment of a selective repertoire of defense mechanisms designed to protect the developing feto-placental unit against diverse viral infections.

### 3.0 CVB ENTRY INTO HUMAN PLACENTAL TROPHOBLASTS

#### 3.1 INTRODUCTION

As discussed in subsection 1.2.2 “**Coxsackievirus B**”, maternal-fetal transmission of Group B coxsackieviruses (CVBs) during pregnancy has been associated with severe pathological outcomes for the fetus, including but not limited to congenital skin lesions [45], neurodevelopmental delays [47], hydrops fetalis [44], the development of type I diabetes [48, 49] and thyroiditis later in life [50], fetal myocarditis [40-42], meningoencephalitis [43], aseptic meningitis [46], fetal sepsis [37], miscarriage [35], stillbirth [36], and/or death [38, 39]. Throughout pregnancy, the placenta is an indispensable tissue that forms a physical and immunological barrier at the maternal-fetal interface. Despite the severity of pathologic disease associated with fetal CVB infection during pregnancy, little is known regarding the strategies used by viruses to gain entry into placental trophoblasts.

In this chapter, we have examined the mechanism(s) by which CVB, a virus that causes fetal pathology, gains entry into polarized placental trophoblasts. Examination of the kinetics of CVB entry and uncoating in placental trophoblasts have revealed similarities to those previously described in polarized intestinal epithelial cells. Similarly, CVB entry into placental trophoblasts requires DAF binding, and involves the relocalization of virus from the apical surface to intercellular tight junctions. In contrast, we have identified a divergent mechanism for CVB entry into polarized trophoblasts that is non-clathrin, non-caveolar, dynamin II-independent, and

lipid-raft dependent, but requires Src family tyrosine kinase signaling. These studies highlight the complexity associated with viral entry into human placental trophoblasts, and may serve as a model for how other pathogens have evolved to disrupt the placental barrier.

## 3.2 RESULTS

### 3.2.1 BeWo cells are an appropriate model to study virus-host interactions at the maternal-fetal interface

To determine that immortalized BeWo human trophoblast cells are a plausible *in vitro* model for investigating CVB entry into polarized placental trophoblasts, we stained for cell markers that demonstrate polarized apical-basolateral localization (**Figure 3.1A**). As expected, we observed distinct localization of tight junction (TJ)-associated protein zonula occludens-1 (ZO-1) at the apical TJ. We also detected the basolateral marker Na<sup>+</sup>/K<sup>+</sup> ATPase at the basolateral domain in BeWo cells, further supporting that BeWo cells are polarized epithelial cell models with the capability to form intercellular junctions [201, 202].

We also investigated whether CVB3-RD receptors DAF and CAR demonstrate polarized localization in BeWo placental trophoblasts (**Figure 3.1B**). DAF was found at the apical surface, and CAR localized to the tight junction (TJ), similar to other polarized cell types [54, 82]. Additionally, it was observed that CVB forms characteristic double-membrane autophagosome-like replication complexes in BeWo trophoblasts (**Figure 3.1F**), similar to that detected in other cell types following picornavirus infection [179, 180, 203]. These data reveal that BeWo placental trophoblasts are an appropriate polarized cell model for studying virus-host interactions at the maternal-fetal interface.

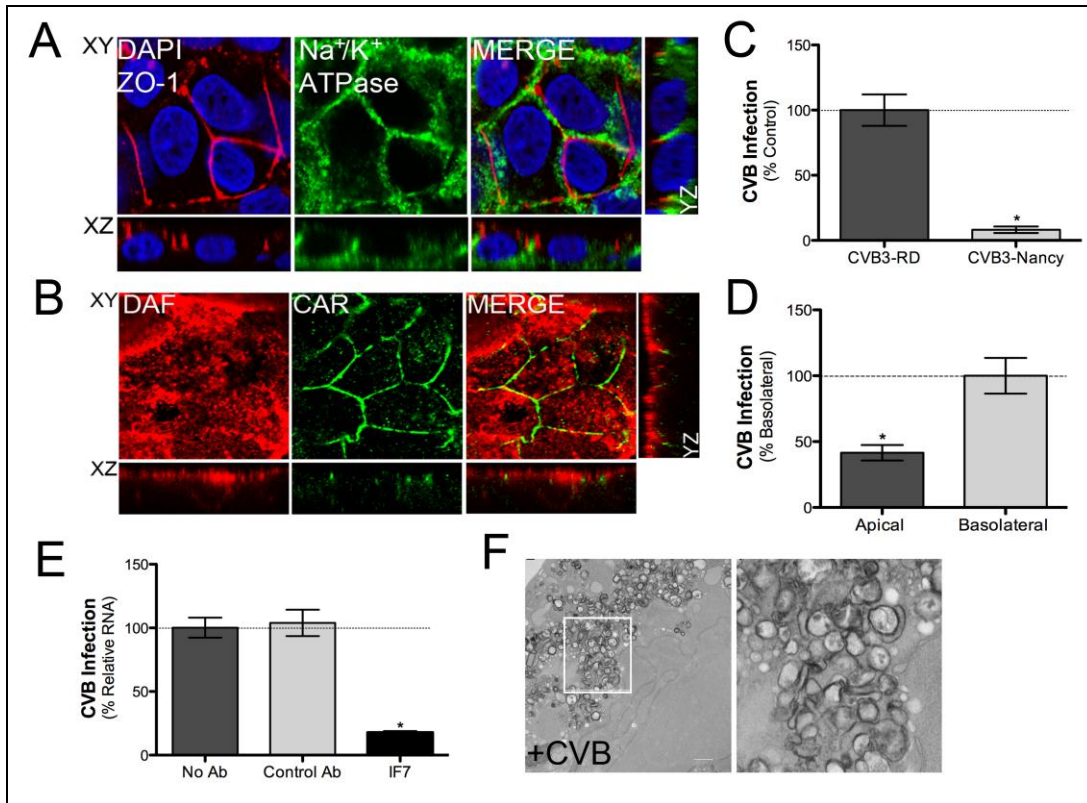


**Figure 3.1. DAF is required for efficient CVB infection of placental trophoblasts.** (A) Confocal micrographs of BeWo cells stained for the TJ marker ZO-1 (red), and the basolateral marker Na<sup>+</sup>/K<sup>+</sup> ATPase (green), DAPI-stained nuclei (blue). (B) Confocal micrographs of BeWo cells fixed and stained for DAF (red) and CAR (green). (C) BeWo cells were grown on collagen-coated chamber slides, then infected with either CVB3-RD or CVB3-Nancy (5 PFU/cell). Images were captured and quantified. Shown is the percent-infected cells (VP1+/DAPI as assessed by IF; \*p<0.0005). (D) BeWo cells were grown on collagen-coated transwells and infected with CVB3-RD from either the apical or basolateral surfaces. Shown is the percent-infected cells (VP1+/DAPI as assessed by IF; \*p<0.0001). (E) BeWo cells were incubated with either control (mock or nonspecific mAb) or anti-DAF mAb (IF7) antibody for 60 min, and then infected with CVB. RNA was isolated and RT-qPCR was performed. Shown is the percent infection assessed by relative RNA (\*p<0.005). (F) CVB-infected BeWo cells demonstrate numerous autophagosome-like structures. (Left) Magnification=30,000x. Bar=500nm. (Right) Zoom of autophagosome structures shown on left. In C-E, data are displayed as mean ±SD.

### 3.2.2 DAF is required for efficient CVB entry

Coxsackievirus B 3 isolate RD (CVB3-RD) requires two virus receptors: DAF (or CD55) – a virus attachment factor – and coxsackie and adenovirus receptor (CAR) – a receptor for virus entry and uncoating [54, 80, 81, 83-87, 139]. To define the requirement of DAF in CVB infection in trophoblasts, we infected with either CVB3-RD (a DAF-binding CVB) or CVB3-Nancy (a non-DAF-binding CVB) (Figure 3.1C). Interestingly, there is only a single amino acid

difference between CVB3-RD and CVB3-Nancy [204]. The ability to bind DAF is conferred to CVB3-Nancy if a glutamate residue within viral capsid protein VP3 (VP3-234E) is substituted with a glutamine residue (Q) [204]. We observed that BeWo cells were poorly infected with CVB3-Nancy (<10%) compared to infection with CVB3-RD, indicating that DAF was necessary for efficient infection of placental trophoblasts (**Figure 3.1C**). (Unless otherwise stated, all subsequent CVB infections were performed with CVB3-RD.) To determine the efficiency of CVB3-RD (a DAF-binding CVB isolate) to facilitate infection in a polarized manner, we cultured BeWo cells on collagen-coated transwells and then initiated infection at either the apical or basolateral domain (**Figure 3.1D**). We found CVB infection initiated at the apical surface to be less efficient (>55%) than infection at the basolateral surface (**Figure 3.1D**). This is consistent with previous work in polarized endothelial cells [88]. We further investigated the requirement of DAF in the CVB infection of trophoblast cells by incubating BeWo cells with an anti-DAF blocking antibody (IF7) [205], a control antibody, or without antibody (**Figure 3.1E**), and then infected with CVB. BeWo cells demonstrated significantly lower levels of CVB infection when incubated in the presence of the IF7 antibody (>80% less) compared to incubation with either mock antibody or no antibody (**Figure 3.1E**). Taken together, these data indicate DAF is critical for mediating efficient CVB infection in the placental trophoblasts.

### **3.2.3 Kinetics of CVB entry into BeWo trophoblasts**

To examine the kinetics of CVB entry in placental trophoblasts, we performed an immunofluorescence-based virus internalization assay and serial staining procedure that distinguishes between surface-associated (in red) and internalized (in green) virus particles in BeWo cells (**Figure 3.2A** and described further in **5.15.2 “Serial staining for virus entry**

assay”). We bound virus (MOI 100-150) to BeWo cells at room temperature, then shifted the cells to 37°C to facilitate synchronized entry in the presence of virus-free medium. Cells were then fixed after the desired time points (0, 30, 60, 90 min). Following binding (0 min), CVB was observed bound at the apical surface (presumably to DAF) (**Figure 3.2A**). By 30 min, CVB relocated to the TJ, for subsequent interaction with CAR (**Figure 3.2A**). Virus internalized to perinuclear compartments by 90 min (**Figure 3.2A**). This time course of entry was very similar to that which we have observed previously with CVB in other polarized cell types [54].

#### **3.2.4 CAR does not internalize with CVB during entry**

We next investigated whether the virus receptor CAR internalized with CVB in polarized trophoblasts (**Figure 3.2B**), as CAR internalization with CVB appears to be cell-type dependent [54, 89]. It was previously found that CAR did not internalize with virus in polarized intestinal epithelial cells [54], but did enter with CVB in non-polarized cells [89]. We found no evidence of CAR internalization by 90 min during CVB entry (**Figure 3.2B**), consistent with CVB entry in polarized intestinal cells [54]. BeWo cells transfected with a small-interfering RNA (siRNA) to CAR effectively silenced CAR expression as assessed by western blot analysis (**Figure 3.2D**). Loss of CAR also inhibited CVB entry (**Figure 3.2C**) and infection (>90%) (**Figure 3.2D**) in BeWo trophoblasts. Taken together, these data indicate that the kinetics and dependence on CAR for virus entry in BeWo trophoblast cells are similar to CVB entry in other polarized cell types [54].

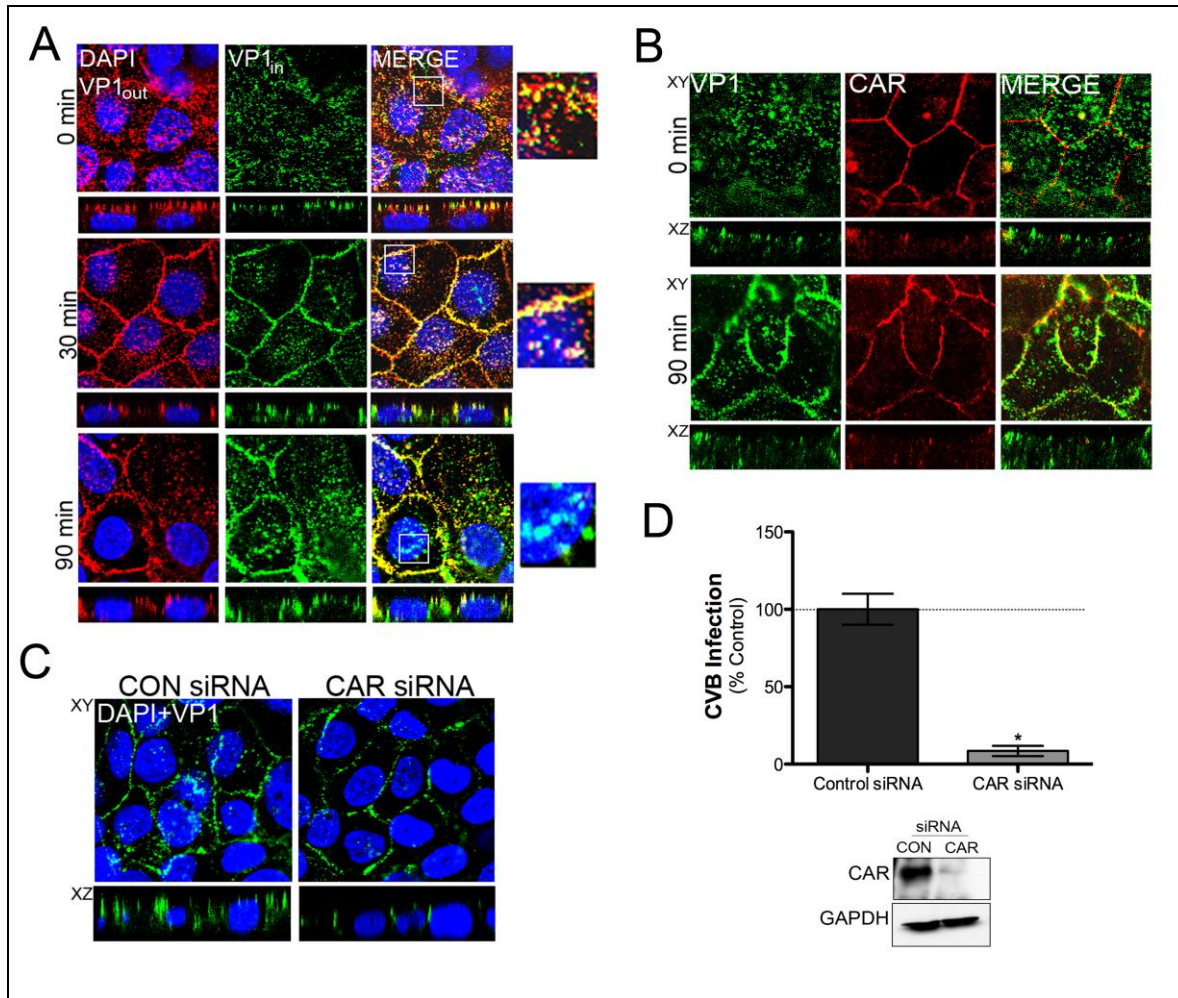


**Figure 3.2. Kinetics of CVB entry into placental trophoblasts.** (A) CVB (100-150 PFU/cell) was bound to BeWo cells at RT, unbound virus removed, and cells were incubated at 37°C to facilitate virus entry. Cells were fixed at the indicated time points and serially stained for virus [prior to permeabilization (VP1<sub>out</sub>) or after permeabilization (VP1<sub>in</sub>)]. Red or colocalized (red and green overlapping) fluorescence denotes virus bound on the cell surface; distinctively green fluorescence (no red) denotes internalized virus. DAPI is shown in blue. Magnified inserts (3x). (B) Cells were bound with CVB (100-150 PFU/cell), washed, and incubated at 37°C to facilitate virus entry for the indicated times prior to fixation. Cells were permeabilized and stained for virus (green) or CAR (red). Confocal micrographs are shown. (C) BeWo cells were transfected with either control or CAR siRNAs for a minimum of 48 hr. Cells were bound with CVB (100-150 PFU/cell), washed, and incubated at 37°C to facilitate virus entry for 90 min prior to fixation. Cells were permeabilized and stained for virus (green). Confocal micrographs are shown. (D) Top, BeWo cells were transfected with either control or CAR siRNAs for a minimum of 48 hr. Scramble siRNA was used as control. Cells were infected with CVB (5 PFU/cell), then fixed and stained for VP1. Images were captured and quantified. Shown are the percent-infected cells (VP1+/DAPI as assessed by IF; \*p=0.0001). Bottom, immunoblot analysis for CAR expression (top) and GAPDH (bottom) in BeWo cells transfected with either control or CAR siRNA.

### **3.2.5 Clathrin endocytosis is not required for CVB entry**

To dissect the entry mechanism by which CVB enters placental trophoblast cells, we generated a neutral-red (NR) containing CVB based on the protocols of other NR incorporated picornaviruses such as poliovirus [206] and echovirus 7 [207]. NR is an RNA-binding dye that, when cultured in the presence of virus, becomes readily incorporated into the viral RNA during viral propagation. After incorporation of the neutral red, the resulting NR-containing CVB virions are light sensitive. All subsequent virus purification, plaquing, and experimentation must be performed under semi-dark conditions to prevent irreversible damage to the virions. Following light exposure, the NR-virions are unable to replicate as the close proximity of the NR dye and RNA within the viral capsid, causes crosslinking of the viral RNA, and the resulting virus particle can no longer replicate [206, 208, 209]. Upon entry of the virus into host cells, and subsequent uncoating and RNA release, the NR dye disengages from the viral RNA, and the virion is able to replicate. In this way, this method has been utilized to screen pharmacological inhibitors of host endocytic and signaling pathways to tease out drugs that act specifically on virus entry from those drugs that may (also) inhibit non-entry events, such as replication. If a drug functions to inhibit CVB entry, light-exposure will inactivate virions bound to the host cell surface, and thus we will not observe virus infection. However, if a drug inhibits a non-entry step of the virus life cycle, light exposure will have no effect on virions that have already entered, uncoated, and released their genomes. We verified that the NR-incorporated CVB was light sensitive by performing plaque assays under both illuminated and non-illuminated conditions, and observed a significant loss of titer (data not shown).

We performed modified neutral-red infectious center (NRIC) assays to assess the propensity of known pharmacological inhibitors of the clathrin endocytic pathway to inhibit

CVB entry and infection in BeWo cells (**Figure 3.3A**). In the NRIC assay, BeWo cells were incubated in the presence of the indicated drug for 60 minutes at 37°C prior to initiating infection (see **Figure 5.2**). Cells were infected with NR-incorporated CVB for 2 hr to allow entry to occur (under semi-dark conditions). Cells undergoing infection were then exposed to a light box for 20 min (illuminated), while a dark only control (non-illuminated) was maintained in the dark. After light exposure, cells were washed with PBS, trypsinized, and equal amounts of cells were seeded onto a fresh, naïve monolayer of cells in media that was absent of both virus and drug. Naïve cells are allowed to infect for about 24 hr to determine if the drug prevented CVB from successfully entering the BeWo cells and uncoating. We observed that chlorpromazine, a pharmacological drug known to induce loss of clathrin and adaptor AP2 from the plasma membrane [210] and *reviewed in* [211] significantly inhibited CVB in the NRIC assay under illuminated (>80%) but not under non-illuminated conditions. We also tested monodansylcadaverine (MDC), an inhibitor of clathrin-endocytosis that functions by stabilizing clathrin-coated pits at the plasma membrane, *reviewed* [211] in the CVB NRIC assay (**Figure 3.3A**). Under illuminated conditions, there was no significant effect on CVB infection; conversely, we observed a partial reduction of CVB infection under non-illuminated conditions (~35%) (**Figure 3.3A**). As a control, we also tested the effects of chlorpromazine and MDC on vesicular VSV infection (**Figure 3.3B**); VSV utilizes a clathrin-dependent pathway to enter and infect host cells [51, 76, 212] and described further in subsection **1.3.2 “VSV Entry”**. Both chlorpromazine and MDC significantly inhibited VSV infection as expected (~95% and >85%, respectively).

To further confirm the results obtained with the pharmacological agents, we performed a standard virus infection assay with BeWo cells transfected with a siRNA targeting clathrin heavy

chain (CHC) (**Figure 3.3C**). Transfection with the CHC siRNA had no effect on CVB infection in BeWo cells, despite good levels of knockdown (**Figure 3.3C**). As a control, we also detected inhibition of transferrin uptake when cells were transfected with the CHC siRNA compared to control (**Figure 3.4**). We also observed colocalization of early endosome marker EEA1 and transferrin in control siRNA-transfected cells but not in cells transfected with the CHC siRNA (**Figure 3.4**). Additionally, we found no role for dynamin II (see subsection **3.2.6 “Dynamin II is not required for CVB entry”**) a GTPase essential for clathrin endocytosis [213], in CVB entry. Taken together, these data indicate that clathrin-mediated endocytosis was not required for CVB entry and infection into placental trophoblasts.

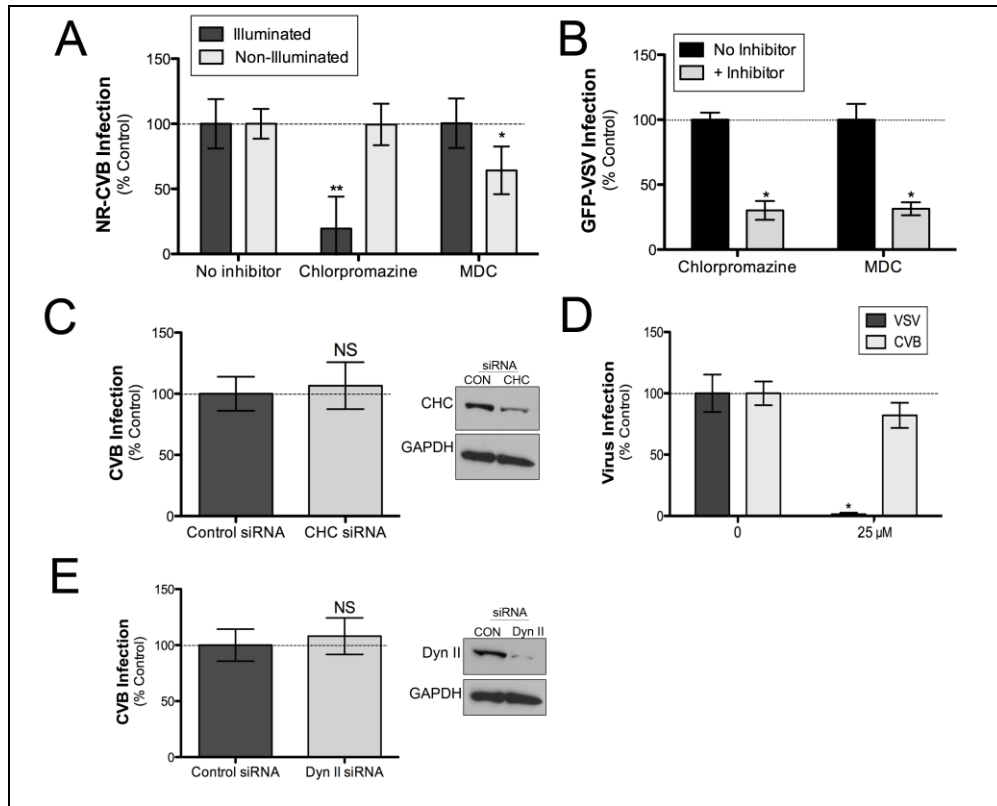


**Figure 3.3. Clathrin-mediated endocytosis is not required for CVB entry into BeWo trophoblast cells.** (A) NRIC assay in cells treated with either chlorpromazine (12.5 μg/mL) or MDC (100 μM). Shown are the percent-infected cells (VP1+/DAPI as assessed by IF; \*p<0.005, \*\*p<0.0001). (B) Cells were pre-treated for 60 min prior to and during GFP-VSV infection with either chlorpromazine (12.5 μg/mL) or MDC (100 μM). Images were captured and quantified. Shown are the percent-infected cells (GFP+/DAPI as assessed by IF; \*p<0.001). (C) Cells were transfected with either control or clathrin heavy chain (CHC) siRNAs for a minimum of 48 hr. (Left) Cells were infected with CVB (5 PFU/cell) then fixed and stained for VP1. Images were captured and quantified. Shown are the percent-infected cells at left (VP1+/DAPI as assessed by IF; not significant). (Right) Immunoblot analysis for CHC expression (top) and GAPDH (bottom). (D) BeWo cells were pre-treated with dynasore (25 μM) for 60 min prior to and during infection with either CVB or GFP-VSV. Cells were fixed and stained for VP1 (CVB) or assessed for GFP-expression (GFP-VSV). Images were captured and quantified. Shown are the percent-infected cells (VP1+ or GFP+/DAPI as assessed by IF; \*p<0.0005). (E) BeWo cells were transfected with either control or dynamin II (dyn II) siRNAs for a minimum of 48 hr. (Left) Cells were infected with CVB (5 PFU/cell), then fixed and stained for VP1. Images were captured and quantified. Shown are the percent-infected cells at left (VP1+/DAPI as assessed by IF; not significant). (Right) Immunoblot analysis for dyn II expression (top) and GAPDH (bottom).

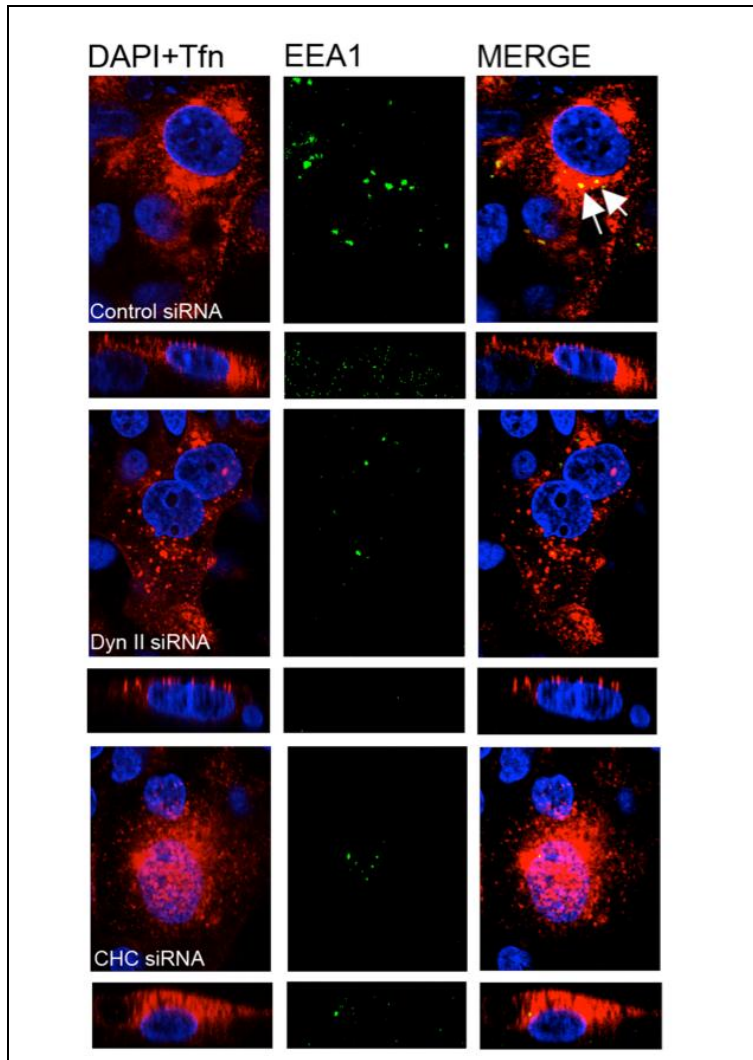


**Figure 3.4. Dynamin II and clathrin heavy chain siRNAs inhibit transferrin uptake.** Shown are confocal micrographs of BeWos transfected with either control scrambled, dynamin II (dyn II), or clathrin heavy chain (CHC) siRNAs for a minimum of 48 hr. Cells were incubated with transferrin conjugated to Alexa Fluor 594 shown in red (Tfn; 10  $\mu$ g/mL) for 30 min then fixed and stained for EEA1 (green). DAPI is shown in blue.

### 3.2.6 Dynamin II is not required for CVB entry into placental trophoblasts

We also investigated whether the small GTPase dynamin II (dyn II), which is critical for the endocytosis of clathrin- [213] and caveolar-vesicles [64, 65], was involved in CVB entry into polarized trophoblasts. Previous work demonstrated that dynamin II was required for CVB entry into polarized human brain microvascular endothelial cells [88] and non-polarized cells [89], but

was not necessary for internalization into polarized intestinal epithelial cells [54]. We found that dynasore, a pharmacological inhibitor of dynamin [214] – had little to no effect on CVB infection, while it potently inhibited VSV infection (>98%) (**Figure 3.3D**). To further validate our findings, we transfected BeWo cells with siRNAs towards dyn II and performed a standard infection assay (**Figure 3.3E**). Transfection with the Dyn II siRNA had no effect on CVB infection in BeWo cells, despite good levels of knockdown (**Figure 3.3E**). As a control, we also detected inhibition of transferrin uptake when cells were transfected with the Dyn II siRNA compared to control (**Figure 3.4**). Transferrin uptake is dependent on clathrin- and dynamin II dependent endocytosis [192]. We also observed colocalization of early endosome marker EEA1 and transferrin in control siRNA-transfected cells but not in cells transfected with the dyn II siRNA (**Figure 3.4**). Taken together, these data indicate that dynamin II-dependent endocytosis was not required for CVB entry and infection into placental trophoblasts.

### **3.2.7 Lipid rafts but not caveolae are required for CVB entry**

As we did not observe a significant role for clathrin-mediated endocytosis in the entry of CVB in BeWo trophoblasts, we examined whether lipid rafts and/or caveolae were involved. Earlier work has demonstrated that caveolin-1 was required for CVB entry into polarized intestinal epithelial cells [54] and human brain microvascular endothelial cells (HBMEC) [88]. However, lipid rafts, but not caveolin, were necessary for CVB entry into non-polarized cells [89]. To determine whether lipid rafts and/or caveolae were required for CVB entry into placental trophoblasts, we tested the lipid raft inhibitors filipin, nystatin, and methyl- $\beta$ -cyclodextrin (M $\beta$ CD) in our modified NRIC assay. However, we found no significant effect using filipin or nystatin on CVB infection either with or without light illumination (**Figure 3.5A**). Filipin and

nystatin are both polene antibiotics that produce aggregates in the plasma membrane, thereby sequestering cholesterol and disturbing the ordered structure of both lipid rafts and caveolae, *reviewed in* [211]. M $\beta$ CD functions by isolating, and thus depleting, cholesterol from cell membranes, and disrupting lipid rafts, *reviewed* [211]. We detected complete inhibition of CVB infection with M $\beta$ CD with light illumination, but no effect without illumination (**Figure 3.5A**), indicating that M $\beta$ CD likely inhibits CVB entry (rather than a non-entry event) in BeWo cells. As a control, we performed cholera toxin B (CTB) uptake assays in BeWo cells in the presence of M $\beta$ CD, and observed a significant lack of CTB internalization in M $\beta$ CD-treated cells compared to untreated (data not shown). M $\beta$ CD targets and depletes both caveolae-dependent and caveolae-independent lipid rafts, *reviewed* [211]. CTB uptake (and other cargo that utilize these pathways such as SV40) is dependent on caveolae in certain cell types [52, 215, 216], but may also use non-caveolar lipid raft pathways as well [56, 217, 218]. Thus, M $\beta$ CD would block either caveolae-dependent or caveolae-independent CTB uptake in this assay.

To further investigate whether caveolae were involved in CVB entry, we transfected BeWo cells with either control or caveolin-1 (cav-1) siRNAs, and infected with CVB (**Figure 3.5B**). Caveolae are a specific type of lipid raft, which form morphologically distinct invaginations (50-100 nm) at the plasma membrane and are dependent on the integral membrane protein caveolin-1 (cav-1), *reviewed* [62]. We observed no significant effect on CVB infection, despite good levels of cav-1 protein knockdown as assessed by western blotting (**Figure 3.5B**). As a control, we examined whether CTB uptake was inhibited by the cav-1 siRNA, and found that CTB uptake was not inhibited (data not shown). However, this is not surprising as CTB may utilize either caveolae-dependent [215], or caveolae-dependent (if the caveolae pathway is not available) mechanisms to internalize [217, 218]. Additionally, we found no role for dynamin

II (see subsection **3.2.6 “Dynamin II is not required for CVB entry”**), a GTPase necessary for caveolar-mediated endocytosis [64, 65], in CVB entry.

To further validate our findings that the cholesterol-depleting agent M $\beta$ CD inhibited CVB entry, we performed a virus entry assay to examine whether M $\beta$ CD specifically blocked virion endocytosis (**Figure 3.5C**). At 90 minutes post-entry, internalized virus was observed within the trophoblast cells under the mock condition; however, in the presence of M $\beta$ CD, virus was detected extracellularly and did not internalize. Based on both the NRIC and CVB entry assays, M $\beta$ CD, a lipid raft disrupting and cholesterol-depleting agent was found to inhibit CVB internalization, suggesting that lipid rafts are necessary for CVB entry into trophoblasts. Taken together, these data indicate that CVB entry in BeWo trophoblasts is independent of caveolin-1 and caveolae. Thus, CVB entry into placental trophoblasts is clathrin, dynamin II, and caveolin-1 independent but is dependent on cholesterol-enriched lipid rafts.

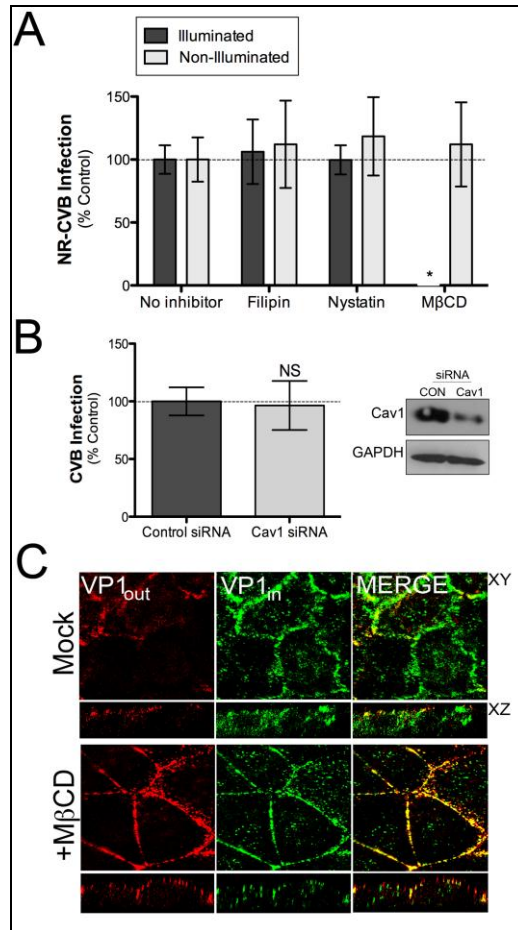


**Figure 3.5. Lipid rafts, but not caveolin, are required for CVB entry.** (A) NRIC assay in BeWo monolayers treated with filipin (3  $\mu\text{g}/\text{mL}$ ), nystatin (25  $\mu\text{g}/\text{mL}$ ), or M $\beta$ CD (5 mM). Shown are the percent-infected cells (VP1+/DAPI as assessed by IF; \* $p < 0.0001$ ). (B) Cells transfected with either control or caveolin-1 (cav-1) siRNAs for a minimum of 48 hr were infected with CVB (5 PFU/cell) then fixed and stained for VP1 (left). Images were captured and quantified. Shown are the percent-infected cells at left (VP1+/DAPI as assessed by IF; not significant). (Right) Immunoblot analysis for cav-1 expression (top) and GAPDH (bottom). (C) Cells were pre-treated with M $\beta$ CD (5 mM) for 60 min prior to and during binding with CVB (100-150 PFU/cell) at RT. Unbound virus was removed, and cells were incubated at 37°C (in the presence of drug) to facilitate virus entry. Cells were fixed at 90 min and serially stained for virus [prior to permeabilization (VP1<sub>out</sub>) and with a green fluorophore after permeabilization (VP1<sub>in</sub>)]. Red or colocalized (red and green overlapping) fluorescence denotes virus bound on the cell surface; distinctively green fluorescence (no red) denotes internalized virus.

### 3.2.8 Macropinocytosis is not required for CVB entry

Macropinocytosis is a non-clathrin, non-caveolar, dynamin-independent mechanism that requires actin for the non-specific uptake of fluid and other cargo, *reviewed* [53, 67]. The incoming vesicles, termed macropinosomes (0.5-10  $\mu\text{m}$ ), are formed by the closure of actin-dependent

membrane ruffles [68, 69]. Previously, it has been shown that CVB entry requires features of macropinocytosis in polarized human intestinal epithelial cells [55]. Therefore, we also investigated the possible role of macropinocytosis in facilitating CVB entry in polarized trophoblasts (**Figure 3.6**). To examine whether macropinocytosis was involved in facilitating CVB entry into placental trophoblasts, we performed the NRIC assay under both illuminated and non-illuminated conditions using pharmacological inhibitors of macropinocytosis – EIPA and rottlerin (**Figure 3.6A**). The pharmacological agent EIPA (ethyl isopropyl amiloride) is an inhibitor of the epithelial  $\text{Na}^+/\text{H}^+$  exchanger [219, 220], and rottlerin is a non-specific inhibitor of PKC (protein kinase C) [212, 221]; both the  $\text{Na}^+/\text{H}^+$  exchanger and PKC are necessary for macropinocytosis. We found that both EIPA and rottlerin inhibited CVB replication under illuminated conditions using the NRIC assay (>97%) (**Figure 3.6A**). Under dark only conditions, EIPA had no effect on CVB infection (**Figure 3.6A**). However, rottlerin also partially reduced CVB replication under non-illuminated conditions (>75%), suggesting that it also inhibited steps in the virus life cycle that occur post-entry (**Figure 3.6A**).

The actin cytoskeleton is a key mediator of macropinocytosis, particularly in the formation and closure of membrane ruffles [68]. To determine if the actin cytoskeleton played a role in mediating CVB entry into BeWo placental trophoblasts, we also tested the actin polymerizing inhibitors cytochalasin D (CytoD) [222] and latrunculin A (LatA) [222, 223] (**Figure 3.6B**). If macropinocytosis were involved in CVB entry into placental trophoblasts, overall infection and entry should be sensitive to treatment with CytoD and LatA [69]. We performed a standard infection assay using NR-CVB and light illumination 2 hr p.i., and found that these drugs had no significant effect on CVB infection in BeWo cells (**Figure 3.6B**). We also investigated whether Rho GTPases were involved in CVB entry into placental trophoblasts

by assessing the effects of toxin B (derived from *Clostridium difficile*), an inhibitor of Rho GTPases [224, 225]. The Rho family of GTPases (Rho, Rac, Cdc42) mediates critical coordination and spatiotemporal regulation of cellular actin dynamics, which enable macropinocytosis and other actin-dependent cell processes such as membrane ruffling, protrusion, and retraction, reviewed in [58, 226]. We found that instead of inhibiting CVB, treatment with toxin B actually enhanced CVB infection in BeWo cells (>200%) (**Figure 3.6B**). We also investigated whether CVB internalization was accompanied by an increased uptake of dextran and/or colocalization with the macropinosome marker rabankyrin-5 [227, 228]. We did not see any evidence of increased dextran uptake when performing a virus internalization assay, and there was no association between CVB particles and dextran or rabankyrin-5 positive vesicles (data not shown). Furthermore, we did not observe any evidence of macropinosome formation when BeWo cells were co-stained for actin (using phalloidin) following a virus entry assay (data not shown). Taken together, these data indicate that macropinocytosis is not involved in facilitating CVB entry into placental trophoblasts.

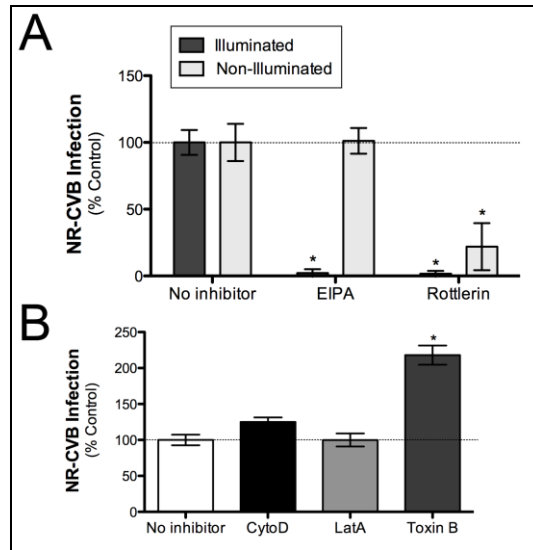


**Figure 3.6. Macropinocytosis is not involved in CVB entry into placental trophoblasts.** (A) NRIC assay in BeWo cells treated with EIPA (102  $\mu$ M) or rottlerin (10  $\mu$ M). Shown are the percent-infected cells (VP1+/DAPI as assessed by IF; \* $p$ <0.0001). (B) BeWo cells were pre-treated for 60 min prior to and during neutral-red CVB (NR-CVB) infection with cytochalasin D (CytoD; 2.5  $\mu$ g/mL), latrunculin A (LatA; 1  $\mu$ M), or toxin B (1 ng/mL). Cells were illuminated 2 hr p.i. to inactivate virions that had not yet entered. Images were captured and quantified. Shown are the percent-infected cells (VP1+/DAPI as assessed by IF; \* $p$ <0.0005).

### 3.2.9 CVB entry is dependent on Src family tyrosine kinases

In addition to examining the endocytic route by which CVB enters, we also investigated potential signaling mechanisms utilized by CVB to enter and infect trophoblasts. We performed an initial pharmacological drug screen using the standard virus infection assay with NR-CVB and light illumination 2 hr p.i., and found that the PI3K inhibitor wortmannin [229] or the tyrosine phosphatase inhibitor pervanadate [230] had no effect on CVB infection (**Figure 3.7A**). In this assay, we also tested additional inhibitors of cellular signaling pathways, which reduced CVB infection including the pan tyrosine kinase inhibitor genistein (>60%) [231], the SFK inhibitor PP2 (~70%) [232], the microtubule depolymerizing agent nocodazole (>70%) [233], and the myosin II inhibitor blebbistatin (>85%) [234] (**Figure 3.7A**). To further verify whether these drugs were acting on CVB entry (rather than a non-specific post-entry event such as

replication), we applied the CVB NRIC assay under both illuminated and non-illuminated conditions. Using the NRIC assay under illuminated conditions, we observed a reduction of CVB infection with genistein (~85%) and PP2 (~90%) but saw no effect on CVB infection under the non-illuminated condition (**Figure 3.7B**). This indicated that any inhibition of CVB infection due to genistein and PP2 was occurring on virus entry rather than a non-entry event, as there was no effect with the drug under the 'dark only' condition.

We also tested nocodazole and blebbistatin under both illuminated and non-illuminated conditions in the NRIC assay (**Figure 3.7C**). We detected near-complete inhibition of CVB with both nocodazole and blebbistatin under illuminated conditions, and significant inhibition (>80%) without light illumination (**Figure 3.7C**). In contrast, we detected near-complete inhibition of CVB with both nocodazole and blebbistatin under illuminated conditions, suggesting that the inhibitory effects of these agents may occur due to inhibition of post-entry events.

Based on the NRIC assay results obtained with genistein and PP2, we sought to verify that SFKs were necessary for CVB entry into BeWo placental trophoblast cells (**Figure 3.7A-B,D**). We performed the immunofluorescence-based virus internalization assay in the presence of either genistein or PP2, and found that both drugs prevented CVB entry into BeWo trophoblasts (**Figure 3.7D**). Thus, SFKs are required for CVB entry into placental trophoblasts. This is similar to the requirement of select members of the SFKs (Fyn and Abl) for CVB entry into human polarized intestinal epithelial [54] and endothelial cells [88], but not for entry into non-polarized cells [89].

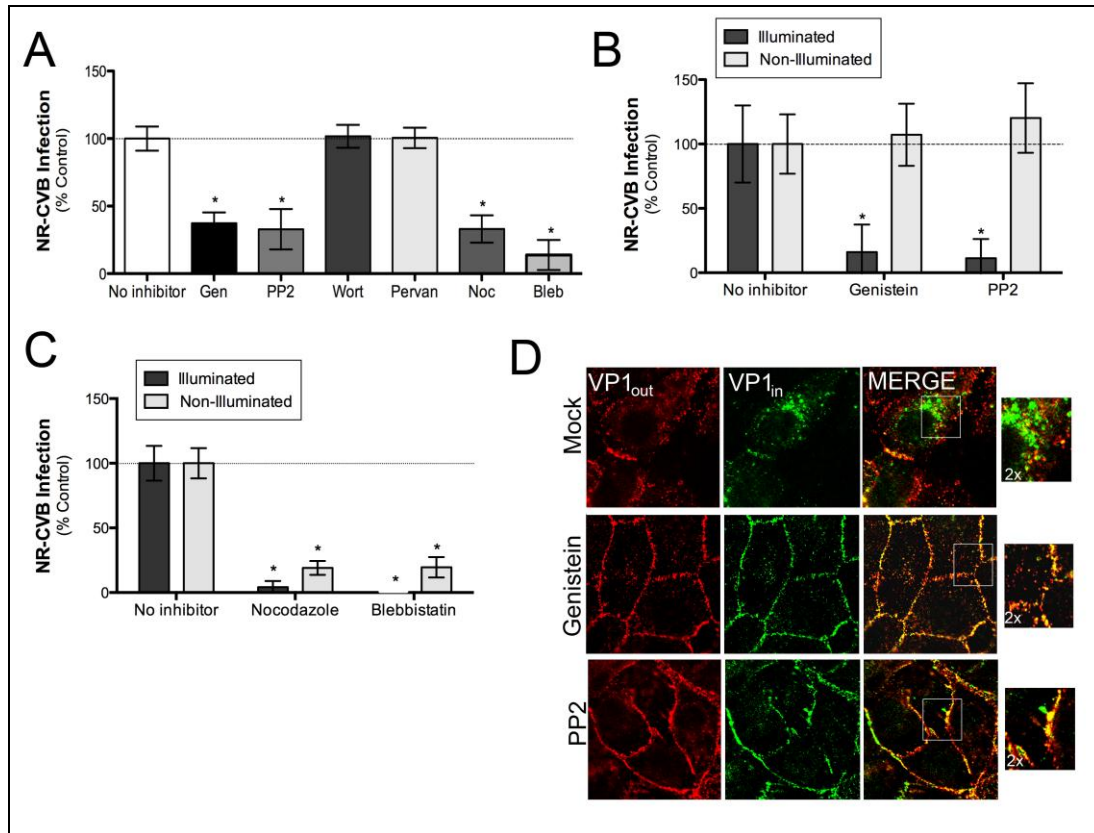


**Figure 3.7. CVB entry is dependent on Src family tyrosine kinases.** (A) BeWo cells were pre-treated for 60 min prior to and during neutral-red CVB (NR-CVB) infection with genistein (74  $\mu$ M), PP2 (30  $\mu$ M), wortmannin (2.5  $\mu$ M), pervanadate (50  $\mu$ M), nocodazole (10  $\mu$ g/mL), or blebbistatin (50  $\mu$ M). Cells were illuminated 2 hr p.i. to inactivate virions that had not yet entered. Images were captured and quantified. Shown are the percent-infected cells (VP1+/DAPI as assessed by IF; \* $p$ <0.001). (B) NRIC assay in BeWo monolayers treated with genistein (74  $\mu$ M) or PP2 (30  $\mu$ M). Shown are the percent-infected cells (VP1+/DAPI as assessed by IF; \* $p$ <0.0001). (C) NRIC assay in BeWo monolayers treated with nocodazole (10  $\mu$ g/mL) or blebbistatin (50  $\mu$ M). Shown are the percent-infected cells (VP1+/DAPI as assessed by IF; \* $p$ <0.001). (D) Cells were pre-treated with (74  $\mu$ M) or PP2 (30  $\mu$ M) for 60 min prior to and during binding with CVB (100-150 PFU/cell) at RT. Unbound virus was removed, and cells were incubated at 37°C (in the presence of drug) to facilitate virus entry. Cells were fixed at 90 min and serially stained for virus [prior to permeabilization (VP1<sub>out</sub>) and after permeabilization (VP1<sub>in</sub>)]. Red or colocalized (red and green overlapping) fluorescence denotes virus bound on the cell surface; distinctively green fluorescence (no red) denotes internalized virus. Magnified inserts (2x).

### 3.2.10 CVB entry into primary human trophoblasts (PHTs)

As these studies utilized an immortalized human trophoblast cell line – BeWo [235, 236], we wanted to investigate whether CVB entry into primary human placental trophoblast cells (PHTs) followed a similar mechanism (Figure 3.8). We found that the entry kinetics of CVB into PHTs were comparable to that in BeWo trophoblasts (Figure 3.2A and Figure 3.8). CVB was bound

to the apical cell surface at 0 min (**Figure 3.8**). Virus was observed to cluster at the apical domain and subsequently shuttle to the junction by 30 min (data not shown), with internalization by 90 min (**Figure 3.8**).

We also investigated whether the cholesterol-depleting agent M $\beta$ CD blocked CVB entry into PHTs, similar to BeWo trophoblasts (**Figure 3.5C** and **Figure 3.8**). Indeed, M $\beta$ CD inhibited CVB entry into PHTs at 90 min post-entry, as assessed by the immunofluorescence-based virus internalization assay (**Figure 3.8**). Thus, CVB utilizes similar entry kinetics and mechanisms in PHTs and BeWo trophoblasts. Additionally, the consistency of CVB entry kinetics and the dependence of CVB on lipid rafts for entry into PHTs and BeWo trophoblasts further demonstrates that BeWo cells are excellent cell culture models for model virus-host interactions *in vitro*.

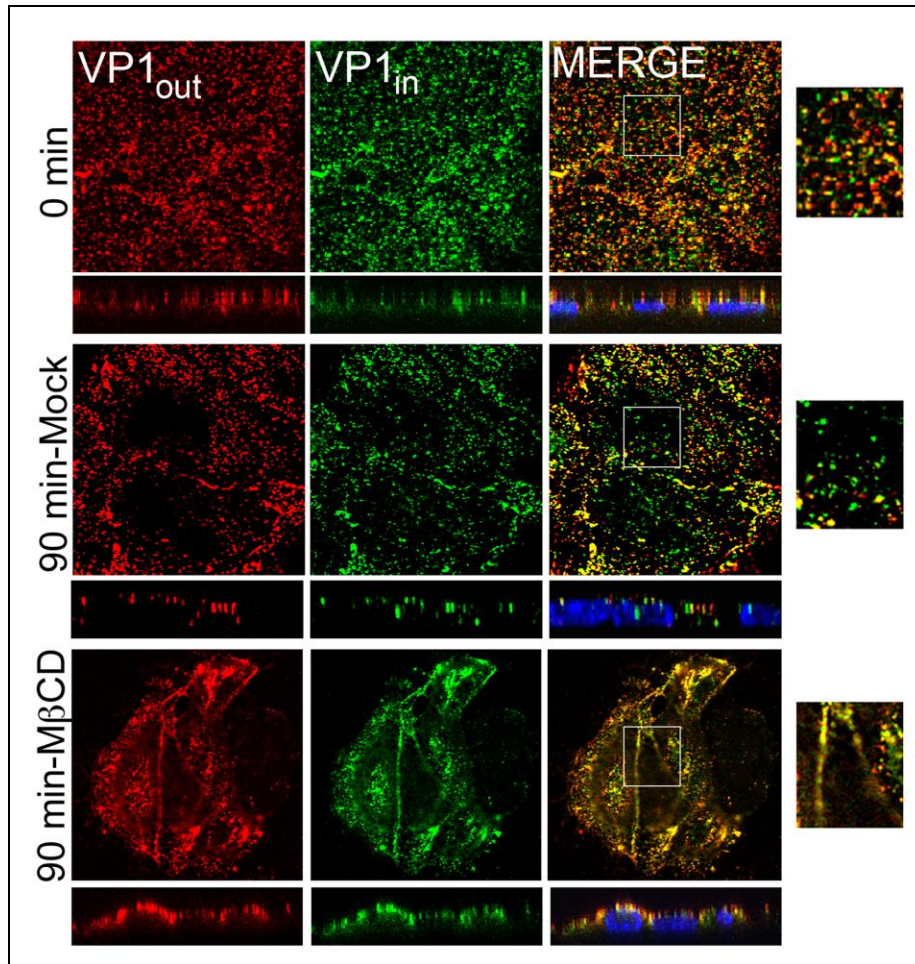


**Figure 3.8. CVB entry into primary human trophoblasts requires lipid rafts.** Primary human trophoblasts (PHT) cells were grown in culture, and CVB (250 PFU/cell) was bound at RT for 1 hr. Unbound virus was removed, and cells were incubated at 37°C to facilitate virus entry. Cells were fixed at the indicated time points and serially stained for virus [prior to permeabilization (VP1<sub>out</sub>) and after permeabilization (VP1<sub>in</sub>)]. Red or colocalized (red and green overlapping) fluorescence denotes virus bound on the cell surface; distinctively green fluorescence (no red) denotes internalized virus. DAPI is shown in blue. (Bottom row) In parallel, cells were pre-treated with MβCD (5 mM) for 1 hr prior to and during binding with CVB (250 PFU/cell) at RT. Unbound virus was removed, and cells were incubated at 37°C (in the presence of drug) to facilitate virus entry. Cells were fixed and serially stained. Magnified inserts (3x).

### 3.3 DISCUSSION

Viruses and other pathogens have clearly evolved mechanisms to subvert the protective placental barrier at the maternal-fetal interface, as incidences of fetal disease have been extensively reported [35-50]. Although the placenta has evolved its own innate immune functions to protect

itself and surrounding maternal tissues from virus infection (see chapter 2.0, “**Placental exosomes confer viral resistance**”), we cannot exclude that gestational stage, placental injury, and/or individual genetic variation may contribute to the propensity of viruses to enter and infect the placenta and/or neighboring cells. To initiate vertical infection and entry into the fetal compartment, viruses must first traverse and exit maternal circulation (possibly via the endothelium) to confront the formidable obstacle presented by the placenta trophoblasts. These findings reveal unprecedented insight into how enteroviruses may hijack the trophoblast cell defense machinery to initiate fetal infection *in utero*.

In this study, we have found that BeWo immortalized trophoblasts serve as excellent *in vitro* polarized cell culture models for investigating host-pathogen interactions at the maternal-fetal interface. BeWo trophoblasts exhibited characteristic junctional complexes and unique polarized localization of apical, junctional, and basolateral proteins (**Figure 3.1A-B**). The virus receptors DAF and CAR localized to the apical surface and tight junction (TJ), respectively (**Figure 3.1B**), which is consistent with what has been observed in other polarized cell types [54, 82, 85, 88]. CVB3-RD also required the co-receptor DAF for efficient infection in BeWo trophoblasts (**Figure 3.1C-E**), which is also consistent with CVB3-RD infection in other polarized cell types [54, 85, 88]. Furthermore, CAR was required for both entry and infection in BeWo trophoblasts (**Figure 3.2C-D**), but did not internalize with virus (**Figure 3.2B**). This is consistent to what has been found in polarized intestinal epithelial cells [54], but in contrast to CVB entry in non-polarized cells [89].

Also presented here is a unique mechanism whereby Coxsackievirus B-3 isolate RD (CVB3-RD) enters and infects polarized human placental trophoblast cells. In both immortalized and primary human trophoblasts (PHTs), we have found that CVB follows entry

kinetics similar to what has been observed in polarized human intestinal epithelial cells (**Figure 3.2A** and **Figure 3.8**; [54]) with virus internalized to areas adjacent to the nucleus by 90 min. Applying a modified NRIC assay with light-sensitive neutral-red CVB3-RD (NR-CVB) has also enabled us to dissect the route by which CVB usurps and hijacks the host cell machinery to enter and infect placental trophoblasts (**Figures 3.3A, 3.5A, 3.6A** and **3.7B-C**). We also detected no role for the clathrin or dynamin II-dependent endocytic machinery by utilizing known pharmacological inhibitors (chlorpromazine, MDC, dynasore) and siRNAs (CHC, dyn II) targeting these cellular components (**Figure 3.3**). Again, this was similar to CVB entry into polarized intestinal epithelia [54]; however, this was also in contrast to CVB entry into polarized endothelia [88] and non-polarized cells [89], wherein dynamin II was required.

We also found that lipid-rafts (but not caveolin-1) were necessary for CVB entry into polarized trophoblasts (**Figure 3.5** and **Figure 3.8**). By screening pharmacological inhibitors of caveolae and lipid rafts (filipin, nystatin, M $\beta$ CD) in the modified NRIC assay, we determined that M $\beta$ CD blocked both CVB infection and entry (**Figure 3.5A,C**). To note, the pharmacological activities of filipin and nystatin differ from M $\beta$ CD [211], which may potentially explain why an inhibitory effect on CVB was observed with M $\beta$ CD but not with filipin or nystatin (**Figure 3.5A**). Furthermore, transfection of a siRNA targeting caveolin-1 (cav-1), the transmembrane protein component critical for the formation of caveolae [62], had no effect on CVB infection in these cells, suggesting that lipid rafts but not caveolae were necessary for CVB entry into BeWo cells (**Figure 3.5B**). This mechanism differs from CVB entry into polarized intestinal epithelial and human brain microvascular endothelial cells in which caveolin-1 was required [54, 88]. However, in non-polarized HeLa cells, both filipin and M $\beta$ CD, but not the loss of cav-1 by siRNA targeting, reduced CVB infection [89].

Surprisingly, we found no role for macropinocytosis in the uptake of CVB into placental trophoblasts (**Figure 3.6** and data not shown). This demonstrates a divergent mechanism for CVB entry in comparison to polarized intestinal epithelial cells, which required features of macropinocytosis [55]. Interestingly, the mechanism of CVB entry into placental trophoblasts is very similar to HIV entry into polarized trophoblasts, which was independent of clathrin-, caveolae, dynamin II, and macropinocytosis but required free-cholesterol and lipid rafts [237]. Furthermore, Vidricaire *et al.* found that filipin, but not M $\beta$ CD, inhibited HIV entry and infection in immortalized JAR trophoblasts [237].

Previous work has demonstrated a significant role for SFK members in mediating various aspects of CVB entry into polarized intestinal epithelial and human brain microvascular endothelial cells [54, 88]. Additionally, SFKs appeared to be important for early stages of CVB infection in non-polarized cells but were not required for virus entry [89]. Applying two pharmacological inhibitors – genistein (a pan tyrosine kinase inhibitor) [231] and PP2 (a SFK selective inhibitor) [232] – in both the CVB NRIC and internalization assays demonstrated that Src family tyrosine kinases were critical for CVB entry into BeWo trophoblasts (**Figure 3.7A-B,D**). Clearly, the inclination of CVB to usurp this cellular signaling pathway to promote its invasion into the host is a common strategy used across multiple polarized and non-polarized cell types (**Figure 3.7A-B,D** and [54]). Given the key cellular functions of SFK members, this is not surprising. SFKs, a family of non-receptor tyrosine kinases, are critical for a myriad of cellular processes. Members of the SFKs are involved in intracellular signaling cascades, cell growth, differentiation, proliferation, motility, and survival, *reviewed* [238]. Furthermore, deregulation of SFKs contributes to the progression of various types of cancer, *reviewed* [239-241].

At the present time, the multitude of endocytic and signaling mechanisms utilized by diverse viruses (such as CVB) to enter and infect placental trophoblasts are unknown. Elucidation of the endocytic pathways and host signaling associated with virus entry are important for modeling pathogen transmission and infection of the placenta. Specific targeting of molecular mediators of CVB entry in the placenta is critical for reducing the incidences of prenatal disease during pregnancy. These studies also have the therapeutic potential for preventing prenatal infections, pre-term labor, birth defects, and fetal death.

## 4.0 CONCLUSIONS

Throughout evolution, viruses and host cells have competed for supremacy. Arguably, without complex pathogen defense strategies, fetal development could not be sustained due to the constant onslaught of microbes in our daily environment. However, we also know that pathogens have developed effective countermeasures to overcome the innate protective mechanisms used by placental trophoblasts. Often, *in utero* pathogen infections cause highly detrimental pathologies in the developing fetus, including pre-term labor, fetal and neonatal disease, birth defects, miscarriage, and even neonatal death [24, 26, 27, 29, 31, 32, 35-50, 190]. Therefore, it is crucial that ongoing studies are aimed at investigating both virus entry (and other pregnancy-associated pathogens) and host defense at the maternal-interface. This dissertation has explored both sides of virus-host interactions at the maternal-fetal interface – virus entry and placental trophoblast defense. These studies have the potential for developing therapeutic strategies designed to reduce the incidence of pre-term labor, miscarriage, prenatal and neonatal pathologies, and birth defects.

### 4.1 PLACENTAL EXOSOMES CONFER VIRAL RESISTANCE

Abundant evidence exists supporting the devastating prenatal and neonatal diseases resulting from *in utero* infections [24, 26, 27, 29, 31, 32, 35-50, 190]. However, little was known

regarding the diverse strategies employed by cells at the maternal-fetal interface to defend against pathogen invasion. As the placenta is an indispensable barrier to the fetal compartment, both functionally and physically, we were particularly interested in investigating the mechanisms by which placental trophoblasts protect the fetus from invading pathogens during pregnancy. Our initial studies investigated virus infection in primary human trophoblast (PHT) cells isolated from healthy, term placentas. Astonishingly, we found that PHTs were resistant to infection by a panel of disparate viruses (e.g. CVB, PV, VSV, VV, HSV-1, CMV). This was very intriguing as our PHT culture conditions promote trophoblast differentiation along the syncytiotrophoblast lineage [242, 243]. Previous work by others has also indicated that the syncytiotrophoblast cells may serve as a bottleneck for pathogen invasion into the placental unit to prevent transmission to the fetus [7, 15, 16, 19]. Evolutionarily, this is the ideal adaptation as the syncytiotrophoblast cells lie in direct contact with the maternal blood, and thus, would serve as the initial target site for any pathogen attempting to invade into the fetal compartment.

Strikingly, we also found that PHTs were able to confer this antiviral effect to non-placental recipient cells via trophoblast conditioned medium, trophoblast-derived exosomes, stable expression of the entire C19MC, or select miRNAs (miR-512-3p, miR-516b-5p, and miR-517-3p) from the primate- and placenta-specific chromosome 19 miRNA cluster (C19MC). Intriguingly, C19MC miRNAs are cargo of PHT exosomes, and their expression levels in PHT-exosomes correlates very closely to their expression levels in PHTs [115]. It is interesting to speculate that, during pregnancy, the secretion of placental-derived exosomes containing antiviral C19MC miRNAs may mediate systemic innate immune defense to the mother. In our studies, we have identified that relevant maternal-fetal cell types including placental fibroblasts, human uterine maternal vascular endothelial cells (HUtMVEC), human umbilical vein

endothelial cells (HUVEC), primary human foreskin fibroblasts (HFF), and human uterine epithelial (RL-95) cells are receptive to PHT exosomes and mediate antiviral effects following exposure to conditioned trophoblast medium. Additionally, we found that a number of non-specific cell types, such as non-polarized (U2OS human osteosarcoma cells, Vero African green monkey kidney cells, Huh 7.5 human liver hepatocellular carcinoma, HT1080 human fibrosarcoma cells, and polarized (Caco-2 human intestinal epithelial cells). This further demonstrates that PHT-derived exosomes are capable of transferring viral resistance to a wide variety of cell types. These data point to the finding of a novel mechanism that may serve to defend the developing fetus and surrounding maternal tissues against microbial invaders.

It has been published that human placental trophoblasts abundantly express both C19MC- and non-C19MC miRNAs and other small RNAs (snRNA, snoRNA, piRNA) throughout pregnancy [115, 116, 139-142]. Interestingly, C19MC miRNAs have been detected in the plasma of pregnant women [115, 116, 139], and the levels of C19MC miRNAs in maternal circulation “decrease dramatically after delivery” [116]. Furthermore, Luo *et al.* found that the blood plasma levels of maternal C19MC miRNAs were lower in the first-trimester of pregnancy compared to full-term pregnancies [116]. Remarkably, several clinical reports have described the pathogenicity of certain prenatal infections as being more detrimental during the first trimester (when according to Luo *et al.*, circulating C19MC miRNA levels would be low) as compared to infection during later in pregnancy (when C19MC levels would be higher) [116, 149, 150]. There appears to be a paradox in terms of the balance of virus infection and virus protection. In our studies, we have observed that PHTs resist infection by a number of diverse viruses (CVB, PV, VSV, VV, HSV-1, CMV). On the other hand, incidences of prenatal infections have been widely reported [24, 26, 27, 29, 31, 32, 35-50, 190]. The possibility exists

that individual variation in the number of and/or low numbers of circulating C19MC miRNAs (either due to genetic contributions or to the developmental stage of the pregnancy) in the maternal blood may offer one possible explanation for a defect in this seemingly perfect defense mechanism, contributing to the aberrant proliferation of incoming pathogens. Altogether, this supports that circulating levels of C19MC miRNAs in the maternal blood contribute to antiviral effects *in vivo*.

In addition to inducing potent antiviral effects, our data support that conditioned trophoblast medium, purified PHT exosomes, and select miRNAs of the C19MC family robustly induce autophagy. Autophagy has recently been identified as a significant antimicrobial host defense mechanism [74, 156, 166-169]. Surprisingly, we found no role for type I IFN signaling in recipient cells, and conditioned PHT medium had potent antiviral effects in cells incapable of inducing downstream ISGs. Inhibition of C19MC-induced autophagy by either the pharmacological agent 3-MA or by siRNA-mediated silencing of beclin-1 was sufficient to restore viral infection (**Figure 2.9a-b**). In contrast to autophagy stimulated in response to virus challenge as an arm of the host defense pathway, C19MC-dependent autophagy occurs *prior* to any viral stimulation. Viruses internalizing through the endosomal pathway may be trafficked along the autophagic route, destined for degradation within lysosomes (and thus preventing viral uncoating and replication). Our data demonstrated that entering VSV virions colocalized with LC3b-positive autophagosomes and that inhibition of viral replication occurs very early during the virus life cycle, further supporting this model. However, additional study to fully elucidate the mechanism by which C19MC-induced autophagy promotes viral trafficking along the autophagic pathway is needed, and future work should be aimed towards this purpose.

Given that we did detect unusually high levels of baseline autophagy in PHT cells

(*without* viral stimulation), PHTs restricted infection very early in the virus life cycle, and the pharmacological inhibitor 3-MA bolstered infection in PHTs, autophagy may be one mechanism PHT cells employ to shield against pathogens. There likely exists a highly complex repertoire of antimicrobial defense mechanisms used by placental trophoblasts to prevent vertical transmission to the fetus, given the inherent necessity to maintain a sterile environment for healthy development. Further study is needed to fully establish the connection between placental trophoblasts and antiviral autophagy. However, additional questions are raised as well. *Do C19MC miRNAs contribute to the antiviral phenotype of PHT cells?* As there are 46 unique miRNAs in this cluster, *what other functions do C19MCs contribute to in the placental trophoblast?* And, *what are the other mechanisms utilized by PHTs to defend against diverse microbial invaders?* Clearly, further investigation is required.

Taken together, these data provides evidence for a novel autocrine, paracrine and/or systemic function of placental trophoblasts as facilitators of maternal-fetal communication via exosome-mediated delivery of trophoblast-derived miRNAs. Although we have not yet identified the *in vivo* effector cells that these exosomes primarily target, the possibility remains that this delivery system may be critical to mediate antiviral effects and/or the upregulation of autophagy throughout the maternal-fetal unit. Autophagy is critical for neonatal survival during the post-birth period [182, 183], *reviewed* [154, 244], and it is exciting to speculate that trophoblast-mediated exosomal transfer of C19MC miRNAs may be a component of this process.

As mentioned in section **2.3 “Discussion,”** out of all of the viruses tested in this study, it is intriguing that CMV infection was considerably enhanced in recipient cells exposed to conditioned trophoblast medium or in cells stably expressing the entire C19MC-BAC. CMV is a

component of the TORCH complex, owing to its highly pathologic effects on the fetus when infections occur *in utero* (see subsection **1.2.1 “TORCH infections”**). CMV infection during pregnancy is associated with fetal abnormalities including liver, lung, and spleen pathologies, jaundice, seizures, IUGR, hearing and/or vision loss, small head, mental disabilities, lack of coordination, seizures, and/or death [29]. Interestingly, CMV is also known to counteract antiviral autophagy in response to virus stimulation [176, 177]. However, in addition to CMV, at least one of the viruses tested in this study (eg. CVB [180, 181]) may actually benefit from autophagy as a mechanism to enhance replication. *So, why does CMV infection increase while the replication of the other viruses tested is inhibited? Is this why CMV remains one of the leading infectious disease concerns during pregnancy? Are other TORCH pathogens upregulated in response to conditioned medium and/or C19MC miRNAs?* Undoubtedly, further study is needed to determine the mechanisms by which C19MC miRNAs enhance CMV replication.

The data presented here demonstrates a role for a novel mechanism of transferrable, autophagy-dependent antiviral responses. Future studies will be aimed towards testing and determining what other pathogens, particularly those among the TORCH complex, are susceptible to either the antiviral or proviral effects of C19MC miRNAs. To expand upon the observations made *in vitro*, the development of a non-human primate animal model would be invaluable to studying virus-host interactions at the maternal-fetal interface. This could also provide additional information on the route by which pathogens traverse the maternal blood to gain access to various trophoblast populations, and ultimately, to enter into the fetal compartment.

However, a major question remains – *what are the mRNA targets of the C19MC miRNAs (both in PHTs and in recipient cells)? Furthermore, what are the mRNA targets of the C19MCs tested (miR-512-3p, -516b-5p, and -517-3p) that are responsible for the robust induction of autophagy?* Ongoing work in the laboratory is directed towards answering these questions. Furthermore, we do not know if these miRNAs act individually or synergistically *in vivo* with the antiviral/pro-autophagy miRNAs we have identified (miR-512-3p, -516b-5p, and -517-3p), or if there are other C19MC miRNAs that have yet to be recognized. Individual miRNAs may potentially act on hundreds of protein targets, either directly or indirectly *reviewed* [245], further complicating mRNA target identification. MiRNA target prediction databases such as TargetScan, miRanda, and PicTar generate predicted hits based on seed region base pairing in the 3'UTR of mRNAs, but many projected targets are not true target mRNAs [245].

*Moreover, what is the therapeutic potential of developing exosome-based C19MC miRNA delivery systems for treating severe and/or chronic viral infections?* The potential for designing therapeutic strategies for combating infections, not only for during pregnancy but for routine applications, is attractive. Currently, the market is limited in terms of the available antiviral treatments, and approved antivirals are mainly for the treatment of pre-existing, chronic viral infections, such as HIV or HSV [70]. Exosomal delivery of miRNAs or other small RNAs could theoretically be engineered to target specific cell populations. The design of novel exosome-mediated delivery system for therapeutic, or even preventative purposes would be a significant advance.

## 4.2 CVB ENTRY INTO HUMAN PLACENTAL TROPHOBLASTS

From the data presented in chapter 2.0 “**PHT exosomes confer viral resistance,**” we know that the placenta mediates its own innate antiviral defense strategies. However, this also raises several questions. *What contributes to the disruption of placental defense factors, resulting in fetal infection? Are the EVTs truly the ‘weak link’ allowing for pathogen invasion?* It is important to also consider that placental injury, hypoxia, individual genetic variation, and defects in exosome packaging, secretion, and recipient cell uptake may potentially contribute to the propensity of prenatal microbial infections, despite existing trophoblast defense mechanisms. Therefore, we also investigated the mechanisms by which CVB, a virus known to cause fetal pathology, enters into human placental trophoblast cells to model virus-host interactions at the maternal-fetal interface.

In these studies, we have utilized both immortalized BeWo and primary human trophoblast (PHT) cells to investigate CVB entry. We found that BeWo cells were excellent *in vitro* polarized models for studying virus-host interactions. As immortalized BeWo cells are a cell line derived from a choriocarcinoma (a malignant trophoblast cancer) [235, 236], we expected there to be possible variability from normal trophoblast tissue. Thus, we validated our key findings in PHT cells, and found strikingly similar results both in the kinetics of entry and in the lipid-raft dependent pathway utilized by the virus.

We found that CVB attachment factor and co-receptor DAF was necessary for efficient binding and entry into human placental trophoblasts. We also uncovered no evidence for CVB receptor CAR internalization with virus, similar to what has been observed in polarized Caco-2 intestinal epithelial cells [54]. However, CAR does internalize with CVB in non-polarized cells [89]. CAR is a junctional transmembrane protein that also interacts with ZO-1 and the multi-

PDZ domain protein-1 (MUPP-1) [82, 246]. Addition of soluble CAR and anti-CAR antibodies disrupts tight junctions, *reviewed* [247]. One possible explanation for why CAR may not internalize with virus in polarized cells is that the virus may usurp normal homeostatic mechanisms for tight junction remodeling to promote its endocytosis [248].

To dissect the route by which CVB enters placental trophoblast cells, we performed a variety of assays and techniques, including immunofluorescence-based infection assays, NR-CVB infections, NRIC assays, virus entry assays, pharmacological inhibitors, and siRNAs targeted towards cellular components involved in endocytosis and signaling. We found that CVB required a non-clathrin, non-caveolar, and dynamin-independent, lipid-raft dependent route that required Src family tyrosine kinase signaling. Although we uncovered similarities between CVB entry into placental trophoblasts with similarities to CVB entry into certain cell types, we also found differences (see section **3.3 “Discussion”**). As pharmacological inhibitors utilized in a standard infection assay can potentially inhibit multiple steps in the virus life cycle, we applied the NRIC assay to specifically discriminate the effects of a particular drug on virus entry v. other non-entry events. For example, in a conventional infection assay, it may be difficult to distinguish between inhibition of virus entry versus a block of a non-entry event such as replication. Given that pharmacological drugs can have a variety of off-target, non-specific effects [211], we also complimented our studies with siRNAs. Taken together, these data identify key pathways necessary for successful CVB entry into human placental trophoblasts.

At the present time, our understanding is limited regarding the molecular events associated with pathogen entry into placental trophoblast cells. In order to develop effective therapeutic strategies to prevent and combat infections during pregnancy, we must have an understanding of the pathways by which viruses associated with causing prenatal disease hijack

host pathways to enter, replicate, and disseminate. Furthermore, microbial infections during pregnancy are associated with a variety of pathologies including induction of pre-term labor, birth defects, and/or fetal death. Further study is required to effectively reduce the incidences of infectious diseases *in utero*.

### 4.3 CONCLUDING REMARKS

Thus far, there is still much to uncover by investigating virus-host interactions at the maternal fetal interface. Here, we present work examining virus entry of a known prenatal pathogen and a novel means of innate transferrable trophoblast-mediated antiviral defense. These studies are critical, not only to further our understanding of the molecular mechanisms involved in virus entry and host defense during *in utero* development, but also to develop therapeutic strategies aimed at preventing fetal disease. Although we have presented here that human placental trophoblasts have complex mechanisms for thwarting viral invasion, infectious diseases continue to cause prenatal and neonatal pathologies [24, 26, 27, 29, 31, 32, 35-50, 190]. The second body of work presented here explored the mechanisms by which a known prenatal pathogen enters into human placental trophoblast cells. Currently, the available therapeutic options for pathogen infections during pregnancy are limited [26, 28, 30, 32]. Even if an infection is identified and a treatment is available, there may be little therapeutic benefit if the infection is too far advanced. Therefore, continued investigation into the development of new therapeutics for treating prenatal infections is essential. The identification of exosome-delivered C19MC miRNAs as potent inducers of viral resistance presents a novel option for prevention and treatment of virus

infections. Undoubtedly, further study into both sides of virus-host interactions at the maternal fetal interface is critical for reducing the rates of preterm birth, birth defects, and fetal death.

## 5.0 MATERIALS AND METHODS

### 5.1 CELLS

Primary human trophoblasts (PHT) and primary placental fibroblasts were provided by Dr. Yoel Sadovsky at the Magee-Womens Research Institute (Pittsburgh, PA). PHT cells were isolated from healthy singleton term placentas using the trypsin-deoxyribonuclease-dispase/Percoll method as described by Kliman *et al.*, with previously published modifications [242, 249] under an exempt protocol approved by the Institutional Review Board at the University of Pittsburgh. Under the protocol, patients provided written consent for the use of de-identified, discarded tissues for research upon admittance to the hospital. Isolated PHTs were maintained in DMEM (Sigma) containing 10% fetal bovine serum (FBS; Hyclone), 2% HEPES (20 mM/L), 1% Fungizone (Invitrogen), and antibiotics at 37°C. Cells were maintained 72 hr after plating, with cell quality monitored both morphologically (by microscopy) and by medium human chorionic gonadotropin (hCG) levels by ELISA (DRG International) showing a characteristic increase in medium hCG as cytotrophoblasts differentiate into syncytiotrophoblasts [242, 243]. Primary placental fibroblasts were isolated and maintained in DMEM-H supplemented with 10% FBS, HEPES, L-glutamine, and antibiotics.

BeWo cells were obtained from the ATCC and cultured in Ham's F-12K medium with Kaighn's modification containing 10% FBS and 1% penicillin/streptomycin. Cells were plated on collagen-coated 8-well chamber slides (LabTek) at a density of  $1.5 \times 10^5$  cells/well, on 24-

well plates at  $2.4 \times 10^5$  cells/well, on 12-mm Transwell-Col inserts (0.4- $\mu$ m pore size) (Costar) at  $1.25 \times 10^6$  cells/well, or collagen-coated 6-well plates at  $1.6 \times 10^6$  cells/well. Cells were grown a minimum of 48 hr prior to study.

Human osteosarcoma U2OS, HFFs, Huh7.5, HeLa, and HT1080 cells were cultured in DMEM-H supplemented with 10% FBS and antibiotics. HFF cells were provided by Dr. Jon Boyle, Department of Biological Sciences, University of Pittsburgh. HuVEC (human umbilical vein endothelial cells) and HUtMVEC (human uterine microvascular endothelial cells) were provided by Dr. Carl Hubel at the Magee-Womens Research Institute (Pittsburgh, PA) and were cultured in phenol-red free GM-2 supplemented with 5% FBS and antibiotics. Vero African green monkey kidney cells were maintained in DMEM-H supplemented with 5% FBS and antibiotics. Caco-2 (ATCC clone) human intestinal epithelial cells were cultured in MEM supplemented with 10% FBS, non-essential amino acids, sodium pyruvate, and antibiotics. All cells were maintained at 37°C in a 5% carbon dioxide (CO<sub>2</sub>)-air atmosphere.

## 5.2 VIRUSES

Experiments were performed with vesicular stomatitis virus (VSV), green fluorescent protein (GFP)-tagged VSV, coxsackievirus B3-Nancy (non-DAF binding) as described [89], coxsackievirus B3-RD isolate (CVB3-RD; DAF-binding) as described [54], recombinant yellow fluorescent protein (YFP)-tagged vaccinia virus (VV) as described [250], poliovirus (PV) as described [251], cytomegalovirus (hCMV Towne strain, obtained from Dr. William Goins (University of Pittsburgh), or GFP-tagged herpes simplex virus-1 (HSV-1, strain KOS) as described [252].

## **5.3 VIRUS EXPANSION AND PREPARATION**

### **5.3.1 VSV**

For VSV and GFP-VSV expansion, Vero cells were seeded on T-150 flasks. One day later, cells were washed twice with phosphate buffered saline (PBS). Virus (0.01 PFU/mL) was added to cells in 7 mL, 2% FBS Vero complete medium. Cells were incubated at 37°C for 1 hr, rocking every 15 min to verify even virus distribution. After 1 hr, virus inoculum was removed by aspiration, and 15 mL, 2% Vero complete medium was added/T-150 flask at 37°C. Cells were dead by 48 hr. The medium was removed from the flask. A debris spin was performed at 1,500 rpm for 15 min. The supernatant was aliquoted and frozen at -80°C.

### **5.3.2 CVB**

For CVB expansion, HeLa (clone 7b) cells were seeded on T-150 flasks. When confluent, cells were washed with PBS. CVB was bound in MEM containing 20 mM HEPES (1 µL virus/8 mL MEM). Cells were incubated at RT for 1 hr, rocking. After 1 hr, virus inoculum was removed. Cells were washed with PBS, and complete medium was added (10 mL/flask). Cells were incubated at 37°C for 24 hr until cell death. Flasks were then freeze (-80°C)/thawed (in warm water) for three times to lyse cells. During the last thaw, four flasks worth of virus-containing media (40 mL) was added to a 50 mL conical, and 2 mL, 10% Triton X-100 was added. The tube was inverted to mix and kept on ice for 10 min. A debris spin was performed with a pre-cooled SW28 rotor at 7,000 rpm for 20 min at 16°C in a Beckman XL-90 ultracentrifuge. Following the debris spin, the supernatant was added to a new 50 mL conical containing 3 mL,

10% SDS. A sucrose cushion was prepared by adding 1.5 mL, 30% sucrose to an ultracentrifuge tube (for SW28 rotor). SDS and supernatant were mixed by pipet, and slowly added to the side of the ultracentrifuge tube. Ultracentrifuge tubes were balanced with PBS. The sucrose cushion spin was performed using a pre-cooled SW28 rotor at 27,000 rpm for 3 hr at 16°C in a Beckman XL-90 ultracentrifuge. Residual sucrose/SDS/PBS were removed (virus should be pelleted at the bottom of the tube). Virus was resuspended in 1 mL PBS, aliquoted, and stored at -80°C.

### **5.3.3 Neutral red labeled CVB**

To prepare neutral red-labeled CVB3-RD (NR-CVB3-RD), CVB3-RD was grown on HeLa cells (clone 7B) (as described in Materials and Methods subsection **5.3.2 “CVB”**) in media containing neutral red dye (10 µg/mL; Sigma) [206, 207]. NR-CVB3-RD was purified and plaque assays were performed as described above. All procedures were performed under semi-dark conditions. To test the light sensitivity of the NR-CVB3-RD, plaque assays were performed, and cells were exposed to a light box after the binding step (as described in Materials and Methods subsection **5.4.2 “CVB”**).

## **5.4 PLAQUE ASSAYS**

### **5.4.1 VSV**

For VSV plaque assays, Vero cells were seeded on 12-well plates ( $4.5 \times 10^5$  cells/well). One day later, serial dilutions of virus ( $10^{-5}$  to  $10^{-9}$  in DMEM) in duplicate were added to confluent cells

(200  $\mu$ L/well). VSV was bound to cells for 1 hr at 37°C, rocking every 15 min. Virus inoculum was removed, and cells were washed with PBS. Agarose overlay<sup>6</sup> was added (1 mL/well). Plaque assays were incubated for ~24 hr at 37°C. Agarose plugs were removed. Plaques were visualized with crystal violet staining (0.05% crystal violet in 10% ethanol) and enumerated to calculate titers.

#### 5.4.2 CVB

For CVB plaque assays, HeLa (7b) cells were seeded on 12-well plates ( $9 \times 10^5$  cells/well). One day later, serial dilutions of virus ( $10^{-2}$  to  $10^{-12}$  in complete medium) in duplicate were added to confluent cells (150  $\mu$ L/well). CVB was bound to cells for 1 hr at RT, rocking every 15 min. Virus inoculum was removed, and cells were washed with PBS. Agar overlay<sup>7</sup> was added (1.5 mL/well). Plaque assays were incubated for ~40 hr at 37°C. Titers were calculated by visualizing and enumerating plaques with 2xMTT/INT.

To prepare the 2xMTT/INT solution, PBS (100 mL) was heated to 90°C, and 60  $\mu$ L glacial acetic acid was added. INT (150 mg; Sigma) was stirred in, and the solution was allowed to cool to 50-60°C. MTT (600 mg) was stirred into solution. Aliquots were stored at -20°C.

---

<sup>6</sup> Agarose overlay was prepared by adding 10 mL media overlay (25 mL 2xMEM, 2.5 mL FBS, 0.5 mL penicillin/streptomycin, 7.5 mL dH<sub>2</sub>O) and 3.5 mL, 1.6% agarose in dH<sub>2</sub>O.

<sup>7</sup> Agar overlay included a 1:1 mixture of agar (0.8% for CVB3-RD and 1.5% for CVB3-Nancy) in dH<sub>2</sub>O with 10 mM MgCl<sub>2</sub>) and media overlay (2xMEM, 10% FBS, 2xNEAA, and 2x penicillin/streptomycin).

### **5.4.3 Neutralizing virus plaque assays**

VSV virus stock was diluted 1:20 in either non-conditioned or conditioned PHT medium, then incubated at 37°C for 1 hr. Plaques assays were performed on Vero cells (as described in subsection 5.4.1 “VSV”). Plaques were visualized after 36 hr by staining with crystal violet.

## **5.5 MODIFIED TCID50 VIRUS TITERING ASSAYS**

Vero or PHT cells were seeded to confluence on 96-well plates. Cells were incubated with serial dilutions of virus (CVB, VV, GFP-VSV, HSV-1) for ~40-45 h, then stained with crystal violet. For experiments performed with conditioned medium, Vero cells were incubated in non-conditioned or conditioned medium 24 hr prior to incubation with virus. Serial dilutions of virus were made in either non-conditioned or conditioned medium, and cells were incubated and developed by staining with crystal violet.

## **5.6 ANTIBODIES**

Mouse anti-VSV-G, mouse anti-hCMV gB glycoprotein, mouse anti-HA, rabbit anti-IRF3, rabbit anti-p65, rabbit anti-GAPDH conjugated to HRP, goat anti-beta-actin, and goat anti-EEA1 antibodies were obtained from Santa Cruz Biotechnology. Mouse anti-enterovirus VP1 (NCI-Enterovirus) monoclonal antibody was purchased from Novacastra Laboratories. Affinity-purified CAR-specific rabbit antibody has been described [85]. Mouse anti-DAF (clone IF7) was a

generous gift from Dr. Jeffrey Bergelson (University of Pennsylvania) [205]. Mouse-anti clathrin heavy chain (CHC) and mouse anti-caveolin 1 (cav-1) antibodies were obtained from BD Transduction Laboratories. Rabbit anti-dynamin II (dyn II) antibody was purchased from Abcam. Rabbit anti-p62 and rabbit anti-Beclin1 antibodies were obtained from Cell Signaling Technology.

## **5.7 PHARMACOLOGICAL AGENTS**

### **5.7.1 Autophagy assays**

Cells were pre-treated with 3-methyladenine (3-MA; 5 mM, Sigma) for 30-60 min prior to infection, and the drug was incubated throughout the duration of infection. For mRFP-LC3b punctae assays, 3-MA was added for 30 min prior to non-conditioned or conditioned media exposure, and was present throughout. Rapamycin (5  $\mu$ M, Calbiochem) treatment or serum-starvation with Hank's balanced salt solution (HBSS, Gibco) for 4 hr was used as a positive control for autophagy.

### **5.7.2 CVB entry assays**

For pharmacological inhibitor studies, cells were pre-treated with inhibitor for 60 min before and during infection or entry assays in complete media. However, for the experiments involving dynasore or drugs targeting lipid-raft disruption (filipin, nystatin, M $\beta$ CD) were incubated in complete medium containing 10% NuSerum (BD Transduction Laboratories) rather than FBS as

the presence of serum can negatively impact the efficacy of these drugs [89, 253]. Dynasore (25  $\mu\text{M}$ ), chlorpromazine (12.5  $\mu\text{g/mL}$ ), monodansylcadaverine (MDC; 100  $\mu\text{M}$ ), filipin (3  $\mu\text{g/mL}$ ), M $\beta$ CD (5 mM), [EIPA 5-(*N*-ethyl-*N*-isopropyl) amiloride; 102  $\mu\text{M}$ ], and rottlerin (10-20  $\mu\text{M}$ ) were purchased from Sigma. Nystatin (25  $\mu\text{g/mL}$ ) and Cytochalasin D (2.5  $\mu\text{g/mL}$ ) were obtained from MP Biomedicals. Genistein (74  $\mu\text{M}$ ), PP2 (30  $\mu\text{M}$ ), wortmannin (2.5  $\mu\text{M}$ ), nocodazole (10  $\mu\text{g/mL}$ ), latrunculin A (1  $\mu\text{M}$ ), blebbistatin (50  $\mu\text{M}$ ), and toxin B (1 ng/mL) were purchased from Calbiochem.

## 5.8 CONDITIONED MEDIUM TREATMENT

Conditioned media from PHT or other cells were harvested between 48-72 hr post plating (**Figure 5.1**). Non-conditioned medium was complete PHT medium (described in section 5.1 “Cells”) that had not been incubated with PHT cells. Conditioned media were subjected to sonication or heat-inactivation for 30 min at 65°C. Recipient cells were exposed to conditioned medium for ~24 hr prior to assay.

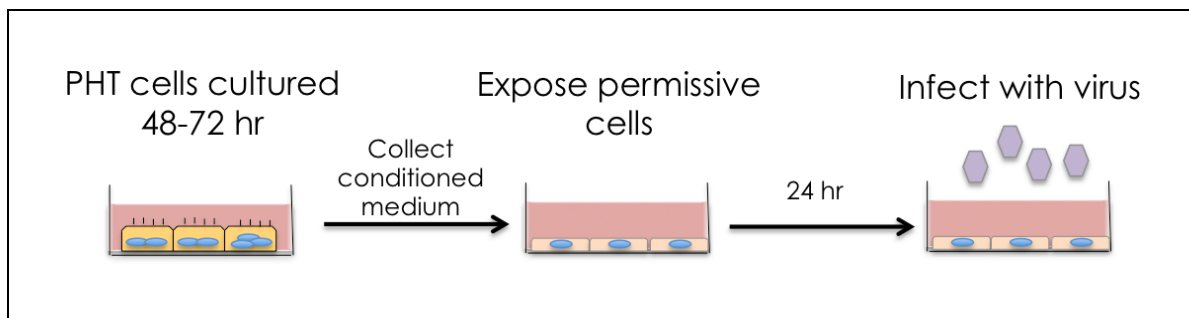


**Figure 5.1. Culturing recipient cells with conditioned PHT medium.** Shown is a schematic of primary human trophoblast cells isolated from term placentas were cultured for approximately 48-72 hr to promote syncytiotrophoblast differentiation. Media supernatant was collected from these cells (thereafter known as conditioned PHT medium). The media was passed onto naïve permissive, non-PHT recipient cells and cultured for ~24 hr. Recipient cells were then infected with virus as indicated. Schematic courtesy of Dr. Carolyn Coyne.

## 5.9 EXOSOME ISOLATION

Purified exosomes were provided by Dr. Yoel Sadovsky, Magee-Womens Research Institute, Pittsburgh, PA and are further detailed in [115, 254]. Briefly, for the isolation of PHT (or JEG-3) exosomes, cells were maintained for 48 hr in DMEM containing 10% FBS that had been previously ultracentrifuged at 108,000g for 10 hr to deplete pre-existing FBS exosomes. Supernatants from 200 million PHT cells were centrifuged at 300g for 5 min, 1,200g for 10 min, and 10,000g for 30 min. Exosomes were concentrated by centrifugation at 2,500g for 25 min using a Vivacell 100 filter (BioExpress), then ultracentrifuged at 108,000g for 1 hr. The pellet was subsequently ultracentrifuged on top of a 30% sucrose/D<sub>2</sub>O density cushion at 108,000g for 1 hr [255]. The exosomal phase was collected and resuspended in PBS.

Dendritic cell (DC) – derived exosomes were purified as previously described [256], from culture supernatants of C57Bl/6 mouse DC generated from bone marrow precursors cultured in medium supplemented 10% fetal calf serum (FCS), GM-CSF (1000 U/ml) and IL-4 (500 U/ml). During the last 48 hr of culture, DCs were maintained in medium supplemented with cytokines and 10% exosome-free FCS (overnight 100,000g centrifugation). At day 6, DCs were incubated for 1 hr with 100 nM ionomycin and culture supernatants were centrifuged at 300g (10 min), 1,200g (20 min), 10,000g (30 min) and then ultrafiltered (2000g, 20 min) through a Vivacell 100 filter. The filtered supernatant was adjusted to 10 mL with PBS and ultracentrifuged (100,000g, 60 min) on top of 1.6 ml 30% sucrose/D<sub>2</sub>O density cushion [255]. The phase containing the exosomes was collected, adjusted to 10 ml PBS, rinsed overnight at 4°C, and centrifuged at 100,000g for 1 hr. The amount of exosome protein was assessed with a NanoDrop 2000c.

## **5.10 TRANSFECTIONS**

### **5.10.1 Plasmid transfection**

Plasmid transfections were performed using X-tremeGENE 9 (Roche) according to manufacturer's protocol. The mRFP-LC3b expression construct was purchased from AddGene (plasmid 21075) and originally constructed by Tamotsu Yoshimori [257]. For experiments with conditioned media and purified exosomes, cells were exposed to media 24 hr post-transfection, and fixed 48 hr post-transfection. For all other experiments, cells were assayed 48 hr post-transfection.

### **5.10.2 miRNA transfection**

Mimics for C19MC miRNAs (miRIDIAN) as well as a non-targeting control miRNA mimic were obtained from Thermo-Fisher Scientific (Dharmacon) as described [115]. U2OS cells were reverse transfected with one or multiple miRNA mimics or miRNA mimic control (final concentration 6 nM for each miRNA mimic) using DharmaFECT-1 transfection reagent (Thermo-Fisher Scientific) or HiPerfect (Qiagen) according to manufacturers' instructions. The total concentration of non-targeting control miRNA mimics was adjusted to that of all active miRNA mimics. Cells were assayed 48 hr post-transfection.

### **5.10.3 siRNA (small interfering RNA) transfection**

For siRNA transfections, U2OS cells ( $3 \times 10^5$  of trypsinized cells/well) were reverse transfected

using HiPerfect transfection reagent (Qiagen). For silencing beclin-1, 40 nM per well of scrambled non-targeting siRNA (siControl) or beclin-1 siRNA (Cell Signaling, #6222S) were transfected.

BeWo cells were transfected with DharmaFECT 1 transfection reagent (Thermo-Fisher Scientific) according to manufacturer's protocol. Final siRNA concentration per well was 25 nM. siRNAs targeting human dynamin II, CHC, and cav-1 were obtained from Thermo-Fisher Scientific. CAR siRNA was obtained from IDT (5'-GGU GGA UCA AGU GAU UAU-3'; 5'-AAU AAU CAC UUG AUC CAC-3'). Cells were assayed 48-72 hr post-transfection.

## 5.11 VIRUS INFECTION ASSAYS

For experiments assessing productive viral infection, PHT cells were infected with CVB, PV, VSV, VV, or HSV-1 for 14-15 hr (MOI=5), or CMV for 24 hr for immunofluorescence. Infections were performed with three individual PHT preparations in duplicate. CMV infections were performed with two individual PHT preparations in triplicate. For 3-MA experiments assessed by RT-qPCR, PHT cells were infected with GFP-VSV for 15 hr at MOI=5. For experiments analyzing immediate early viral gene expression measured by RT-qPCR, PHT cells were infected with CVB, VSV, VV, or HSV-1 for 6-7 hr at MOI=1. HeLa cells were infected with CVB or PV at an MOI = 5 for 8 hr. HFF cells were infected with CMV for 24 hr, VSV or CVB (MOI=5), or HSV-1 (MOI=2.5) for 15 hr. Vero cells were infected with VSV for 6 hr (MOI=5). Caco-2 cells were infected with VSV or CVB for 7 hr (MOI = 5). RL-95 cells were infected with CVB for 15 hr (MOI=5). For immunofluorescence, U2OS cells were infected with CVB for 7 hr (MOI=5), VSV (MOI=5), VV, or HSV-1 (MOI=1) for 15 hr. For RT-qPCR,

U2OS cells were infected with CMV, VSV, HSV-1 or VV for 5-6 h (MOI = 1).

For infection of polarized BeWo cells, monolayers were cultured on collagen-coated 8-well chamber slides (LabTek) at a density of  $1.5 \times 10^5$  or on 12-mm Transwell-Col inserts (0.4- $\mu$ m pore size; Costar) at  $1.25 \times 10^6$  cells/well, or on 6-well plates at  $1.7 \times 10^6$  cells/well at 37°C. Cells were grown a minimum of 48 hr prior to study. Virus infection experiments were performed at a multiplicity of 5 plaque-forming units (PFU) per cell with CVB3-RD, CVB3-Nancy, or GFP-VSV. For immunofluorescence-based infection assays, cellular infection occurred for 7-8 hr 37°C. For NR-CVB infections, cells were infected (MOI=5) for 7-8 hr. At 2 hr p.i., cells were illuminated on a light box for 20 min. For RT-qPCR based infection assays, cells were infected with CVB (MOI=5) for 6-7 hr. For EM-based infection assays, cells were infected with CVB (MOI=10) for 14.5 hr. CVB-infected cells were fixed with ice-cold 3:1 methanol-acetone for 5 min, and GFP-VSV-infected cells fixed with 4% paraformaldehyde (PFA) at room temperature (RT).

## 5.12 NEUTRAL RED INFECTIOUS CENTER ASSAY

This assay was modified from [206, 207]. BeWo cells were pre-treated with the indicated inhibitors then infected with NR-CVB in the presence of inhibitor for 2 hr under semi-dark conditions (**Figure 5.2**). Cells were then illuminated on a light box for 20 min. Duplicate monolayers were maintained in the dark to control for non-specific effects of the pharmacological inhibitor on events unrelated to entry. Cells were then washed, trypsinized, and spun down at 2,000 rpm. Trypsin was removed, and cell pellets were resuspended in drug-free media. Known amounts of cells were plated onto naïve cells (on collagen-coated 8-well

chamber slides). Cells were allowed to infect for approximately 20-24 hr. Cells were then fixed and stained for VP1. Infection levels were assessed by immunofluorescence microscopy as described (5.15.3 “Immunofluorescence and confocal microscopy” and 5.15.4 “Quantification and analysis”).

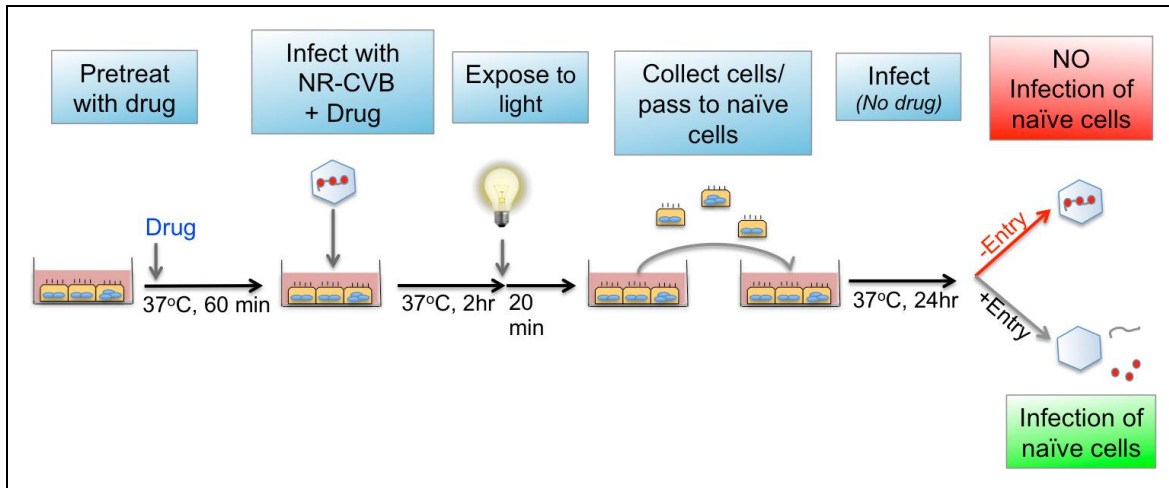


**Figure 5.2. Modified NRIC (Neutral Red Infectious Center) Assay.** Shown is a schematic of the NRIC assay. To determine the mechanism by which CVB enters placental trophoblasts, a modified NRIC assay was performed (adapted from [206, 207]). CVB was propagated in the presence of neutral red (NR) dye under semi-dark conditions. After incorporation of NR, the CVB virions become light sensitive and all subsequent virus purification and experimentation was performed under semi-dark conditions. This method enabled for the screening for inhibitors of various cellular endocytic and signaling pathways to dissect that may be required for CVB entry into placental trophoblasts. BeWo cells were incubated in the presence of the indicated drug for 60 min at 37°C prior to initiating infection. Cells were infected with NR-incorporated CVB for 2 hr to allow for virus entry. Infected cells were exposed to a light box for 20 min (illuminated) while a dark only, (non-illuminated) control condition was maintained in the dark. After light exposure, cells were washed, trypsinized, and equal amounts of cells were seeded onto a fresh, naïve monolayer of cells in media absent of both virus and drug. Naïve cells were allowed to infect for ~24 hr. Cells were fixed and stained for CVB capsid protein VP1. Infections were imaged and quantified as virus positive cells/DAPI using Image J software. Schematic courtesy of Dr. Carolyn Coyne.

## 5.13 VIRUS ENTRY ASSAYS

### 5.13.1 U2OS

VSV entry assays in U2OS cells exposed to either non-conditioned or conditioned PHT medium for 24 hr prior to assay was performed by incubating cells with virus (MOI=500) for 1 hr at 37°C until fixation in 4% PFA followed by permeabilization in 0.25% Triton X-100. VSV particles were visualized with anti-VSV-G antibody.

### 5.13.2 BeWo cells

CVB entry assays were performed with CVB3-RD (MOI=100-200) as indicated. Virus in binding buffer was allowed to bind to cells for 1 hr at RT. For BeWo cells, binding buffer was F12K with 20 mM HEPES. Unbound virus was washed off, complete medium was added, and cells were placed at 37°C to initiate virus particle entry. Virus entry was stopped by fixation with 4% PFA for 10 min at RT. PFA was removed and cells were washed with PBS. Cells were quenched 50 mM NH<sub>4</sub>Cl in PBS for 10 min. Virus was visualized with anti-VP1 antibody following a serial staining procedure as further detailed in (5.15.2 “Serial staining for virus entry assay”).

### 5.13.3 PHTs

Virus entry assays in PHT cells were performed with CVB as described (in subsection 5.13.2 “BeWo cells” and [54, 251]). For PHTs, binding buffer was minimal essential media (MEM)

with 20 mM HEPES. VV and HSV-1 internalization assays were performed by incubating PHT cells with virus (MOI=25) at 37°C until fixation at various time points (30, 60, 90 min). VV and HSV-1 were visualized by GFP expression.

## **5.14 CHOLERA TOXIN B AND TRANSFERRIN UPTAKE ASSAY**

Cholera toxin B (CTB) conjugated to Alexa Fluor 488 (8 µg/mL; Invitrogen) and transferrin conjugated to Alexa Fluor 594 (Invitrogen) uptake was performed essentially as previously described [89].

## **5.15 IMMUNOSTAINING**

### **5.15.1 General protocol**

Cell monolayers were cultured on 8-well chamber slides (Nunc LabTek) at 37°C. Cells were then washed and fixed as indicated with either ice cold methanol or 3:1 methanol-acetone for 5 min, or 4% paraformaldehyde in PBS (10 min) and permeabilized with 0.25% Triton X-100 in PBS (10 min). Fixed monolayers were incubated with the primary antibody (1:500 in PBS, 1 hr RT), washed twice with PBS, incubated with 1:1000 Alexa Fluor-488 or -594-conjugated secondary antibodies (Invitrogen) in 10% species-specific serum/PBS for 30 min RT, washed three times with PBS, and then mounted with Vectashield (Vector Laboratories) containing 4',6-diamidino-2-phenylindole (DAPI). For GFP-expressing viruses or RFP-LC3b experiments,

fixed monolayers were fixed with 4% PFA, permeabilized with 0.25% Triton X-100 for 5 min, and then mounted with Vectashield containing DAPI.

### **5.15.2 Serial staining for virus entry assay**

For CVB virus entry, a serial staining procedure was used to distinguish surface-associated virus under non-permeabilizing conditions from internalized virus under permeabilized conditions [251]. Following fixation with 4% PFA and quenching with  $\text{NH}_4\text{Cl}$  (50 mM in PBS) (non-permeabilizing condition), surface-associated virus was detected with VP1 primary antibody (1:500 in PBS, 1 hr RT), washed twice with PBS, incubated with 1:1000 Alexa Fluor-594 secondary antibodies (Invitrogen) in 10% species-specific serum/PBS for 30 min RT, and washed three times with PBS. Cells were refixed with 4% PFA, washed, and permeabilized with 0.25% Triton X-100 for 10 min (permeabilizing condition). Internalized virus was detected with VP1 primary antibody (1:500 in PBS, 1 hr RT), washed twice with PBS, incubated with 1:1000 Alexa Fluor-488 secondary antibodies (Invitrogen) in 10% species-specific serum/PBS for 30 min at RT, and washed three times with PBS. Slides were mounted with Vectashield containing DAPI.

### **5.15.3 Immunofluorescence and confocal microscopy**

For imaging of virus infection, cells were fixed and stained for markers of virus infection [CVB and PV (VP1), VSV (VSV-G), hCMV (gB)] or assessed for fluorescence-expression (VV-YFP, HSV-1-GFP, VSV-GFP). Images were captured with an IX81 inverted microscope equipped with a motorized stage or with an Olympus Fluoview 1000 laser scanning confocal microscope.

Images of infected cells were taken using an Olympus PlanApo 10x/0.40 NA dry or Apo 20x/0.75 NA dry objective, whereas all other images were taken with an Olympus PlanApo 60x/1.42 NA oil objective. For three-dimensional analysis of, XZ- or YZ-series stacks were acquired at 0.35-0.5  $\mu\text{m}$  intervals through the cell monolayer.

#### **5.15.4 Quantification and analysis**

For virus infection assays, a minimum of three independent fields per condition were counted (at least 500 cells total) per replicate. Infection levels are reported as the percentage of virus positive cells among the total number of cells, determined by DAPI staining using ImageJ (NIH) analysis. In some cases (where indicated), results were normalized to control and reported (% control).

For LC3b autophagy assays, at least 20 individual cells from a minimum of four independent fields were captured per condition. The total number of mRFP-LC3b-positive punctae was quantified per cell using ImageJ analysis with identical settings per condition. Analysis of the extent of VSV-G and mRFP-LC3b punctae colocalization was performed using ImageJ.

### **5.16 TRANSMISSION ELECTRON MICROSCOPY (TEM)**

Cells were seeded onto 6-well plates, assayed as noted, fixed with 2.5% glutaraldehyde in PBS for 1 hr, and then processed for electron microscopy as previously described [258]. Briefly, fixative was removed, and samples were washed three times in PBS at RT. Samples were post-

fixed in 1% osmium tetroxide ( $\text{OsO}_4$ ) containing 1% potassium ferricyanide ( $\text{K}_3\text{Fe}(\text{CN})_6$ ) for 1 hr, then washed three times in PBS. Samples were dehydrated in a series of alcohol/PBS washes (10 min each): 30% EtOH, 50% EtOH, 70% EtOH, 90% EtOH, and three times in 100% EtOH. The samples were infiltrated with in 1:1 propylene oxide:Polybed 812 epoxy resin (Polysciences) for 1 hr at RT or overnight at 4°C. Following subsequent changes of 100% resin the following day, the samples were embedded in molds, cured at 37°C overnight, and then 65°C for 48 hr. The technicians at CBI collected ultrathin sections (60 nm) on 100 mesh copper grids, then stained with 2% uranyl acetate in 50% methanol for 10 min, followed by 1% lead citrate for 7 min. Sections were imaged, and digital TEM images were captured using a JEOL JEM 1011 transmission electron microscope at 80 kV fitted with a bottom mount AMT 2k digital camera (Advanced Microscopy Techniques). The number of autophagosomes per cell (including amphisomes, autophagosomes, autophagic vacuoles, and autolysosomes) was manually quantified.

## **5.17 RNA EXPRESSION STUDIES**

### **5.17.1 RNA isolation**

For cellular mRNA analysis, total RNA was extracted using TRI reagent (MRC) or RNeasy (Qiagen) according to manufacturer's protocol. RNA samples were treated with RNase-free DNase (Qiagen).

### **5.17.2 cDNA synthesis**

Total RNA was reverse transcribed using iScript cDNA synthesis kit (Bio-Rad) or RT<sup>2</sup> First Strand kit (SABiosciences). For each sample, 1 µg RNA was used for cDNA synthesis. Autophagy and TLR RT-qPCR arrays (SABiosciences) were performed with 1 µg RNA per 96 well plate and subjected to RT-qPCR using SYBR/ROX RT<sup>2</sup> qPCR 2x master mix (SABiosciences) according to manufacturer's protocol.

### **5.17.3 RT-qPCR (Real time quantitative polymerase chain reaction)**

RT-qPCR was performed using iQ SYBR Green Supermix (Bio-Rad) in an Applied Biosystems StepOnePlus real-time PCR machine according to the manufacturer's instructions. Gene expression was calculated using the  $2^{-\Delta\Delta CT}$  method normalized to human  $\beta$ -actin. Relevant primer sequences are detailed below in **Table 5.1**. For the autophagy and TLR qPCR arrays (SABiosciences), gene expression was defined from the threshold cycle (Ct), and relative expression levels were calculated using SABiosciences RT<sup>2</sup> Profiler PCR array analysis automated software (<http://pcrdataanalysis.sabiosciences.com/pcr/arrayanalysis.php>).

**Table 5.1. Real-time PCR primers.**

Target	Forward (5'-3')	Reverse (5'-3')
Actin	ACTGGGACGACATGGAGAAAA	GCCACACGCAGCTC
VSV	TGCAAGGAAAGCATTGAACAA	GAGGAGTCACCTGGACAATCACT
CVB	ACGAATCCCAGTGTGTTTTGG	TGCTCAAAAACGGTATGGACAT
GFP	CACATGAAGCAGCAGCACTTCT	AACTCCAGCAGGACCATGTGAT
CMV Towne Strain	GCGGTGGTTGCCCAACAGGA	ACGACCCGTGGTCATCTTA
Tk	ACCCGC TTAACAGCGTCAACA	CCAAAGAGGTGCGGGAGTTT
VV rpo35 early	GCCAATGAGGGTTCGAGTTC	AACAACATCCCGTCGTTTCATC
ISG56	CAACCAAGCAAATGTGAGGA	GGAGACTTGCCTGGTGAAAA

## 5.18 IMMUNOBLOTS

Cells were grown in 24-well plates and lysates and prepared with RIPA buffer [50 mM Tris-HCl (pH 7.4); 1% NP-40; 0.25% sodium deoxycholate; 150 mM NaCl; 1 mM EDTA; 1 mM phenylmethanesulfonyl fluoride; 1 mg/ml aprotinin, leupeptin, and pepstatin; 1 mM sodium orthovanadate], and insoluble material was precipitated by brief centrifugation. Protein concentration of lysates was determined by BCA protein assay (Thermo Scientific). Lysates containing equal amounts of protein were loaded onto 4-20% Tris-HCl gels (Bio-Rad) and transferred to polyvinylidene difluoride (PVDF) or nitrocellulose membranes. Membranes were blocked in 5% nonfat dry milk, probed with the indicated antibodies, and developed with horseradish peroxidase-conjugated secondary antibodies (Santa Cruz Biotechnology) and SuperSignal West Pico or Dura, chemiluminescent substrates (Pierce Biotechnology).

Densitometry was performed using Image J.

### **5.19 REPORTER GENE ASSAY**

Data for reporter gene assays was provided by Dr. Carolyn Coyne, University of Pittsburgh, Pittsburgh, PA. Activation of IFN $\beta$  or ISRE promoters was measured by reporter assay. U2OS cells were transfected with 1  $\mu$ g of DNA/well of a 24-well plate, a 30:1 ratio of p-125 luc (IFN $\beta$ ) or ISRE reporter plasmids to pRL-null as per manufacturer's protocol (Promega). Cells were lysed in 100  $\mu$ L of lysis buffer and the levels of firefly and renilla luciferase levels quantified using the Dual-Luciferase Reporter Assay System with a dual injector equipped Synergy 2 SL Luminescence Microplate Reader (BioTek). Levels of firefly luciferase were normalized to control renilla luciferase levels. For poly(I:C) treatment, cells were transfected with 1  $\mu$ g poly(I:C)/well using XtremeGene-9 for 16 hr as per the manufacturer's protocol.

### **5.20 STATISTICAL ANALYSIS**

Data are presented as mean  $\pm$  SD. Except where specified, Student's t-test was used to determine statistical significance for virus infection and autophagy assays when two sets were compared, and one-way analysis of variance (ANOVA) with Bonferroni's correction for post-hoc multiple comparisons were used to determine statistical significance for reporter gene assays. A  $p < 0.05$  was determined significant.

## APPENDIX A

### ABBREVIATIONS

**3-MA:** 3-methyl-adenine

**ADP:** Adenosine diphosphate

**Ago2:** Argonaute2

**ANOVA:** Analysis of variance

**ANXA2:** Annexin A2

**AP2:** Adaptor protein 2

**APPs:** Antimicrobial proteins and peptides

**Arf6:** ADP-ribosylation factor 6

**ATCC:** American type culture collection

**ATG:** Autophagy-related gene

**BAC:** Bacterial artificial chromosome

**BCA assay:** Bicinchoninic acid assay

**C:** Celsius

**C19MC:** Chromosome 19 miRNA cluster

**CAR:** Coxsackievirus and adenovirus receptor

**Cav-1:** Caveolin-1

**CHC:** Clathrin heavy chain

**CME:** Clathrin-mediated endocytosis

**CMV:** Cytomegalovirus

**CO<sub>2</sub>:** Carbon dioxide

**CRH:** Corticotropin-releasing hormone

**CTB:** Cholera toxin B

**CVB:** Coxsackievirus B

**CVB3-Nancy:** Coxsackievirus B3 isolate Nancy

**CVB3-RD:** Coxsackievirus B3 isolate RD

**CytoD:** Cytochalasin D

**D<sub>2</sub>O:** Heavy water

**DAI:** DNA-dependent activator of IFN-regulatory factors

**DAF:** Decay-accelerating factor

**DAPI:** 4',6-diamidino-2-phenylindole

**DGCR8:** DiGeorge syndrome critical region gene 8

**DMEM:** Dulbecco's modified Eagle medium

**DMEM-H:** Dulbecco's modified Eagle medium-high glucose

**dsDNA:** Double-stranded DNA

**Dyn II:** Dynamin II

**EBV:** Epstein Barr virus

**ECM:** Extracellular matrix

**EDTA:** Ethylenediaminetetraacetic acid

**EEA1:** Endosome early antigen 1

**EIF2 $\alpha$ :** Eukaryotic initiation factor-2 $\alpha$

**EIPA:** 5-(*N*-ethyl-*N*-isopropyl) amiloride

**ELISA:** Enzyme-linked immunosorbent assay

**Eps15:** Epidermal growth factor receptor substrate 15

**ERK1/2:** Extracellular signal-regulated kinase 1/2

**ESCRT:** Endosomal sorting complex required for transport

**EtOH:** Ethanol

**EVTs:** Extravillous trophoblasts

**FBS:** Fetal bovine serum

**FCS:** Fetal calf serum

**g:** Gram

**GAPDH:** Glyceraldehyde 3-phosphate dehydrogenase

**gB:** Glycoprotein B

**GEEC:** GPI-enriched endocytic compartments

**GFP:** Green fluorescent protein

**GFP-VSV:** Green fluorescent protein expressing vesicular stomatitis virus

**GI:** Gastrointestinal

**GM-CSF:** Granulocyte macrophage colony-stimulating factor

**GPI:** Glycosylphosphatidylinositol

**GTP:** Guanosine triphosphate

**GW182:** Glycine-tryptophan repeat containing protein of 182 kDa

**HA:** Hemagglutinin

**HBMEC:** Human brain microvascular endothelial cells

**HBSS:** Hank's balanced salt solution

**HBV:** Hepatitis B virus

**hCG:** Human chorionic gonadotropin

**hCMV:** Human cytomegalovirus

**hCS:** Human chorionic somatotropin

**HCV:** Hepatitis C virus

**HEPES:** 4-(2-hydroxyethyl)-1-piperazineethanesulfonic acid

**HFF:** Human foreskin fibroblast

**hGHs:** Human growth hormones

**HIV:** Human immunodeficiency virus

**hPL:** Human placental lactogen

**hPRL:** Human prolactin

**HPV:** Human papilloma virus

**Hr:** Hours

**HUtMVEC:** Human uterine microvascular endothelial cell

**HUVEC:** Human umbilical vein endothelial cell

**HSV-1:** Herpes simplex virus-1

**HSV-2:** Herpes simplex virus-2

**IGF:** Insulin growth factor

**IFN:** Interferon

**IFNAR1/2:** Type I IFN- $\alpha/\beta$  receptors 1 and 2

**IL:** Interleukin

**ILVs:** Intraluminal vesicles

**INT:** Iodonitrotetrazolium chloride

**IRF:** Interferon regulatory factor

**ISG:** Interferon stimulated gene

**ISRE:** IFN-stimulated response elements

**IUGR:** Intrauterine growth restriction

**JAK:** Janus kinases

**JNK1:** C-jun-N-terminal kinase-1

**K<sub>3</sub>Fe(CN)<sub>6</sub>:** Potassium ferricyanide

**Kb:** Kilobases

**KSHV:** Kaposi's sarcoma herpesvirus

**L:** Liter

**LatA:** Latrunculin A

**LC3:** Microtubule-associated protein light chain-3

**LMP1:** Latent membrane protein 1

**LPS:** Lipopolysaccharide

**MAL:** MyD88-adaptor-like

**M $\beta$ CD:** Methyl- $\beta$ -cyclodextrin

**MCMV:** Murine cytomegalovirus

**MDA5:** melanoma differentiation associated gene 5

**MDC:** Monodansylcadaverine

**MEM:** Minimum essential medium

**mg:** Milligram

**μg:** Microgram

**MgCl<sub>2</sub>:** Magnesium chloride

**MHV-68:** Murine herpesvirus-68

**Min:** Minutes

**miRISC:** miRNA-induced silencing complex

**miRNA:** MicroRNA

**mL:** Milliliter

**μL:** Microliter

**mM:** Millimolar

**μM:** Micromolar

**μm:** Micrometer

**MMR:** Measles, mumps, and rubella

**MOI:** Multiplicity of infection

**mRFP:** Monomeric red-fluorescent protein

**mRNA:** Messenger RNA

**mTOR:** Mammalian target of rapamycin

**mTORC1:** Mammalian target of rapamycin complex-1

**MTT:** Thiazolyl blue tetrazolium bromide

**MUPP-1:** Multi-PDZ domain protein-1

**MVBs:** Multivesicular bodies

**Mx:** Myxovirus-resistance protein

**NaCl:** Sodium chloride

**NEAA:** Non-essential amino acids

**NF- $\kappa$ B:** Nuclear factor- $\kappa$ B

**ng:** Nanogram

**NH<sub>4</sub>Cl:** Ammonium chloride

**NIH:** National Institutes of Health

**nm:** Nanometer

**NPC:** Nasopharyngeal carcinomas

**N-Rh-PE:** Sulfonyl dioleoylphosphatidylethanolamine

**NR:** Neutral red

**NR-CVB:** Neutral red incorporated Coxsackievirus B

**NRIC:** Neutral red infectious center

**nt:** Nucleotide

**OAS:** Oligo-adenylate synthetase

**OsO<sub>4</sub>:** Osmium tetroxide

**PBS:** Phosphate buffered saline

**PCR:** Polymerase chain reaction

**pDCs:** Plasmacytoid dendritic cells

**PAMP:** Pathogen associated molecular pattern

**PE:** Phosphatidylethanolamine

**PFA:** Paraformaldehyde

**PFU:** Plaque forming unit

**PHT:** Primary human trophoblast

**P.i.:** Post-infection

**PI3K:** Phosphoinositide 3-kinase

**PI3P:** Phosphatidylinositol-3-phosphate

**PKC:** Protein kinase C

**PKR:** RNA-dependent protein kinase

**Pol:** Polymerase

**Poly(I:C):** Polyinosinic-polycytidylic acid

**Pre-miRNAs:** Precursor miRNAs

**Pri-miRNA:** Primary miRNA

**PRR:** Pattern recognition receptor

**PTHrP:** Parathyroid hormone-related protein

**PV:** Poliovirus

**PVDF:** Polyvinylidene difluoride

**RAN-GTP:** RAS-related nuclear protein-guanosine triphosphate

**RAS:** Rat sarcoma

**RBPs:** RNA-binding proteins

**RIG-I:** Retinoic-acid-inducible gene I

**RISC:** RNA-induced silencing complex

**RLH:** RIG-I-like helicase

**RNA:** Ribonucleic acid

**RNase:** ribonuclease

**RNA seq:** Next-generation RNA sequencing

**Rpm:** Revolutions per minute

**RT:** Room temperature

**RT-qPCR:** Real-time quantitative PCR

**SDS:** Sodium dodecyl sulfate

**siRNA:** Small-interfering RNA

**SFKs:** Src family kinases

**SFV:** Semliki forest virus

**ssRNA:** Single-stranded RNA

**STAT:** Signal transduction and activators of transcription

**SV40:** Simian virus-40

**TAR:** Trans-activating response

**TCID<sub>50</sub>:** 50% Tissue culture infectious dose 50

**TEM:** Transmission electron microscopy

**Tfn:** Transferrin

**TICAM1:** TIR-domain-containing-molecule 1

**TIR:** Toll/IL-1R homology domain

**TIRAP:** TIR-associated protein

**TJ:** Tight junction

**Tk:** Thymidine kinase

**TLR:** Toll-like receptor

**TORCH:** *T*oxoplasma *g*ondii, *o*ther, *r*ubella virus, *C*MV, and *H*SV-1 and -2

**TORCHES:** *T*oxoplasma *g*ondii, *o*ther, *r*ubella virus, *C*MV, *H*SV-1 and -2, and *s*yphilis

**TRAM:** TRIF-related adaptor molecule

**TRBP:** HIV TAR RNA binding protein

**TRIF:** TIR-domain-containing adaptor protein-inducing IFN- $\beta$

**Tris-HCl:** Tris(hydroxymethyl)aminomethane-hydrochloride

**U:** Units

**UTR:** Untranslated region

**UVRAG:** Ultraviolet radiation resistance-associated gene protein

**VP:** Virus protein

**VPS:** Vacuolar protein-sorting

**VSV:** Vesicular stomatitis virus

**VSVG:** Vesicular stomatitis virus glycoprotein

**VV:** Vaccinia virus

**VZV:** Varicella zoster virus

**Wt:** Wild-type

**YFP:** Yellow fluorescent protein

**ZO-1:** Zonula occludens-1

## APPENDIX B

### EXPRESSION CHANGES IN AUTOPHAGY- AND TLR-RELATED TRANSCRIPTS

Gene	Fold-change	Gene	Fold-change	Gene	Fold-change	Gene	Fold-change
ATG4C	3.2861	MAP1LC3B	1.2209	HMGB1	0.9027	ATG10	0.724
UVRAG	3.2696	CHUK	1.2054	TNFRSF1A	0.901	FADD	0.7218
CCL2	3.1764	HSPA1A	1.1822	ELK1	0.8971	BAX	0.7145
DAPK1	3.119	ATG12	1.1791	IL1B	0.8966	PIK3R4	0.7073
CTSS	3.1154	RIPK2	1.1446	UBE2V1	0.8948	MK3	0.6992
EIF2AK2	2.5184	ATG16L1	1.1417	GABARAP	0.8913	HSPA8	0.6945
RB1	2.3295	PTGS2	1.1354	IKBKB	0.8859	MAPK8	0.68385
BNIP3	2.3171	TOLLIP	1.124	PTEN	0.8814	ATG7	0.6794
MAP1LC3A	2.1561	EIF2AK3	1.1192	EIF4G1	0.8792	MAPK8IP3	0.6767
PIK3C3	2.1554	IL8	1.1002	GABARAPL2	0.8772	NFRKB	0.6665
BID	2.149	UBE2N	1.0968	MAP4K4	0.8748	TAB1	0.6663
AMBRA1	1.9193	MAP3K7	1.0954	CD180	0.8699	ULK1	0.6621
ARSA	1.849	TLR4	1.0872	CLN3	0.8339	TICAM1	0.6597
BCL2L1	1.7855	APP	1.0846	PRKAA1	0.8324	CDKN1B	0.6285
PRKRA	1.7526	PPARA	1.0624	FAM176A	0.8304	TGM2	0.6192
ATG4D	1.7454	PELI1	1.0265	TRAF6	0.8257	DRAM2	0.6166
SQSTM1	1.7187	PRKAA2	1.0185	MAP2K4	0.8234	RPS6KB1	0.6072
NFKBIA	1.6335	FAS	1.0149	NR2C2	0.8234	RGS19	0.6005
ATG4A	1.6288	BECN1	1.0139	BCL2	0.8218	NFKB2	0.5946
LY96	1.4979	HSP90AA1	1.0107	HTT	0.8135	TMEM74	0.576
NFKB1	1.45885	HSPD1	0.9957	TLR6	0.809	ATG9A	0.5758
TBK1	1.3469	CSF2	0.9879	ECSIT	0.804	CASP8	0.57545
TP53	1.3446	HGS	0.9745	BAD	0.8011	JUN	0.5644
MAP3K1	1.3294	REL	0.9743	BAK1	0.7987	SARM1	0.5564
DRAM1	1.3204	CXCR4	0.9529	MYD88	0.7962	NFKBIL1	0.5528
ATG3	1.289	MAPK14	0.9497	GAA	0.7936	IRAK1	0.5404
AKT1	1.2812	IRF3	0.9437	IRF1	0.7825	FOS	0.5091
TLR3	1.2655	TICAM2	0.9347	CASP3	0.7749	TP73	0.5061

ATG16L2	1.2457	ATG4B	0.9261	GABARAPL1	0.7581	TNFSF10	0.4193
TGFB1	1.2354	ATG5	0.9159	HDAC1	0.7541	IRGM	0.2952
ULK2	1.2352	HRAS	0.9159	RAB24	0.7351	TNF	0.2475
SNCA	1.2286	CTSB	0.9132	RELA	0.7325	ATG9B	0.2436
						IFNA4	0.1286

## BIBLIOGRAPHY

1. Aplin, J.D., *The cell biological basis of human implantation*. Baillieres Best Pract Res Clin Obstet Gynaecol, 2000. **14**(5): p. 757-64.
2. Huppertz, B., *The anatomy of the normal placenta*. J Clin Pathol, 2008. **61**(12): p. 1296-302.
3. Benirschke, K., P. Kaufmann, and R.N. Baergen, *Pathology of the Human Placenta*. 5th ed2006, New York: Springer Science+Business Media, Inc.
4. Khong, T.Y. and J.M. Pearce, *Development and Investigation of the Placenta and Its Blood Supply in The Human Placenta: Clinical Perspectives*, J.P. Lavery, Editor 1987, Aspen Publishers: Rockville, MD. p. 25-33.
5. Lunghi, L., et al., *Control of human trophoblast function*. Reprod Biol Endocrinol, 2007. **5**: p. 6.
6. Levy, O., *Innate immunity of the newborn: basic mechanisms and clinical correlates*. Nat Rev Immunol, 2007. **7**(5): p. 379-90.
7. Robbins, J.R., et al., *Placental syncytiotrophoblast constitutes a major barrier to vertical transmission of Listeria monocytogenes*. PLoS Pathog, 2010. **6**(1): p. e1000732.
8. Zeldovich, V.B., et al., *Invasive extravillous trophoblasts restrict intracellular growth and spread of listeria monocytogenes*. PLoS Pathog, 2011. **7**(3): p. e1002005.
9. Sanchez, L., M. Calvo, and J.H. Brock, *Biological role of lactoferrin*. Arch Dis Child, 1992. **67**(5): p. 657-61.
10. Kim, H.S., et al., *Endotoxin-neutralizing antimicrobial proteins of the human placenta*. J Immunol, 2002. **168**(5): p. 2356-64.
11. White, S.H., W.C. Wimley, and M.E. Selsted, *Structure, function, and membrane integration of defensins*. Curr Opin Struct Biol, 1995. **5**(4): p. 521-7.
12. Mor, G. and I. Cardenas, *The immune system in pregnancy: a unique complexity*. Am J Reprod Immunol, 2010. **63**(6): p. 425-33.
13. Mor, G., et al., *Inflammation and pregnancy: the role of the immune system at the implantation site*. Ann N Y Acad Sci, 2011. **1221**: p. 80-7.
14. Gabbe, S.G., Niebyl, Jennifer R., Galan, Henry, Jauniaux, Eric R. M., Landon, Mark, Simpason, Joe Leigh, and Deborah Driscoll *Obstetrics: Normal and Problem Pregnancies* 5th ed2007: Churchill Livingstone.
15. Chan, G., et al., *Human cytomegalovirus-caused damage to placental trophoblasts mediated by immediate-early gene-induced tumor necrosis factor-alpha*. Am J Pathol, 2002. **161**(4): p. 1371-81.
16. Fisher, S., et al., *Human cytomegalovirus infection of placental cytotrophoblasts in vitro and in utero: implications for transmission and pathogenesis*. J Virol, 2000. **74**(15): p. 6808-20.

17. Maidji, E., et al., *Transmission of human cytomegalovirus from infected uterine microvascular endothelial cells to differentiating/invasive placental cytotrophoblasts*. Virology, 2002. **304**(1): p. 53-69.
18. Maidji, E., et al., *Developmental regulation of human cytomegalovirus receptors in cytotrophoblasts correlates with distinct replication sites in the placenta*. J Virol, 2007. **81**(9): p. 4701-12.
19. Robbins, J.R., et al., *Tissue Barriers of the Human Placenta to Infection with Toxoplasma gondii*. Infect Immun, 2012. **80**(1): p. 418-28.
20. Nahmias, A.J., et al., *Perinatal risk associated with maternal genital herpes simplex virus infection*. Am J Obstet Gynecol, 1971. **110**(6): p. 825-37.
21. Kinney, J.S. and M.L. Kumar, *Should we expand the TORCH complex? A description of clinical and diagnostic aspects of selected old and new agents*. Clin Perinatol, 1988. **15**(4): p. 727-44.
22. Kaur, R., et al., *Screening for TORCH infections in pregnant women: a report from Delhi*. Southeast Asian J Trop Med Public Health, 1999. **30**(2): p. 284-6.
23. Stegmann, B.J. and J.C. Carey, *TORCH Infections. Toxoplasmosis, Other (syphilis, varicella-zoster, parvovirus B19), Rubella, Cytomegalovirus (CMV), and Herpes infections*. Curr Womens Health Rep, 2002. **2**(4): p. 253-8.
24. Chicago, U.o. *TORCH Infections Pediatrics Clerkship*, 2013.
25. Brumback, R.A., *TORCHES*. Pediatrics, 1976. **58**.
26. CDC *Parasites - Toxoplasmosis (Toxoplasma infection)*. 2013.
27. CDC *Rubella*. 2009.
28. Caserta, M.T. *Congenital Rubella The Merck Manual for Health Care Professionals* 2009.
29. CDC *Cytomegalovirus (CMV) and Pregnancy*. 2012.
30. Schleiss, M.R., *Congenital cytomegalovirus infection: update on management strategies*. Curr Treat Options Neurol, 2008. **10**(3): p. 186-92.
31. Pereira, L., et al., *Insights into viral transmission at the uterine-placental interface*. Trends Microbiol, 2005. **13**(4): p. 164-74.
32. Anzivino, E., et al., *Herpes simplex virus infection in pregnancy and in neonate: status of art of epidemiology, diagnosis, therapy and prevention*. Virol J, 2009. **6**: p. 40.
33. Pallansch, M.A., Roos, R.P. , *Enteroviruses: Polioviruses, Coxsackieviruses, Echoviruses, and Newer Enteroviruses*. 5th ed2001, Philadelphia: Lippincott Williams & Wilkins.
34. Huber, S. and A.I. Ramsingh, *Coxsackievirus-induced pancreatitis*. Viral Immunol, 2004. **17**(3): p. 358-69.
35. Axelsson, C., et al., *Coxsackie B virus infections in women with miscarriage*. J Med Virol, 1993. **39**(4): p. 282-5.
36. McClure, E.M. and R.L. Goldenberg, *Infection and stillbirth*. Semin Fetal Neonatal Med, 2009. **14**(4): p. 182-9.
37. Strong, B.S. and S.A. Young, *Intrauterine coxsackie virus, group B type 1, infection: viral cultivation from amniotic fluid in the third trimester*. Am J Perinatol, 1995. **12**(2): p. 78-9.
38. Wikswa, M.E., et al., *Increased activity of Coxsackievirus B1 strains associated with severe disease among young infants in the United States, 2007-2008*. Clin Infect Dis, 2009. **49**(5): p. e44-51.

39. Satosar, A., et al., *Histologic correlates of viral and bacterial infection of the placenta associated with severe morbidity and mortality in the newborn*. Hum Pathol, 2004. **35**(5): p. 536-45.
40. Verma, N.A., et al., *Outbreak of life-threatening coxsackievirus B1 myocarditis in neonates*. Clin Infect Dis, 2009. **49**(5): p. 759-63.
41. Lu, J.C., et al., *Neonate with coxsackie B1 infection, cardiomyopathy and arrhythmias*. J Natl Med Assoc, 2005. **97**(7): p. 1028-30.
42. Bendig, J.W., et al., *Coxsackievirus B3 sequences in the blood of a neonate with congenital myocarditis, plus serological evidence of maternal infection*. J Med Virol, 2003. **70**(4): p. 606-9.
43. Konstantinidou, A., et al., *Transplacental infection of Coxsackievirus B3 pathological findings in the fetus*. J Med Virol, 2007. **79**(6): p. 754-7.
44. Ouellet, A., et al., *Antenatal diagnosis of intrauterine infection with coxsackievirus B3 associated with live birth*. Infect Dis Obstet Gynecol, 2004. **12**(1): p. 23-6.
45. Sauerbrei, A., et al., *Congenital skin lesions caused by intrauterine infection with coxsackievirus B3*. Infection, 2000. **28**(5): p. 326-8.
46. Callen, J. and B.A. Paes, *A case report of a premature infant with coxsackie B1 meningitis*. Adv Neonatal Care, 2007. **7**(5): p. 238-47.
47. Euscher, E., et al., *Coxsackie virus infection of the placenta associated with neurodevelopmental delays in the newborn*. Obstet Gynecol, 2001. **98**(6): p. 1019-26.
48. Elfving, M., et al., *Maternal enterovirus infection during pregnancy as a risk factor in offspring diagnosed with type 1 diabetes between 15 and 30 years of age*. Exp Diabetes Res, 2008. **2008**: p. 271958.
49. Dahlquist, G., et al., *Indications that maternal coxsackie B virus infection during pregnancy is a risk factor for childhood-onset IDDM*. Diabetologia, 1995. **38**(11): p. 1371-3.
50. Svensson, J., et al., *Intrauterine exposure to maternal enterovirus infection as a risk factor for development of autoimmune thyroiditis during childhood and adolescence*. Thyroid, 2004. **14**(5): p. 367-70.
51. Sun, X., et al., *Role of clathrin-mediated endocytosis during vesicular stomatitis virus entry into host cells*. Virology, 2005. **338**(1): p. 53-60.
52. Anderson, H.A., Y. Chen, and L.C. Norkin, *Bound simian virus 40 translocates to caveolin-enriched membrane domains, and its entry is inhibited by drugs that selectively disrupt caveolae*. Mol Biol Cell, 1996. **7**(11): p. 1825-34.
53. Mercer, J. and A. Helenius, *Gulping rather than sipping: macropinocytosis as a way of virus entry*. Curr Opin Microbiol, 2012. **15**(4): p. 490-9.
54. Coyne, C.B. and J.M. Bergelson, *Virus-induced Abl and Fyn kinase signals permit coxsackievirus entry through epithelial tight junctions*. Cell, 2006. **124**(1): p. 119-31.
55. Coyne, C.B., et al., *Coxsackievirus entry across epithelial tight junctions requires occludin and the small GTPases Rab34 and Rab5*. Cell Host Microbe, 2007. **2**(3): p. 181-92.
56. Damm, E.M., et al., *Clathrin- and caveolin-1-independent endocytosis: entry of simian virus 40 into cells devoid of caveolae*. J Cell Biol, 2005. **168**(3): p. 477-88.
57. Schelhaas, M., et al., *Entry of human papillomavirus type 16 by actin-dependent, clathrin- and lipid raft-independent endocytosis*. PLoS Pathog, 2012. **8**(4): p. e1002657.

58. Delorme-Axford, E. and C.B. Coyne, *The actin cytoskeleton as a barrier to virus infection of polarized epithelial cells*. *Viruses*, 2011. **3**(12): p. 2462-77.
59. McMahon, H.T. and E. Boucrot, *Molecular mechanism and physiological functions of clathrin-mediated endocytosis*. *Nat Rev Mol Cell Biol*, 2011. **12**(8): p. 517-33.
60. Doherty, G.J. and H.T. McMahon, *Mechanisms of endocytosis*. *Annu Rev Biochem*, 2009. **78**: p. 857-902.
61. Grant, B.D. and J.G. Donaldson, *Pathways and mechanisms of endocytic recycling*. *Nat Rev Mol Cell Biol*, 2009. **10**(9): p. 597-608.
62. Kiss, A.L., *Caveolae and the regulation of endocytosis*. *Adv Exp Med Biol*, 2012. **729**: p. 14-28.
63. Nabi, I.R. and P.U. Le, *Caveolae/raft-dependent endocytosis*. *J Cell Biol*, 2003. **161**(4): p. 673-7.
64. Henley, J.R., et al., *Dynamin-mediated internalization of caveolae*. *J Cell Biol*, 1998. **141**(1): p. 85-99.
65. Oh, P., D.P. McIntosh, and J.E. Schnitzer, *Dynamin at the neck of caveolae mediates their budding to form transport vesicles by GTP-driven fission from the plasma membrane of endothelium*. *J Cell Biol*, 1998. **141**(1): p. 101-14.
66. Schlegel, A., et al., *Crowded little caves: structure and function of caveolae*. *Cell Signal*, 1998. **10**(7): p. 457-63.
67. Mercer, J., M. Schelhaas, and A. Helenius, *Virus entry by endocytosis*. *Annu Rev Biochem*, 2010. **79**: p. 803-33.
68. Swanson, J.A., *Shaping cups into phagosomes and macropinosomes*. *Nat Rev Mol Cell Biol*, 2008. **9**(8): p. 639-49.
69. Mercer, J. and A. Helenius, *Virus entry by macropinocytosis*. *Nat Cell Biol*, 2009. **11**(5): p. 510-20.
70. Flint, S.J., Enquist, L.W., Racaniello, V.R., and Akalka, A.M., *Principles of virology*. 3rd ed2009, Washington, D.C.: ASM Press.
71. Mire, C.E., et al., *Glycoprotein-dependent acidification of vesicular stomatitis virus enhances release of matrix protein*. *J Virol*, 2009. **83**(23): p. 12139-50.
72. Belkowski, L.S. and G.C. Sen, *Inhibition of vesicular stomatitis viral mRNA synthesis by interferons*. *J Virol*, 1987. **61**(3): p. 653-60.
73. Lee, H.K., et al., *Autophagy-dependent viral recognition by plasmacytoid dendritic cells*. *Science*, 2007. **315**(5817): p. 1398-401.
74. Shelly, S., et al., *Autophagy is an essential component of Drosophila immunity against vesicular stomatitis virus*. *Immunity*, 2009. **30**(4): p. 588-98.
75. Nakamoto, M., et al., *Virus recognition by Toll-7 activates antiviral autophagy in Drosophila*. *Immunity*, 2012. **36**(4): p. 658-67.
76. Johannsdottir, H.K., et al., *Host cell factors and functions involved in vesicular stomatitis virus entry*. *J Virol*, 2009. **83**(1): p. 440-53.
77. Carneiro, F.A., A.S. Ferradosa, and A.T. Da Poian, *Low pH-induced conformational changes in vesicular stomatitis virus glycoprotein involve dramatic structure reorganization*. *J Biol Chem*, 2001. **276**(1): p. 62-7.
78. White, J., K. Matlin, and A. Helenius, *Cell fusion by Semliki Forest, influenza, and vesicular stomatitis viruses*. *J Cell Biol*, 1981. **89**(3): p. 674-9.
79. Sousa, S., M. Lecuit, and P. Cossart, *Microbial strategies to target, cross or disrupt epithelia*. *Curr Opin Cell Biol*, 2005. **17**(5): p. 489-98.

80. Bergelson, J.M., et al., *Isolation of a common receptor for Coxsackie B viruses and adenoviruses 2 and 5*. *Science*, 1997. **275**(5304): p. 1320-3.
81. Martino, T.A., et al., *The coxsackie-adenovirus receptor (CAR) is used by reference strains and clinical isolates representing all six serotypes of coxsackievirus group B and by swine vesicular disease virus*. *Virology*, 2000. **271**(1): p. 99-108.
82. Cohen, C.J., et al., *The coxsackievirus and adenovirus receptor is a transmembrane component of the tight junction*. *Proc Natl Acad Sci U S A*, 2001. **98**(26): p. 15191-6.
83. Bergelson, J.M., et al., *Clinical coxsackievirus B isolates differ from laboratory strains in their interaction with two cell surface receptors*. *J Infect Dis*, 1997. **175**(3): p. 697-700.
84. Shafren, D.R., et al., *Coxsackieviruses B1, B3, and B5 use decay accelerating factor as a receptor for cell attachment*. *J Virol*, 1995. **69**(6): p. 3873-7.
85. Shieh, J.T. and J.M. Bergelson, *Interaction with decay-accelerating factor facilitates coxsackievirus B infection of polarized epithelial cells*. *J Virol*, 2002. **76**(18): p. 9474-80.
86. Shafren, D.R., D.T. Williams, and R.D. Barry, *A decay-accelerating factor-binding strain of coxsackievirus B3 requires the coxsackievirus-adenovirus receptor protein to mediate lytic infection of rhabdomyosarcoma cells*. *J Virol*, 1997. **71**(12): p. 9844-8.
87. Milstone, A.M., et al., *Interaction with coxsackievirus and adenovirus receptor, but not with decay-accelerating factor (DAF), induces A-particle formation in a DAF-binding coxsackievirus B3 isolate*. *J Virol*, 2005. **79**(1): p. 655-60.
88. Bozym, R.A., et al., *Release of intracellular calcium stores facilitates coxsackievirus entry into polarized endothelial cells*. *PLoS Pathog*, 2010. **6**(10).
89. Patel, K.P., C.B. Coyne, and J.M. Bergelson, *Dynamin- and lipid raft-dependent entry of DAF-binding and non-DAF-binding Coxsackieviruses into non-polarized cells*. *J Virol*, 2009.
90. Lee, Y., S. El Andaloussi, and M.J. Wood, *Exosomes and microvesicles: extracellular vesicles for genetic information transfer and gene therapy*. *Hum Mol Genet*, 2012. **21**(R1): p. R125-34.
91. Thery, C., L. Zitvogel, and S. Amigorena, *Exosomes: composition, biogenesis and function*. *Nat Rev Immunol*, 2002. **2**(8): p. 569-79.
92. Record, M., et al., *Exosomes as intercellular signalosomes and pharmacological effectors*. *Biochem Pharmacol*, 2011. **81**(10): p. 1171-82.
93. Skog, J., et al., *Glioblastoma microvesicles transport RNA and proteins that promote tumour growth and provide diagnostic biomarkers*. *Nat Cell Biol*, 2008. **10**(12): p. 1470-6.
94. Valadi, H., et al., *Exosome-mediated transfer of mRNAs and microRNAs is a novel mechanism of genetic exchange between cells*. *Nat Cell Biol*, 2007. **9**(6): p. 654-9.
95. Kosaka, N., et al., *Secretory mechanisms and intercellular transfer of microRNAs in living cells*. *J Biol Chem*, 2010. **285**(23): p. 17442-52.
96. Mittelbrunn, M. and F. Sanchez-Madrid, *Intercellular communication: diverse structures for exchange of genetic information*. *Nat Rev Mol Cell Biol*, 2012. **13**(5): p. 328-35.
97. Pan, B.T., et al., *Electron microscopic evidence for externalization of the transferrin receptor in vesicular form in sheep reticulocytes*. *J Cell Biol*, 1985. **101**(3): p. 942-8.
98. Mincheva-Nilsson, L. and V. Baranov, *The role of placental exosomes in reproduction*. *Am J Reprod Immunol*, 2010. **63**(6): p. 520-33.
99. Yang, C., et al., *Exosomes released from Mycoplasma infected tumor cells activate inhibitory B cells*. *PLoS One*, 2012. **7**(4): p. e36138.

100. Kim, S.H., et al., *Exosomes derived from IL-10-treated dendritic cells can suppress inflammation and collagen-induced arthritis*. J Immunol, 2005. **174**(10): p. 6440-8.
101. Pegtel, D.M., et al., *Functional delivery of viral miRNAs via exosomes*. Proc Natl Acad Sci U S A, 2010. **107**(14): p. 6328-33.
102. Meckes, D.G., Jr., et al., *Human tumor virus utilizes exosomes for intercellular communication*. Proc Natl Acad Sci U S A, 2010. **107**(47): p. 20370-5.
103. Dreux, M., et al., *Short-range exosomal transfer of viral RNA from infected cells to plasmacytoid dendritic cells triggers innate immunity*. Cell Host Microbe, 2012. **12**(4): p. 558-70.
104. Booth, A.M., et al., *Exosomes and HIV Gag bud from endosome-like domains of the T cell plasma membrane*. J Cell Biol, 2006. **172**(6): p. 923-35.
105. Baietti, M.F., et al., *Syndecan-syntenin-ALIX regulates the biogenesis of exosomes*. Nat Cell Biol, 2012. **14**(7): p. 677-85.
106. Tamai, K., et al., *Exosome secretion of dendritic cells is regulated by Hrs, an ESCRT-0 protein*. Biochem Biophys Res Commun, 2010. **399**(3): p. 384-90.
107. Fevrier, B. and G. Raposo, *Exosomes: endosomal-derived vesicles shipping extracellular messages*. Curr Opin Cell Biol, 2004. **16**(4): p. 415-21.
108. Trajkovic, K., et al., *Ceramide triggers budding of exosome vesicles into multivesicular endosomes*. Science, 2008. **319**(5867): p. 1244-7.
109. Schorey, J.S. and S. Bhatnagar, *Exosome function: from tumor immunology to pathogen biology*. Traffic, 2008. **9**(6): p. 871-81.
110. Feng, D., et al., *Cellular internalization of exosomes occurs through phagocytosis*. Traffic, 2010. **11**(5): p. 675-87.
111. Parolini, I., et al., *Microenvironmental pH is a key factor for exosome traffic in tumor cells*. J Biol Chem, 2009. **284**(49): p. 34211-22.
112. Rana, S. and M. Zoller, *Exosome target cell selection and the importance of exosomal tetraspanins: a hypothesis*. Biochem Soc Trans, 2011. **39**(2): p. 559-62.
113. Taylor, D.D., S. Akyol, and C. Gercel-Taylor, *Pregnancy-associated exosomes and their modulation of T cell signaling*. J Immunol, 2006. **176**(3): p. 1534-42.
114. Sabapatha, A., C. Gercel-Taylor, and D.D. Taylor, *Specific isolation of placenta-derived exosomes from the circulation of pregnant women and their immunoregulatory consequences*. Am J Reprod Immunol, 2006. **56**(5-6): p. 345-55.
115. Donker, R.B., et al., *The expression profile of C19MC microRNAs in primary human trophoblast cells and exosomes*. Mol Hum Reprod, 2012. **18**(8): p. 417-24.
116. Luo, S.S., et al., *Human villous trophoblasts express and secrete placenta-specific microRNAs into maternal circulation via exosomes*. Biol Reprod, 2009. **81**(4): p. 717-29.
117. Lodish, H.F., et al., *Micromanagement of the immune system by microRNAs*. Nat Rev Immunol, 2008. **8**(2): p. 120-30.
118. Vasudevan, S., Y. Tong, and J.A. Steitz, *Switching from repression to activation: microRNAs can up-regulate translation*. Science, 2007. **318**(5858): p. 1931-4.
119. Ma, F., et al., *MicroRNA-466l upregulates IL-10 expression in TLR-triggered macrophages by antagonizing RNA-binding protein tristetraprolin-mediated IL-10 mRNA degradation*. J Immunol, 2010. **184**(11): p. 6053-9.
120. Lee, Y., et al., *MicroRNA genes are transcribed by RNA polymerase II*. EMBO J, 2004. **23**(20): p. 4051-60.

121. Cai, X., C.H. Hagedorn, and B.R. Cullen, *Human microRNAs are processed from capped, polyadenylated transcripts that can also function as mRNAs*. RNA, 2004. **10**(12): p. 1957-66.
122. Borchert, G.M., W. Lanier, and B.L. Davidson, *RNA polymerase III transcribes human microRNAs*. Nat Struct Mol Biol, 2006. **13**(12): p. 1097-101.
123. Fabian, M.R. and N. Sonenberg, *The mechanics of miRNA-mediated gene silencing: a look under the hood of miRISC*. Nat Struct Mol Biol, 2012. **19**(6): p. 586-93.
124. Chendrimada, T.P., et al., *TRBP recruits the Dicer complex to Ago2 for microRNA processing and gene silencing*. Nature, 2005. **436**(7051): p. 740-4.
125. Liu, J., et al., *Argonaute2 is the catalytic engine of mammalian RNAi*. Science, 2004. **305**(5689): p. 1437-41.
126. Meister, G., et al., *Human Argonaute2 mediates RNA cleavage targeted by miRNAs and siRNAs*. Mol Cell, 2004. **15**(2): p. 185-97.
127. Okamura, K., N. Liu, and E.C. Lai, *Distinct mechanisms for microRNA strand selection by Drosophila Argonautes*. Mol Cell, 2009. **36**(3): p. 431-44.
128. Lin, S.L., D. Chang, and S.Y. Ying, *Asymmetry of intronic pre-miRNA structures in functional RISC assembly*. Gene, 2005. **356**: p. 32-8.
129. Khvorovova, A., A. Reynolds, and S.D. Jayasena, *Functional siRNAs and miRNAs exhibit strand bias*. Cell, 2003. **115**(2): p. 209-16.
130. Winter, J., et al., *Many roads to maturity: microRNA biogenesis pathways and their regulation*. Nat Cell Biol, 2009. **11**(3): p. 228-34.
131. Lim, L.P., et al., *Microarray analysis shows that some microRNAs downregulate large numbers of target mRNAs*. Nature, 2005. **433**(7027): p. 769-73.
132. Selbach, M., et al., *Widespread changes in protein synthesis induced by microRNAs*. Nature, 2008. **455**(7209): p. 58-63.
133. Baek, D., et al., *The impact of microRNAs on protein output*. Nature, 2008. **455**(7209): p. 64-71.
134. Arroyo, J.D., et al., *Argonaute2 complexes carry a population of circulating microRNAs independent of vesicles in human plasma*. Proc Natl Acad Sci U S A, 2011. **108**(12): p. 5003-8.
135. Santhakumar, D., et al., *Combined agonist-antagonist genome-wide functional screening identifies broadly active antiviral microRNAs*. Proc Natl Acad Sci U S A, 2010. **107**(31): p. 13830-5.
136. Plaisance-Bonstaff, K. and R. Renne, *Viral miRNAs*. Methods Mol Biol, 2011. **721**: p. 43-66.
137. Pedersen, I.M., et al., *Interferon modulation of cellular microRNAs as an antiviral mechanism*. Nature, 2007. **449**(7164): p. 919-22.
138. Witwer, K.W., et al., *MicroRNA regulation of IFN-beta protein expression: rapid and sensitive modulation of the innate immune response*. J Immunol, 2010. **184**(5): p. 2369-76.
139. Mouillet, J.F., et al., *The levels of hypoxia-regulated microRNAs in plasma of pregnant women with fetal growth restriction*. Placenta, 2010. **31**(9): p. 781-4.
140. Noguer-Dance, M., et al., *The primate-specific microRNA gene cluster (C19MC) is imprinted in the placenta*. Hum Mol Genet, 2010. **19**(18): p. 3566-82.
141. Bortolin-Cavaille, M.L., et al., *C19MC microRNAs are processed from introns of large Pol-II, non-protein-coding transcripts*. Nucleic Acids Res, 2009. **37**(10): p. 3464-73.

142. Morales-Prieto, D.M., et al., *MicroRNA expression profiles of trophoblastic cells. Placenta*, 2012. **33**(9): p. 725-34.
143. Li, M., et al., *Frequent amplification of a chr19q13.41 microRNA polycistron in aggressive primitive neuroectodermal brain tumors. Cancer Cell*, 2009. **16**(6): p. 533-46.
144. Nobusawa, S., et al., *Analysis of chromosome 19q13.42 amplification in embryonal brain tumors with ependymoblastic multilayered rosettes. Brain Pathol*, 2012. **22**(5): p. 689-97.
145. Toffanin, S., et al., *MicroRNA-based classification of hepatocellular carcinoma and oncogenic role of miR-517a. Gastroenterology*, 2011. **140**(5): p. 1618-28 e16.
146. Flor, I. and J. Bullerdiek, *The dark side of a success story: microRNAs of the C19MC cluster in human tumours. J Pathol*, 2012. **227**(3): p. 270-4.
147. Bentwich, I., et al., *Identification of hundreds of conserved and nonconserved human microRNAs. Nat Genet*, 2005. **37**(7): p. 766-70.
148. Mouillet, J.F., T. Chu, and Y. Sadovsky, *Expression patterns of placental microRNAs. Birth Defects Res A Clin Mol Teratol*, 2011. **91**(8): p. 737-43.
149. Enders, G., et al., *Intrauterine transmission and clinical outcome of 248 pregnancies with primary cytomegalovirus infection in relation to gestational age. J Clin Virol*, 2011. **52**(3): p. 244-6.
150. Pass, R.F., et al., *Congenital cytomegalovirus infection following first trimester maternal infection: symptoms at birth and outcome. J Clin Virol*, 2006. **35**(2): p. 216-20.
151. He, C. and D.J. Klionsky, *Regulation mechanisms and signaling pathways of autophagy. Annu Rev Genet*, 2009. **43**: p. 67-93.
152. Sumpter, R., Jr. and B. Levine, *Selective autophagy and viruses. Autophagy*, 2011. **7**(3): p. 260-5.
153. Kroemer, G., G. Marino, and B. Levine, *Autophagy and the integrated stress response. Mol Cell*, 2010. **40**(2): p. 280-93.
154. Mizushima, N. and B. Levine, *Autophagy in mammalian development and differentiation. Nat Cell Biol*, 2010. **12**(9): p. 823-30.
155. Hosokawa, N., et al., *Nutrient-dependent mTORC1 association with the ULK1-Atg13-FIP200 complex required for autophagy. Mol Biol Cell*, 2009. **20**(7): p. 1981-91.
156. Levine, B., N. Mizushima, and H.W. Virgin, *Autophagy in immunity and inflammation. Nature*, 2011. **469**(7330): p. 323-35.
157. Noda, T. and Y. Ohsumi, *Tor, a phosphatidylinositol kinase homologue, controls autophagy in yeast. J Biol Chem*, 1998. **273**(7): p. 3963-6.
158. Yang, Z. and D.J. Klionsky, *Eaten alive: a history of macroautophagy. Nat Cell Biol*, 2010. **12**(9): p. 814-22.
159. Kudchodkar, S.B. and B. Levine, *Viruses and autophagy. Rev Med Virol*, 2009. **19**(6): p. 359-78.
160. Hailey, D.W., et al., *Mitochondria supply membranes for autophagosome biogenesis during starvation. Cell*, 2010. **141**(4): p. 656-67.
161. Mari, M., S.A. Tooze, and F. Reggiori, *The puzzling origin of the autophagosomal membrane. F1000 Biol Rep*, 2011. **3**: p. 25.
162. Levine, B. and G. Kroemer, *Autophagy in the pathogenesis of disease. Cell*, 2008. **132**(1): p. 27-42.
163. Xie, Z. and D.J. Klionsky, *Autophagosome formation: core machinery and adaptations. Nat Cell Biol*, 2007. **9**(10): p. 1102-9.

164. Sarkar, S., et al., *Lithium induces autophagy by inhibiting inositol monophosphatase*. J Cell Biol, 2005. **170**(7): p. 1101-11.
165. Nishida, Y., et al., *Discovery of Atg5/Atg7-independent alternative macroautophagy*. Nature, 2009. **461**(7264): p. 654-8.
166. Talloczy, Z., H.W.t. Virgin, and B. Levine, *PKR-dependent autophagic degradation of herpes simplex virus type 1*. Autophagy, 2006. **2**(1): p. 24-9.
167. Liang, X.H., et al., *Protection against fatal Sindbis virus encephalitis by beclin, a novel Bcl-2-interacting protein*. J Virol, 1998. **72**(11): p. 8586-96.
168. Delgado, M.A., et al., *Toll-like receptors control autophagy*. EMBO J, 2008. **27**(7): p. 1110-21.
169. Shi, C.S. and J.H. Kehrl, *MyD88 and Trif target Beclin 1 to trigger autophagy in macrophages*. J Biol Chem, 2008. **283**(48): p. 33175-82.
170. Law, A.H., et al., *Cellular response to influenza virus infection: a potential role for autophagy in CXCL10 and interferon-alpha induction*. Cell Mol Immunol, 2010. **7**(4): p. 263-70.
171. Manuse, M.J., C.M. Briggs, and G.D. Parks, *Replication-independent activation of human plasmacytoid dendritic cells by the paramyxovirus SV5 Requires TLR7 and autophagy pathways*. Virology, 2010. **405**(2): p. 383-9.
172. Liu, Y., et al., *Autophagy regulates programmed cell death during the plant innate immune response*. Cell, 2005. **121**(4): p. 567-77.
173. Gobeil, P.A. and D.A. Leib, *Herpes simplex virus gamma34.5 interferes with autophagosome maturation and antigen presentation in dendritic cells*. MBio, 2012. **3**(5): p. e00267-12.
174. Lussignol, M., et al., *The Herpes Simplex Virus 1 Us11 Protein Inhibits Autophagy through Its Interaction with the Protein Kinase PKR*. J Virol, 2013. **87**(2): p. 859-71.
175. Orvedahl, A., et al., *HSV-1 ICP34.5 confers neurovirulence by targeting the Beclin 1 autophagy protein*. Cell Host Microbe, 2007. **1**(1): p. 23-35.
176. Chaumorcel, M., et al., *Human cytomegalovirus controls a new autophagy-dependent cellular antiviral defense mechanism*. Autophagy, 2008. **4**(1): p. 46-53.
177. Chaumorcel, M., et al., *The human cytomegalovirus protein TRS1 inhibits autophagy via its interaction with Beclin 1*. J Virol, 2012. **86**(5): p. 2571-84.
178. Dreux, M., et al., *The autophagy machinery is required to initiate hepatitis C virus replication*. Proc Natl Acad Sci U S A, 2009. **106**(33): p. 14046-51.
179. Schlegel, A., et al., *Cellular origin and ultrastructure of membranes induced during poliovirus infection*. J Virol, 1996. **70**(10): p. 6576-88.
180. Kemball, C.C., et al., *Coxsackievirus infection induces autophagy-like vesicles and megaphagosomes in pancreatic acinar cells in vivo*. J Virol, 2010. **84**(23): p. 12110-24.
181. Wong, J., et al., *Autophagosome supports coxsackievirus B3 replication in host cells*. J Virol, 2008. **82**(18): p. 9143-53.
182. Kuma, A., et al., *The role of autophagy during the early neonatal starvation period*. Nature, 2004. **432**(7020): p. 1032-6.
183. Efeyan, A., et al., *Regulation of mTORC1 by the Rag GTPases is necessary for neonatal autophagy and survival*. Nature, 2012.
184. Schiaffino, S., C. Mammucari, and M. Sandri, *The role of autophagy in neonatal tissues: just a response to amino acid starvation?* Autophagy, 2008. **4**(5): p. 727-30.

185. Katze, M.G., Y. He, and M. Gale, Jr., *Viruses and interferon: a fight for supremacy*. Nat Rev Immunol, 2002. **2**(9): p. 675-87.
186. Bonjardim, C.A., P.C. Ferreira, and E.G. Kroon, *Interferons: signaling, antiviral and viral evasion*. Immunol Lett, 2009. **122**(1): p. 1-11.
187. Akira, S., S. Uematsu, and O. Takeuchi, *Pathogen recognition and innate immunity*. Cell, 2006. **124**(4): p. 783-801.
188. Novick, D., B. Cohen, and M. Rubinstein, *The human interferon alpha/beta receptor: characterization and molecular cloning*. Cell, 1994. **77**(3): p. 391-400.
189. Boo, K.H. and J.S. Yang, *Intrinsic cellular defenses against virus infection by antiviral type I interferon*. Yonsei Med J, 2010. **51**(1): p. 9-17.
190. Ornoy, A. and A. Tenenbaum, *Pregnancy outcome following infections by coxsackie, echo, measles, mumps, hepatitis, polio and encephalitis viruses*. Reprod Toxicol, 2006. **21**(4): p. 446-57.
191. Horstmann, D.M., *Viral infections in pregnancy*. Yale J Biol Med, 1969. **42**(2): p. 99-112.
192. van der Blik, A.M., et al., *Mutations in human dynamin block an intermediate stage in coated vesicle formation*. J Cell Biol, 1993. **122**(3): p. 553-63.
193. Amegadzie, B.Y., B.Y. Ahn, and B. Moss, *Identification, sequence, and expression of the gene encoding a Mr 35,000 subunit of the vaccinia virus DNA-dependent RNA polymerase*. J Biol Chem, 1991. **266**(21): p. 13712-8.
194. Wang, Z., et al., *Skin mast cells protect mice against vaccinia virus by triggering mast cell receptor SIPR2 and releasing antimicrobial peptides*. J Immunol, 2012. **188**(1): p. 345-57.
195. Lin, S., et al., *Computational identification and characterization of primate-specific microRNAs in human genome*. Comput Biol Chem, 2010. **34**(4): p. 232-41.
196. Seglen, P.O. and P.B. Gordon, *3-Methyladenine: specific inhibitor of autophagic/lysosomal protein degradation in isolated rat hepatocytes*. Proc Natl Acad Sci U S A, 1982. **79**(6): p. 1889-92.
197. Okahira, S., et al., *Interferon-beta induction through toll-like receptor 3 depends on double-stranded RNA structure*. DNA Cell Biol, 2005. **24**(10): p. 614-23.
198. Klionsky, D.J., et al., *Guidelines for the use and interpretation of assays for monitoring autophagy in higher eukaryotes*. Autophagy, 2008. **4**(2): p. 151-75.
199. Liang, X.H., et al., *Induction of autophagy and inhibition of tumorigenesis by beclin 1*. Nature, 1999. **402**(6762): p. 672-6.
200. Kang, R., et al., *The Beclin 1 network regulates autophagy and apoptosis*. Cell Death Differ, 2011. **18**(4): p. 571-80.
201. Cerneus, D.P. and A. van der Ende, *Apical and basolateral transferrin receptors in polarized BeWo cells recycle through separate endosomes*. J Cell Biol, 1991. **114**(6): p. 1149-58.
202. Liu, F., M.J. Soares, and K.L. Audus, *Permeability properties of monolayers of the human trophoblast cell line BeWo*. Am J Physiol, 1997. **273**(5 Pt 1): p. C1596-604.
203. Suhy, D.A., T.H. Giddings, Jr., and K. Kirkegaard, *Remodeling the endoplasmic reticulum by poliovirus infection and by individual viral proteins: an autophagy-like origin for virus-induced vesicles*. J Virol, 2000. **74**(19): p. 8953-65.
204. Pan, J., et al., *Single amino acid changes in the virus capsid permit coxsackievirus B3 to bind decay-accelerating factor*. J Virol, 2011. **85**(14): p. 7436-43.

205. Bergelson, J.M., et al., *Decay-accelerating factor (CD55), a glycosylphosphatidylinositol-anchored complement regulatory protein, is a receptor for several echoviruses*. Proc Natl Acad Sci U S A, 1994. **91**(13): p. 6245-8.
206. Brandenburg, B., et al., *Imaging poliovirus entry in live cells*. PLoS Biol, 2007. **5**(7): p. e183.
207. Kim, C. and J.M. Bergelson, *Echovirus 7 entry into polarized intestinal epithelial cells requires clathrin and Rab7*. MBio, 2012. **3**(2).
208. Crowther, D. and J.L. Melnick, *The incorporation of neutral red and acridine orange into developing poliovirus particles making them photosensitive*. Virology, 1961. **14**: p. 11-21.
209. Wilson, J.N. and P.D. Cooper, *ASPECTS OF THE GROWTH OF POLIOVIRUS AS REVEALED BY THE PHOTODYNAMIC EFFECTS OF NEUTRAL RED AND ACRIDINE ORANGE*. Virology, 1963. **21**: p. 135-45.
210. Wang, L.H., K.G. Rothberg, and R.G. Anderson, *Mis-assembly of clathrin lattices on endosomes reveals a regulatory switch for coated pit formation*. J Cell Biol, 1993. **123**(5): p. 1107-17.
211. Ivanov, A.I., *Pharmacological inhibition of endocytic pathways: is it specific enough to be useful?* Methods Mol Biol, 2008. **440**: p. 15-33.
212. Schlegel, R., et al., *Amantadine and dansylcadaverine inhibit vesicular stomatitis virus uptake and receptor-mediated endocytosis of alpha 2-macroglobulin*. Proc Natl Acad Sci U S A, 1982. **79**(7): p. 2291-5.
213. Damke, H., et al., *Induction of mutant dynamin specifically blocks endocytic coated vesicle formation*. J Cell Biol, 1994. **127**(4): p. 915-34.
214. Macia, E., et al., *Dynasore, a cell-permeable inhibitor of dynamin*. Dev Cell, 2006. **10**(6): p. 839-50.
215. Orlandi, P.A. and P.H. Fishman, *Filipin-dependent inhibition of cholera toxin: evidence for toxin internalization and activation through caveolae-like domains*. J Cell Biol, 1998. **141**(4): p. 905-15.
216. Pelkmans, L., J. Kartenbeck, and A. Helenius, *Caveolar endocytosis of simian virus 40 reveals a new two-step vesicular-transport pathway to the ER*. Nat Cell Biol, 2001. **3**(5): p. 473-83.
217. Massol, R.H., et al., *Cholera toxin toxicity does not require functional Arf6- and dynamin-dependent endocytic pathways*. Mol Biol Cell, 2004. **15**(8): p. 3631-41.
218. Torgersen, M.L., et al., *Internalization of cholera toxin by different endocytic mechanisms*. J Cell Sci, 2001. **114**(Pt 20): p. 3737-47.
219. West, M.A., M.S. Bretscher, and C. Watts, *Distinct endocytotic pathways in epidermal growth factor-stimulated human carcinoma A431 cells*. J Cell Biol, 1989. **109**(6 Pt 1): p. 2731-9.
220. Meier, O., et al., *Adenovirus triggers macropinocytosis and endosomal leakage together with its clathrin-mediated uptake*. J Cell Biol, 2002. **158**(6): p. 1119-31.
221. Sarkar, K., et al., *Selective inhibition by rottlerin of macropinocytosis in monocyte-derived dendritic cells*. Immunology, 2005. **116**(4): p. 513-24.
222. Peterson, J.R. and T.J. Mitchison, *Small molecules, big impact: a history of chemical inhibitors and the cytoskeleton*. Chem Biol, 2002. **9**(12): p. 1275-85.
223. Coue, M., et al., *Inhibition of actin polymerization by latrunculin A*. FEBS Lett, 1987. **213**(2): p. 316-8.

224. Just, I., et al., *Probing the action of Clostridium difficile toxin B in Xenopus laevis oocytes*. J Cell Sci, 1994. **107 ( Pt 6)**: p. 1653-9.
225. Just, I., et al., *Clostridium difficile toxin B acts on the GTP-binding protein Rho*. J Biol Chem, 1994. **269**(14): p. 10706-12.
226. Spiering, D. and L. Hodgson, *Dynamics of the Rho-family small GTPases in actin regulation and motility*. Cell Adh Migr, 2011. **5**(2): p. 170-80.
227. Schnatwinkel, C., et al., *The Rab5 effector Rabankyrin-5 regulates and coordinates different endocytic mechanisms*. PLoS Biol, 2004. **2**(9): p. E261.
228. Kerr, M.C. and R.D. Teasdale, *Defining macropinocytosis*. Traffic, 2009. **10**(4): p. 364-71.
229. Ui, M., et al., *Wortmannin as a unique probe for an intracellular signalling protein, phosphoinositide 3-kinase*. Trends Biochem Sci, 1995. **20**(8): p. 303-7.
230. Huyer, G., et al., *Mechanism of inhibition of protein-tyrosine phosphatases by vanadate and pervanadate*. J Biol Chem, 1997. **272**(2): p. 843-51.
231. Akiyama, T., et al., *Genistein, a specific inhibitor of tyrosine-specific protein kinases*. J Biol Chem, 1987. **262**(12): p. 5592-5.
232. Hanke, J.H., et al., *Discovery of a novel, potent, and Src family-selective tyrosine kinase inhibitor. Study of Lck- and FynT-dependent T cell activation*. J Biol Chem, 1996. **271**(2): p. 695-701.
233. De Brabander, M.J., et al., *The effects of methyl (5-(2-thienylcarbonyl)-1H-benzimidazol-2-yl) carbamate, (R 17934; NSC 238159), a new synthetic antitumoral drug interfering with microtubules, on mammalian cells cultured in vitro*. Cancer Res, 1976. **36**(3): p. 905-16.
234. Straight, A.F., et al., *Dissecting temporal and spatial control of cytokinesis with a myosin II Inhibitor*. Science, 2003. **299**(5613): p. 1743-7.
235. Pattillo, R.A., et al., *Human hormone production in vitro*. Science, 1968. **159**(3822): p. 1467-9.
236. Pattillo, R.A. and G.O. Gey, *The establishment of a cell line of human hormone-synthesizing trophoblastic cells in vitro*. Cancer Res, 1968. **28**(7): p. 1231-6.
237. Vidricaire, G. and M.J. Tremblay, *A clathrin, caveolae, and dynamin-independent endocytic pathway requiring free membrane cholesterol drives HIV-1 internalization and infection in polarized trophoblastic cells*. J Mol Biol, 2007. **368**(5): p. 1267-83.
238. Parsons, S.J. and J.T. Parsons, *Src family kinases, key regulators of signal transduction*. Oncogene, 2004. **23**(48): p. 7906-9.
239. Yeatman, T.J., *A renaissance for SRC*. Nat Rev Cancer, 2004. **4**(6): p. 470-80.
240. Sen, B. and F.M. Johnson, *Regulation of SRC family kinases in human cancers*. J Signal Transduct, 2011. **2011**: p. 865819.
241. Zhang, S. and D. Yu, *Targeting Src family kinases in anti-cancer therapies: turning promise into triumph*. Trends Pharmacol Sci, 2012. **33**(3): p. 122-8.
242. Nelson, D.M., et al., *Hypoxia limits differentiation and up-regulates expression and activity of prostaglandin H synthase 2 in cultured trophoblast from term human placenta*. Am J Obstet Gynecol, 1999. **180**(4): p. 896-902.
243. Chen, B., D.M. Nelson, and Y. Sadovsky, *N-myc down-regulated gene 1 modulates the response of term human trophoblasts to hypoxic injury*. J Biol Chem, 2006. **281**(5): p. 2764-72.

244. Levine, B., *Eating oneself and uninvited guests: autophagy-related pathways in cellular defense*. Cell, 2005. **120**(2): p. 159-62.
245. Thomson, D.W., C.P. Bracken, and G.J. Goodall, *Experimental strategies for microRNA target identification*. Nucleic Acids Res, 2011. **39**(16): p. 6845-53.
246. Coyne, C.B., et al., *The coxsackievirus and adenovirus receptor interacts with the multi-PDZ domain protein-1 (MUPP-1) within the tight junction*. J Biol Chem, 2004. **279**(46): p. 48079-84.
247. Coyne, C.B. and J.M. Bergelson, *CAR: a virus receptor within the tight junction*. Adv Drug Deliv Rev, 2005. **57**(6): p. 869-82.
248. Bergelson, J.M., *Intercellular junctional proteins as receptors and barriers to virus infection and spread*. Cell Host Microbe, 2009. **5**(6): p. 517-21.
249. Kliman, H.J., et al., *Purification, characterization, and in vitro differentiation of cytotrophoblasts from human term placentae*. Endocrinology, 1986. **118**(4): p. 1567-82.
250. Moser, T.S., et al., *A kinome RNAi screen identified AMPK as promoting poxvirus entry through the control of actin dynamics*. PLoS Pathog, 2010. **6**(6): p. e1000954.
251. Coyne, C.B., K.S. Kim, and J.M. Bergelson, *Poliovirus entry into human brain microvascular cells requires receptor-induced activation of SHP-2*. EMBO J, 2007. **26**(17): p. 4016-28.
252. Desai, P. and S. Person, *Incorporation of the green fluorescent protein into the herpes simplex virus type 1 capsid*. J Virol, 1998. **72**(9): p. 7563-8.
253. Kirchhausen, T., E. Macia, and H.E. Pelish, *Use of dynasore, the small molecule inhibitor of dynamin, in the regulation of endocytosis*. Methods Enzymol, 2008. **438**: p. 77-93.
254. Montecalvo, A., et al., *Exosomes as a short-range mechanism to spread alloantigen between dendritic cells during T cell allorecognition*. J Immunol, 2008. **180**(5): p. 3081-90.
255. Lamparski, H.G., et al., *Production and characterization of clinical grade exosomes derived from dendritic cells*. J Immunol Methods, 2002. **270**(2): p. 211-26.
256. Montecalvo, A., et al., *Mechanism of transfer of functional microRNAs between mouse dendritic cells via exosomes*. Blood, 2012. **119**(3): p. 756-66.
257. Kimura, S., T. Noda, and T. Yoshimori, *Dissection of the autophagosome maturation process by a novel reporter protein, tandem fluorescent-tagged LC3*. Autophagy, 2007. **3**(5): p. 452-60.
258. Gao, W., et al., *Biochemical isolation and characterization of the tubulovesicular LC3-positive autophagosomal compartment*. J Biol Chem, 2010. **285**(2): p. 1371-83.